

NAVAL POSTGRADUATE SCHOOL

Monterey, California



APPLICATION OF HOLOGRAPHIC INTERFEROMETRY TO
DENSITY FIELD DETERMINATION IN
TRANSONIC CORNER FLOW

by

D. J. Collins

and

R. A. Kosakoski

December 1972

Approved for public release; distribution unlimited

NAVAL POSTGRADUATE SCHOOL
Monterey, California 93940

Rear Admiral A. S. Goodfellow
Superintendent

M. U. Clauser
Provost

ABSTRACT

The successful application of holographic interferometry to the study of density fields around opaque bodies in wind tunnel experiments has been reported in the literature. The present report extends this technique to the study of the asymmetric flow fields encountered near the wing-fuselage junction of an aerodynamic model in the transonic flow regime. Finite fringe interferometry has been used to investigate the three-dimensional density field about a partially transparent wing-body structure. The resulting asymmetric density field and shock wave structure are shown to be an accurate representation of the phenomena encountered in aerodynamic corner flow.

This report was supported by : ONR Req. 00014-2-000033, 15 Sep 71 and NASC W. R. 2-6059, 12 Jul 71.

TABLE OF CONTENTS

Introduction	1
Appendix I	I-1

INTRODUCTION

This is a report on holographic investigations directed towards the determination of three-dimensional density fields in transonic corner flows. The report consists essentially of Appendix I, which includes the thesis of LT R. A. Kosakoski on holographic investigations of transonic corner flow. This investigation is the first to use transparent models in holographic interferometry.

A paper based on this thesis, "Application of Holographic Interferometry to Density Field Determination in Transonic Corner Flow," by R. A. Kosakoski and D. J. Collins (No. 73-156) has been presented at the AIAA 11th Aerospace Sciences Meeting in Washington, D. C. The paper is now under consideration for publication in the AIAA Journal.

The integral inversion method used in the thesis and paper has now been essentially superseded by a more efficient method based on Fourier Transforms. This latter method is the subject of another report.

Further work on investigation into the application of fiber optics in holographic interferometry is continuing. This study also involves the consideration of flow with limited fields of view.

APPENDIX I

NAVAL POSTGRADUATE SCHOOL

Monterey, California



THESIS

APPLICATION OF
HOLOGRAPHIC INTERFEROMETRY
TO
DENSITY FIELD DETERMINATION
IN TRANSONIC CORNER FLOW

by

Robert Anthony Kosakoski

Thesis Advisor

D. J. Collins

December 1972

Approved for public release; distribution unlimited.

Application of Holographic Interferometry
to Density Field Determination
in Transonic Corner Flow

by

Robert Anthony Kosakoski
Lieutenant, United States Navy
B.S.M.E., University of Rochester, 1965

Submitted in partial fulfillment of the
requirements for the degree of

AERONAUTICAL ENGINEER

from the
NAVAL POSTGRADUATE SCHOOL
December 1972

ABSTRACT

The successful application of holographic interferometry to the study of density fields around opaque bodies in wind tunnel experiments has been reported in the literature. The present report extends this technique to the study of the three-dimensional asymmetric flow fields encountered near the wing-fuselage junction of an aerodynamic model in the transonic flow regime. Finite fringe interferometry has been used to obtain fringe information about a partially transparent wing-body structure. A FORTRAN computer program was utilized to invert the fringe information and produce a plot of the density field around the model. The resulting asymmetric density field and shock wave structure are shown to be an accurate representation of the phenomena encountered in aerodynamic corner flow.

TABLE OF CONTENTS

I.	INTRODUCTION-----	5
II.	EXPERIMENTAL APPARATUS -----	7
	A. THE WIND TUNNEL -----	7
	B. THE HOLOGRAPHIC ARRANGEMENT -----	8
	C. THE WIND TUNNEL MODEL -----	9
III.	ANALYTICAL EVALUATION OF THE DENSITY FIELD----	10
	A. THE BASIC EQUATION OF INTERFEROMETRY -----	10
	B. THE INTEGRAL INVERSION-----	12
	C. THE NUMERICAL PROCEDURE -----	15
IV.	EXPERIMENTAL PROCEDURE -----	18
	A. LABORATORY TECHNIQUES -----	18
	B. PHOTOGRAPHIC TECHNIQUES -----	20
	C. DATA REDUCTION -----	21
V.	EXPERIMENTAL RESULTS AND DISCUSSION -----	24
VI.	CONCLUSIONS -----	30
APPENDIX A: Reduction Of An Interferogram To Obtain		
	Fringe Shift Data-----	64
APPENDIX B: Application Of Computer Program "HOLOFER"--		
		67
LIST OF REFERENCES -----		117
INITIAL DISTRIBUTION LIST -----		119
FORM DD-1473-----		120

ACKNOWLEDGEMENTS

This writer wishes to gratefully acknowledge Dr. D. J. Collins for his most valuable guidance and assistance during the course of this investigation; the Aerodynamics Division of the Naval Ship Research and Development Center, Carderock, Maryland, under Dr. R. Furey, particularly B. Ellis and O. Gilmore, for their tireless effort during the wind tunnel testing phase; the technical staff of the Department of Aeronautics under R. Besel and T. Dunton, particularly N. Leckenby and G. Middleton, for their able assistance in the fabrication and assembly of the models and equipment used in this study; and my wife and family for their noble patience and encouragement.

I. INTRODUCTION

The field of flow measurement has been revolutionized in recent years with the perfection of holography and holographic interferometry techniques. High power Q-switched and dye-switched lasers and sophisticated double-pulsing trigger mechanisms provide exposure times on the order of twenty nanoseconds, thereby "freezing" the flow during the hologram production process. The precision optical quality components and measurement techniques of Mach-Zehnder interferometry have given way to the much less restrictive requirements of holographic interferometry which provide high quality interferograms in three dimensions.

Techniques for the application of holography to interferometry have been reported by Heflinger, et al. [1], and by Brooks [2]. In the determination of the density field around a free jet in the supersonic regime, Matulka [3, 4] expressed the fringe data in a series of orthogonal polynomials and transformed them to polynomials representing density using an inversion technique reported in [5, 6]. The method was extended by Jagota [7, 8] to the determination of the three-dimensional density field around a ten-degree half angle cone in a supersonic wind tunnel. The ability to produce readable holograms in wind tunnel studies using transparent phase objects was verified by Heyer [9]. In the present report the aforementioned techniques

have been combined to study the three-dimensional density field near the wing-fuselage junction of an aerodynamic model in transonic flow. The experiment was conducted at the Naval Ship Research and Development Center, Carderock, Maryland in an eighteen inch transonic blow-down wind tunnel at a Mach number of 0.937, using a semi-transparent model of original design.

Since reasonably small variations in density were anticipated, a finite fringe technique was used in obtaining the interferograms. The horizontal finite fringe field was produced by a vertical translation of a diffusing glass in the scene beam a distance of 0.003 inches between the two exposures of the holographic plate. Fringe data obtained from the interferograms were reduced to density information using a modified form of the inversion computer program used in [7]. A self-testing procedure incorporated in the program verified the resulting density data as an accurate representation of the actual flow around the model.

II. EXPERIMENTAL APPARATUS

A. THE WIND TUNNEL

The investigation was conducted in the Naval Ship Research and Development Center blowdown supersonic wind tunnel. Transonic flow conditions were produced through incorporation of slotted upper and lower tunnel walls. The tunnel is a nominal eighteen inch blow-down-to-vacuum facility with a test section fourteen inches by eighteen inches in cross-section and twenty-nine inches in length with the slotted surfaces installed. Optical quality windows twenty-two inches in diameter in the side walls provided complete viewing of the flow in the test section as the model was rolled through 180 degrees for hologram production. A functional schematic of the wind tunnel is shown in Figure 1.

B. THE MACH NUMBER AND PRESSURE MEASUREMENT PROCEDURE

The Mach number at the test section is determined as a function of total and static pressure measurements and is maintained by carefully controlled butterfly valve settings. Total pressure is determined by recording atmospheric pressure prior to tunnel operation and accounting for the pressure loss between the plenum and the test section during operation. Static pressure is measured directly at a central wall port in the test section. Data recordings

were made on a Beckman Instruments Company 210 Digital Recorder, shown in Figure 2, and were read out on line via a Franklin Strip Tape Printer.

C. THE HOLOGRAPHIC ARRANGEMENT

The holographic arrangement is illustrated in Figure 3 and shown in photographs included as Figures 4, 5, 6, and 7. Two large wooden tables were constructed and linked together with two-by-four beams under the tunnel to form the experimental platform. Thick rubber pads were attached to the table legs to dampen possible floor vibrations. The bulk of the platform provided sufficient stability and vibration damping for the experiment. The monochromatic light source used was a KORAD K-1 pulsed ruby laser operating at a wavelength of 6943 Angstroms, together with a Pockels cell Q-switching device. The resultant effective exposure time was approximately twenty nanoseconds, eliminating the problems due to possible model vibration during hologram exposure. To maintain the laser head and output etalon at a constant temperature of 27.0 degrees Centigrade, a LAUDA constant temperature circulator Model K2R was used.

The reference beam was directed under the wind tunnel by four front surface mirrors, and the beam size was manipulated by means of lenses (Figure 3). The scene beam was routed through the test section to intersect the reference beam on the holographic plate at an angle of approximately fifty degrees. A diffuse glass, mounted on

a precision X-Y translation table in the scene beam, was used to produce light field holograms. Alignment of the Q-switched laser and system optics was accomplished using a continuous wave, low-power helium-neon laser. Reference grids were mounted accurately on the outer surfaces of the tunnel windows using a surveyor's transit. Details of the model mounting and reference grids are shown in Figure 7. To enable hologram production during daylight hours, the entire tunnel room was blacked out using drop curtains and light shields.

D. THE WIND TUNNEL MODEL

The aerodynamic model used is shown in Figures 8, 9, and 10. The metal portions of the model were stainless steel. The greater part of the modified double wedge platform wing was constructed of optical lucite, as was the portion of the fuselage at the wing root. Detailed model dimensions are shown in Figure 11. The choice of aerodynamic design provided good flow characteristics and a relatively stable lambda-type shock wave on the wing; the largely transparent construction facilitated hologram production through 180 degrees of view.

The model was rotated about its sting mount in the wind tunnel from the zero degree position, wings level, to the 180 degree position, wings level inverted. Alignment for the desired rotation angle was accomplished by manually aligning prescribed lines on the sting mount collar with a scribed mark on the sting support.

III. ANALYTICAL EVALUATION OF THE DENSITY FIELD

A. THE BASIC EQUATION OF INTERFEROMETRY

Interferograms are created when two originally coherent light beams are superimposed and projected on a viewing screen. The two rays will reinforce or annul each other, depending on their relative phase difference at the screen. This phase difference is directly a function of the optical pathlengths traversed by the two waves. Consider a coherent beam which is split and then recombined on a viewing screen. A difference in optical pathlengths of the two component beams may be achieved by causing the beams to traverse through different media prior to recombination, with their physical pathlengths maintained equal. Each component beam will travel at a speed c_0/n where c_0 is the speed of light in a vacuum and n is the index of refraction of the medium traversed. The difference in optical pathlength is then given by

$$L = L (n_2 - n_1) = c_0 \Delta t \quad (1)$$

where Δt is the time difference of travel in the two media. If the optical pathlength is changed by an amount $N\lambda$, where λ is the wavelength of the light source and N is an integer, then the order of interference changes by an amount N . In other words, a shift of N fringes occurs in the interference pattern. The fringe shift may be expressed as

$$g = L/\lambda \quad (2)$$

where

g = fringe shift

λ = light source wavelength

L = change in optical pathlength

Substituting equation (1) into equation (2) yields

$$g = \frac{L}{\lambda} (n_2 - n_1) \quad (3)$$

The index of refraction for a given medium is a function of density. In the case of gases, since the speed of light is very nearly the same as in a vacuum, the index of refraction is well represented by the first two terms of a Taylor series expansion [10]:

$$n = 1 + \beta \frac{\rho}{\rho_s} \quad (4)$$

where β = dimensionless constant related to the Gladstone-Dale constant by $K = \beta/\rho_s$

ρ_s = reference density at 0° C, 760 mm. Hg.

The value of β for air at $\lambda = 5893$ Angstroms (deep red light) is 0.000292; variation with wavelength is very small.

For a fixed difference in the index of refraction between the two component beams the fringe shift relation becomes:

$$g = \beta \frac{L}{\lambda} \left(\frac{\rho_2 - \rho_\infty}{\rho_s} \right) \quad (5)$$

For variable density in the test section, the net change in optical pathlength is the integrated effect along the beam path, or

$$g = \frac{\beta}{\lambda \rho_s} \int_0^L (\rho - \rho_\infty) ds = Q \int_0^L f(x, y, z_c) ds \quad (6)$$

where:

$$Q = \frac{\beta \rho_{\infty}}{\lambda \rho_s} \quad (7)$$

$$f(x, y, z_c) = \frac{\rho(x, y, z_c)}{\rho_{\infty}} - 1 \quad (8)$$

z_c = plane of constant z

ds = incremental distance along beam path

Equation (6) is the basic integral equation for the unknown density.

With known fringe shift values from an interferogram, the equation is inverted to obtain the density along a beam path.

B. THE INTEGRAL INVERSION

The integral inversion procedure utilized in this investigation was first reported by C. D. Maldonado, et al [5, 6]. It was used subsequently by R. D. Matulka [3] and R. C. Jagota [7] to determine the density variation in an asymmetric free jet and about a cone at angle of attack in supersonic flow, respectively. The procedure involves the representation of the function $f(x, y, z_c)$ of Equation (6) in a complete set of orthogonal functions, with the expansion coefficients evaluated by use of the orthogonality condition between the functions f and g of Equation (6). The set of functions used is orthogonal over the entire (x, y) plane for every z_c and remains an orthogonal set under a rotation of the coordinate system. The coordinate system used for the inversion is shown in Figure 12. It consists of (a) a set of fixed coordinates x, y and (b) a set of moving coordinates

x', y' in which the fringe number function is defined and which rotates with respect to x, y as the viewing angle through the test section is varied.

In operator form, Equation (6) can be represented as

$$g(\xi, y', z_c) = \mathbb{T} f(x, y, z_c) \quad (9)$$

and f is evaluated by inversely transforming the equation to obtain

$$f(x, y, z_c) = \mathbb{T}^{-1} g(\xi, y', z_c) \quad (10)$$

This inversion is achieved by utilizing a pair of orthogonal polynomials $U_{m+2k}^{+m}(\alpha x, \alpha y)$ and $H_{m+2k}(\alpha y')$ which are related by the transform relationship

$$\mathbb{T} [U_{2k}(\alpha x, \alpha y) e^{-\alpha^2 x'^2}] = \frac{e^{\pm im\xi}}{[k!(m+k)!]^{1/2}} \cdot \frac{1}{2^{m+2k}} \cdot H_{m+2k}(\alpha y') \quad (11)$$

where $H_{m+2k}(\alpha y')$ are Hermite polynomials of order $m+2k$. The unknown function $f(x, y, z_c)$ is expanded in a set of functions U_{m+2k}^{+m} as

$$f(x, y, z_c) = \sum_{m=0}^{\infty} \sum_{k=0}^{\infty} \varepsilon_m \left\{ C_{m+2k}^{+m}(\alpha) U_{m+2k}^{+m}(\alpha x, \alpha y) + C_{m+2k}^{-m}(\alpha) U_{m+2k}^{-m}(\alpha x, \alpha y) \right\} e^{-(\alpha^2 x^2 + \alpha^2 y^2)} \quad (12)$$

where $\varepsilon_m = 1/2$ for $m = 0$, $\varepsilon_m = 1$ for $m = 1, 2, 3, \dots$, and

C_{m+2k}^{+m} are the unknown coefficients of the expansion. α is an arbitrary scale factor which may be considered the reciprocal of a non-dimensionalizing coefficient.

Utilizing the transform relation of Equation (11), Equation (6)

becomes

$$g(\xi, y', z_c) = \sum_{m=0}^{\infty} \sum_{k=0}^{\infty} \varepsilon_m [k!(m+k)! 2^{2(m+2k)}]^{1/2} \times [C_{m+2k}^{+m}(\alpha) e^{im\xi} + C_{m+2k}^{-m}(\alpha) e^{-im\xi}] H_{m+2k}(\alpha) e^{-\alpha^2 y'^2} \quad (13)$$

Equation (13) is subject to the orthogonality condition

$$\int_{-\pi}^{\pi} e^{\pm im\xi} e^{\mp in\xi} d\xi \int_{-\infty}^{+\infty} H_{m+2k}(\alpha y') H_{n+2l}(\alpha y') e^{-\alpha^2 y'^2} dy' = \frac{2\pi^{3/2}}{\alpha} [(m+2k)!(n+2l)! 2^{m+2k} 2^{n+2l} \delta_{mn} \delta_{(m+2k)(n+2l)}] \quad (14)$$

where δ is the Kronecker delta function. The solution of Equation

(14) applied to Equation (13) yields the series coefficients

$$C_{m+2k}^{\pm m}(\alpha) = \frac{\alpha}{2\pi^{3/2}} \left[\frac{k!(m+k)!}{(m+2k)!} \right] \int_{-\pi}^{\pi} \int_{-\infty}^{\infty} g(\xi, y', z_c) H_{m+2k}(\alpha y') e^{\mp im\xi} dy' d\xi \quad (15)$$

With the substitution of the coefficients of Equation (15), Equation (7)

becomes

$$f(x, y, z_c) = \frac{\alpha}{\pi^{3/2}} \sum_{m=0}^{\infty} \sum_{k=0}^{\infty} \varepsilon_m \frac{[k!(m+k)!]^{1/2}}{(m+2k)!} e^{-(\alpha^2 x^2 + \alpha^2 y^2)} \times \text{Re} \left[\int_{-\pi}^{\pi} \int_{-\infty}^{\infty} g(\xi, y', z_c) e^{-im\xi} H_{m+2k}(\alpha y') dy' d\xi \times U_{m+2k}^m(\alpha x, \alpha y) \right] \quad (16)$$

The functions $U_{m+2k}^{\pm m}$ are defined as

$$U_{m+2k}^{\pm m}(\alpha x, \alpha y) = (-1)^k \alpha \left[\frac{k!(\alpha^2 x^2 + \alpha^2 y^2)^m}{\pi(m+k)!} \right]^{1/2} e^{\pm im\phi} L_k^m(\alpha^2 x^2 + \alpha^2 y^2) \quad (17)$$

where $\phi = \tan^{-1}(y/x) - (\pi/2)$ and L_k^m are the associated Laguerre polynomials

$$\left[L_k^m(\alpha^2 x^2 + \alpha^2 y^2) \right]^S = \sum_{s=0}^{\infty} \frac{(m+k)!}{(k-s)!(m+s)! s!} \left[(-1)^s (\alpha^2 x^2 + \alpha^2 y^2) \right]^S \quad (18)$$

Insertion of Equation (17) into Equation (16) yields

$$f(x, y, z_c) = \left(\frac{\alpha}{\pi} \right)^2 \sum_{m=0}^{\infty} \sum_{k=0}^{\infty} \epsilon_m \frac{(-1)^k k!}{(m+2k)!} (\alpha^2 x^2 + \alpha^2 y^2)^{m/2} \left[L_k^m(\alpha^2 x^2 + \alpha^2 y^2) \right]^S \quad (19)$$

$$\times \left[B_{m+2k}^m(\alpha) \cos(m\phi) + D_{m+2k}^m(\alpha) \sin(m\phi) \right] e^{-(\alpha^2 x^2 + \alpha^2 y^2)}$$

where

$$B_{m+2k}^m(\alpha) = \int_{-\pi}^{\pi} \int_{-\infty}^{\infty} g(\xi, y', z_c) \cos(m\xi) H_{m+2k}(\alpha y') dy' d\xi \quad (20)$$

$$D_{m+2k}^m(\alpha) = \int_{-\pi}^{\pi} \int_{-\infty}^{\infty} g(\xi, y', z_c) \sin(m\xi) H_{m+2k}(\alpha y') dy' d\xi \quad (21)$$

Equations (19), (20), and (21) are the basic equations used to obtain the density distribution from the experimentally determined fringe variations in a completely asymmetric flow field.

C. THE NUMERICAL PROCEDURE

Because the function $g(\xi, y', z_c)$ is an experimentally determined quantity the unknown coefficients $B_{m+2k}^m(\alpha)$ and $D_{m+2k}^m(\alpha)$ in the series representation of $f(x, y, z_c)$ in Equation (19) cannot be calculated analytically. It is therefore necessary to evaluate the double integrals of Equations (20) and (21) numerically. This is accomplished by noting in Figure 12 and Equation (8) that there is an area outside which the density is invariant, namely outside the test

section where the known density is ρ_{∞} . Since the function $f(x, y, z_c) = 0$ outside this circular domain, the limits of integration of $+\infty$ and $-\infty$ in Equations (20) and (21) can be replaced by finite values. The fringe distribution is then approximated by small increments over the test domain, resulting in the representation of the B and D coefficients as double series:

$$B_{m+2k}^m(\alpha) = \sum_{i=1}^{I-1} \sum_{j=0}^{J-1} g(\xi_j + \Delta \xi_j, x_i + \Delta x_i) \int_{\xi_j}^{\xi_{j+1}} \cos(m\xi) d\xi \int_{x_i}^{x_{i+1}} H_{m+2k}(\alpha x) dx \quad (22)$$

and

$$D_{m+2k}^m(\alpha) = \sum_{i=1}^{I-1} \sum_{j=0}^{J-1} g(\xi_j + \Delta \xi_j, x_i + \Delta x_i) \int_{\xi_j}^{\xi_{j+1}} \sin(m\xi) d\xi \int_{x_i}^{x_{i+1}} H_{m+2k}(\alpha x) dx \quad (23)$$

Using the derivative formula for Hermite polynomials, Equations (22) and (23) can be manipulated to yield workable series expressions:

$$B_{m+2k}^m(\alpha) = \left[\frac{1}{2\alpha m} \cdot \frac{1}{(m+2k+1)} \right] \sum_{i=0}^{I-1} \sum_{j=0}^{J-1} g(\xi_j + \Delta \xi_j, x_i + \Delta x_i) \times \left[\sin(m\xi_{j+1}) - \sin(m\xi_j) \right] \left[H_{m+2k+1}(\alpha x_{i+1}) - H_{m+2k+1}(\alpha x_i) \right] \quad (24)$$

$$D_{m+2k}^m(\alpha) = - \left[\frac{1}{2\alpha m} \cdot \frac{1}{(m+2k+1)} \right] \sum_{i=0}^{I-1} \sum_{j=0}^{J-1} g(\xi_j + \Delta \xi_j, x_i + \Delta x_i) \times \left[\cos(m\xi_{j+1}) - \cos(m\xi_j) \right] \left[H_{m+2k+1}(\alpha x_{i+1}) - H_{m+2k+1}(\alpha x_i) \right] \quad (25)$$

Since it is impossible to sum over an infinite number of terms,

Equation (19) is necessarily expressed as the sum of a finite series:

$$f(x, y, z_c) = \left(\frac{\alpha}{\pi}\right)^2 \sum_{k=0}^K \sum_{m=0}^M \varepsilon_m (-1)^k \left[\frac{k!}{(m+2k)!} \right] (\alpha^2 x^2 + \alpha^2 y^2) \quad (26)$$

$$\times \int_k^m (\alpha^2 x^2 + \alpha^2 y^2) \left[B_{m+2k}^m(\alpha) \cos(m\phi) + D_{m+2k}^m(\alpha) \sin(m\phi) \right] e^{-(\alpha^2 x^2 + \alpha^2 y^2)}$$

It has been demonstrated that judicious selection of the parameters

$\Delta \xi$, Δx , K , M , and α yields density distributions with very good accuracy [3, 6].

IV. EXPERIMENTAL PROCEDURE

A. LABORATORY TECHNIQUES

In order to visualize the general flow patterns and localize shock or expansion waves about the model a series of standard Schlieren photographs were taken at varying flow Mach numbers. Pictures were produced for roll angles of 0° , 45° , and 90° at Mach numbers from 0.925 to 1.10. A representative series of Schlieren photographs is shown in Figures 13, 14, and 15. Analysis of the Schlieren photographs dictated a flow Mach number of 0.937 for the experimental study; this Mach number yielded uniform upstream flow conditions and located the lambda-type shock wave ideally near the center of the lucite section of the model wing.

The coherence length of the pulsed ruby laser was approximately ten centimeters for the output power utilized. This reduced the normally critical requirement for pathlength equality in the scene and reference beams that must be fulfilled in the classical Mach-Zehnder interferometric approach. Consequently, a length of string proved to be a sufficiently accurate measuring device to maintain the two beam pathlengths within the coherence length of the laser, a requirement for interferogram production. To compensate for the fact that the scene beam traversed approximately five inches of glass tunnel walls and lucite grids which the reference beam did not, the scene beam

was adjusted to be some 2.5 inches shorter than the reference beam. Reference beam pathlength was maintained at approximately 138 inches throughout the experiment.

Holograms produced using the basic holographic setup shown in Figure 3 exhibited clear, well-defined fringe patterns in nearly every instance. In deciding on the final arrangement, several techniques were tested to improve upon fringe pattern definition. Horizontal, vertical and diagonal translations of the diffuser plate in the scene beam were considered, varying from 0.001 inches to 0.005 inches. A vertical translation of 0.003 inches yielded clear horizontal fringes that were quite easily analyzed. The transverse mode selector aperture was varied from 1.0 mm. to 3.0 mm. in increments of 0.5 mm; best lighting of the model resulted with use of a 2.5 mm. aperture. The temperature of the cooling water circulated through the laser head and etalon was varied from 26.0°C. to 28.0°C. in increments of 0.2°C., with 27.0°C. providing the best fringe definition. Finally, a variety of beam splitters and lenses were tested prior to final selection of the best available optics arrangement for the experiment. A 2:1 reference to scene beam strength ratio was found to yield very good holograms.

Two double exposure holograms were taken for each model viewing angle. The first, labeled a double-static exposure, consisted of two exposures in a no-flow condition with a 0.003 inch vertical translation of the diffuser plate between exposures. The fringe

patterns in this hologram provided a measure of the effect of tunnel wall glass, grid plexiglass and model lucite on the subsequent double exposure. The second, or static-dynamic, exposure consisted of a no-flow exposure, a 0.003 inch diffuser translation, and finally an exposure at flow Mach number 0.937. The fringe deviations recorded in the region behind the lucite portion of the model by the double-static hologram were measured and subtracted from the fringe shifts measured in the corresponding static-dynamic hologram.

Holograms were produced on Agfa-Gaevert 8E75 holographic plates, 4 inches by 5 inches in size. As recommended by Collier, et al. [11] the development process included:

1. Five minutes in Kodak D-19 developer
2. Thirty seconds in a flowing water bath
3. Five minutes in standard rapid fixer
4. Thirty seconds in a flowing water bath
5. One and one-half minutes in Kodak Hypo Clearing agent
6. Five minutes in a flowing water bath
7. Five minutes in methanol bath
8. One minute in a flowing water bath
9. Drying

B. PHOTOGRAPHIC TECHNIQUES

Normal reconstructions of the original scene were made by illuminating the holograms with a seven milliwatt continuous wave

helium-neon laser beam at a wavelength of 6328 Angstroms. There was some slight distortion in the reconstructed scene because of the difference in wavelengths of the original scene beam and the reconstruction beam; however, the effect was almost totally negated by shrinkage of the holographic plate emulsion during the development process.

A common technique of image reconstruction was employed, utilizing a conjugate reference beam to reilluminate the exposed hologram, as shown in Figure 16. The resulting scene was recorded on photographic film. Individual points on the photograph are produced by a series of non-parallel rays originating from various source points on the diffuser plate in the scene beam. Using a reilluminating beam of small diameter has the effect of a small aperture at the focal point of the imaging lens, filtering out all but a set of nearly parallel rays, as shown in Figure 17. The real images produced in this manner have a large depth of field, permitting simultaneous projection on the film of front and rear grids, the model and the fringe patterns. The imaging lens was focused as near to the plane of the fringes as possible, producing photographs at various planes of constant z_c .

C. DATA REDUCTION

Photographic interferograms were obtained using the arrangement shown in Figure 16, with the camera viewing screen in the position of the real image. The line of sight in the plane desired was achieved by translating and elevating the hologram until common points on the

front and rear grids were aligned. The Graphic View camera, with the wide angle lens aperture set fully open at $f7.8$, was adjusted to yield the best focus on the fringe plane. Exposure times of from $1/5$ to $3/4$ seconds were used to produce workable interferogram photographs on Polaroid Type 55 P/N film.

Fringe shift analysis was accomplished on 8 inch by 10 inch enlargements of the 4 inch by 5 inch film used to record the images. The enlargements were placed face down on a light table, and the fringes, model contours and shock wave were traced on the back surface at the desired cross-sectional plane. Fringe shift values were recorded by measuring the distance between (1) the intersection of the hypothetically undeviated fringe and the cross-sectional plane and (2) the intersection of the deviated fringe with the same plane. Fringe shifts so obtained were corroborated by placing the negative in a photographic enlarger and tracing the lines of interest directly onto graph paper.

The known model fuselage diameter of 1.1 inches was compared with that measured in each individual photograph to yield magnification factors relating projected dimensions to actual dimensions. These factors were then used as corrections to the fringe shift measurements. A grid reference point located on the cross-sectional plane of interest served as the datum for all fringe shift measurements. A base point was located at the intersection of the cross-sectional plane of interest and the body longitudinal axis. Fringe shift measurements were

corrected using this base point as the new datum so that the inversion circle was properly centered on the body axis. The radius of the inversion circle was selected to be nearly equal to the semi-span of the wing. Fringe shift measurements were converted to fringe numbers using the average free stream spacing, while fringe locations were nondimensionalized using the inversion circle diameter. From the data so obtained, the radial variation of fringe number was plotted for each viewing angle. Fringe numbers at 201 equidistant points, as required for input into Mode 3 of the computer program, HOLOFER, were recorded from the resulting curves. Further details concerning this inversion computer program are outlined in Appendix B. A typical reduction of an interferogram to obtain the radial variation of fringe number at a particular cross-sectional plane is detailed in Appendix A.

V. EXPERIMENTAL RESULTS AND DISCUSSION

A pair of double exposure holograms was taken of the model at $11\frac{1}{4}$ degree intervals through a 180 degree field of view. Experimental data from the wind tunnel runs are recorded in Table I. Initial resulting density patterns indicated relatively smooth contours across adjacent intervals; the interval was therefore doubled to $22\frac{1}{2}$ degrees to simplify and speed the analysis. Fringe data were first inserted into the inversion computer program along nine lines of sight in the 180 degree field of view. A numerical comparison of views from 0 degrees to 90 degrees and from 90 degrees to 180 degrees verified to within 0.20 percent the assumption of a single plane of symmetry in the experiment. The fringe data input was then reduced to five lines of sight in a 90 degree field of view, as shown in Figure 18. The resulting output was an inverted density field along nine radial lines spanning a 180 degree field of view, with a mirror image on the opposite side of the plane of symmetry, as shown in Figure 19.

The static-dynamic photographic interferogram for the 0 degree view, along with its corresponding double-static interferogram, is shown in Figure 20. The diffraction effects caused by the presence of the lucite portions of the model are clearly visible in the double-static exposure, where the free stream fringe lines are bent and displaced toward the model axis. This displacement was measured

and subtracted from subsequent measurements made on the static-dynamic exposure, as outlined in Section IV.A. Photographic interferograms of the remainder of the static-dynamic exposures are shown in Figures 21 through 24. Clearly visible and reduceable in nearly all views were (1) the region of uniform subsonic flow, commonly called the free stream condition, (2) the transition from local subsonic to local supersonic flow, and (3) the lambda-type shock wave on the model wing. These characteristics are shown in schematic representation in Figure 25.

Contour plots of the density function, as expressed in Equation (8) of Section III.A., for successive z-planes of analysis are shown in Figures 26 and 27. The cross-sectional plane of analysis for the plot of Figure 26 was located at 186.75 mm. from the model nose along the longitudinal axis. For Figure 27, the plane of interest was 195.25 mm. from the model nose. It is apparent from both contour plots that the model went to a very small angle of attack under the loading forces produced during tunnel operation; this is evidenced by the compression of the contour lines above the model and the corresponding expansion of the contours below the model. Measurements made from photographic interferograms confirm this angle of attack to be, at most, 0.05 degrees. The closed contours above and adjacent to the wing surface in both figures may very well be the result of a vortex originating at the intersection of the wing leading edge and the

fuselage on either side of the model and traveling aft and outward over the wing surface.

A comprehensive quantitative analysis of the shock wave structure was not undertaken, with the exception of estimating the strength of the shock by comparison of fringe line separation immediately ahead of and aft of the shock wave. Fringe line separation measurements on either side of the shock wave were converted first to density information and thence to pressure information, disregarding compressibility effects. An approximate strength value of 0.207 was computed using the accepted definition of $(p_2 - p_1)/p_1$. This corresponds to a local Mach number of 1.08 in the supersonic region just ahead of the shock wave. Qualitative shock wave analysis resulted in the construction of a three-dimensional structural representation as shown in Figure 28, using input information from several interferogram viewing angles. While location of the leading and trailing edges of the lambda-type shock wave was very accurate, interior structure was largely indefinable due to "smearing" and blurring of the fringes transiting the shock wave itself.

As a preliminary step to possible future studies in this field, photographic interferograms were made from holograms produced with the aerodynamic model set at small angles of attack. Orientations included angles of attack of five and ten degrees, with roll angles varying from zero to ninety degrees. Although the holograms themselves were of very good quality, the photographic reproductions

were relatively poor due to the fact that an inferior photographic arrangement had to be used. They were therefore omitted from this report. It was inferred from the holograms, however, that a complete study at angle of attack using the basic procedures followed in the present study would be both totally feasible and rewardingly fruitful.

The original character of the experimental data prevented comparison with published results. Qualitative studies of transonic phenomena are widely available, and the general characteristics of the resulting density field and shock wave structure serve to bear out the schematics based on theoretical and mathematical models. Moreover, the self-testing mode of the inversion computer program, HOLOFER, verified the consistency and reproducibility of the resulting density distributions to within 2.0 percent through proper choice of the input parameters, primarily the slope-matching parameter α . The errors encountered in the final results are due primarily to errors in the fringe data input to the inversion program. The intrinsic presence of laser speckle, the extended pathlengths of the scene and reference beams and the unavoidable beam scattering and diffraction within the lucite model sections, created difficulty in obtaining precisely the slope of the fringe lines behind the lucite sections. Fringe spacing measurements in the free stream flow were conservatively judged accurate to within 0.5 mm. This assumption was quite reasonable since all measurements were effected with a scale graduated at half millimeter intervals. This figure of 0.5 mm.,

combined with the mean free stream fringe spacing of 5.197 mm. for all interferograms, indicated measurement accuracy to within one tenth (0.1) of a fringe. The mean systematic error of the free stream spacing in each view was computed to be a maximum of 3.9 percent. Associated with this systematic error was a random error of 2.1 percent in the measurement of fringe shifts in each view to a conservative accuracy of 0.5 mm. The resulting error for each viewing angle was therefore a maximum of 6.0 percent, found by merely adding the two types of error for each view. The minimum error limit was found by considering the error resulting from the reproduction of the same interferogram view five separate times. Statistically, with 6.0 percent error in each view, the composite error for the repeated view is 2.6 percent. As five different views, or lines of sight, were used for the data between zero and ninety degrees, the final total error in the analysis was therefore in the interval between 2.6 percent and 6.0 percent. To insure contour clarity and guard against overlapping, the maximum error figure of 6.0 percent was used in construction of the plots shown in Figures 26 and 27. In general, the rather large fringe shifts led to a very low mean fringe sensitivity value of 0.1259. This coefficient indicated a resulting density function (Equation (8)) inaccuracy of less than 1.5 percent for a fringe shift measurement misreading of 0.5 mm.

Physical limitations of beam diameter and hologram plate area dictated the choice of an inversion circle diameter somewhat smaller

than the full data circle normally used in the finite fringe procedure. This, in effect, introduced an inconsistency in reference density into the analysis since the density on the selected circle and immediately outside it was not the calculated ρ_{∞} ; the density function was therefore not zero outside the actual inversion region. To alleviate this inconsistency, a new, updated reference density was computed for each cross-sectional plane of analysis by averaging the density values on the selected circle from the first inversion process. The actual reference densities used were $\rho = 1.777$ mg/cc for the 186.75 mm. plane and $\rho = 1.642$ mg/cc for the 195.25 mm. plane. This procedure was justified since all density values between the selected circle and the full data circle were constant to within approximately fifteen percent. The updated reference densities were then used to produce the final output density field. The net effect was a scaled, uniform shift toward density function values slightly lower than those computed on the basis of the original reference density.

VI. CONCLUSIONS

The finite fringe procedure for the production of holographic interferograms has been applied successfully to the determination of the three-dimensional density distribution of the flow near the wing-fuselage junction of a partially transparent aerodynamic model in the transonic regime. Density contours accurate to within six percent enabled a thorough analysis of the flow field to be conducted, highlighting flow characteristics and the presence of the shock wave. Subsequent studies of similar models at angle of attack have been shown to be entirely feasible. Procedures used in the experiment also exhibit promise for the direct analysis of duct and inlet flows as well as comprehensive study of shock wave structure.

The inversion computer program, HOLOFER, was found to be adequate in handling a general asymmetric flow field analysis. However, it was considered quite cumbersome and difficult to modify for various experimental situations. Subsequent analysts will find the procedures advocated by Sweeney and Vest [12] for the recording and analyzing of interferograms of considerable interest. In addition, the efforts of Van Houton [13], who utilized the method proposed by Junginger and van Haeringen [14], may prove valuable in reducing computer time significantly.

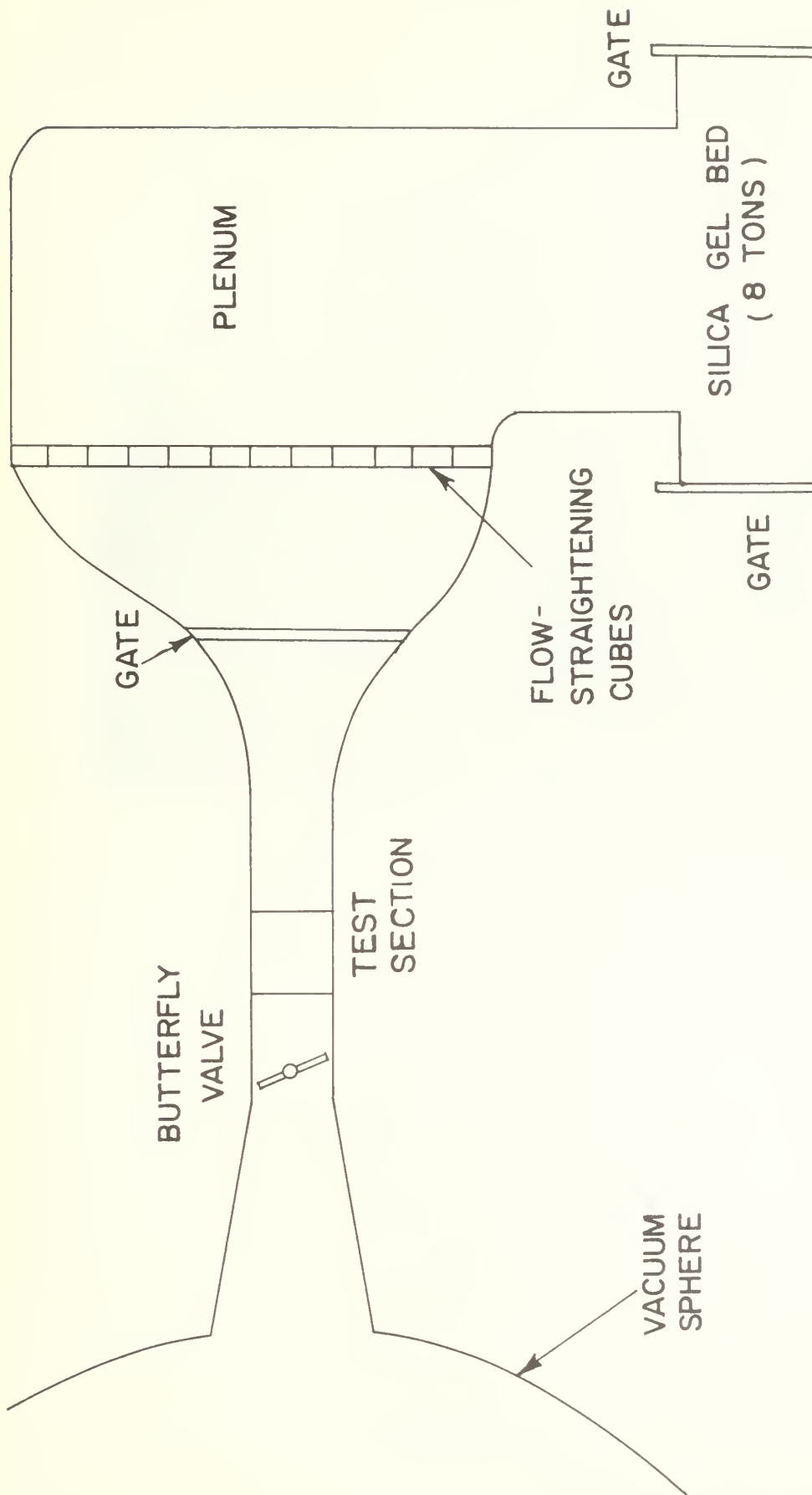


FIGURE 1. FUNCTIONAL SCHEMATIC OF NSRDC WIND TUNNEL

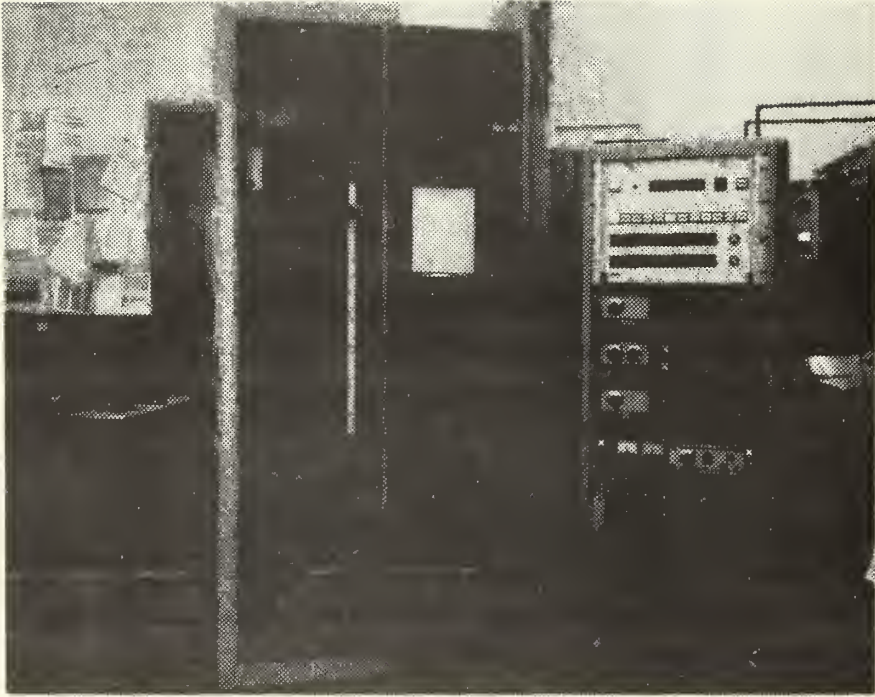


FIGURE 2. BECKMAN 210 DATA RECORDING SYSTEM

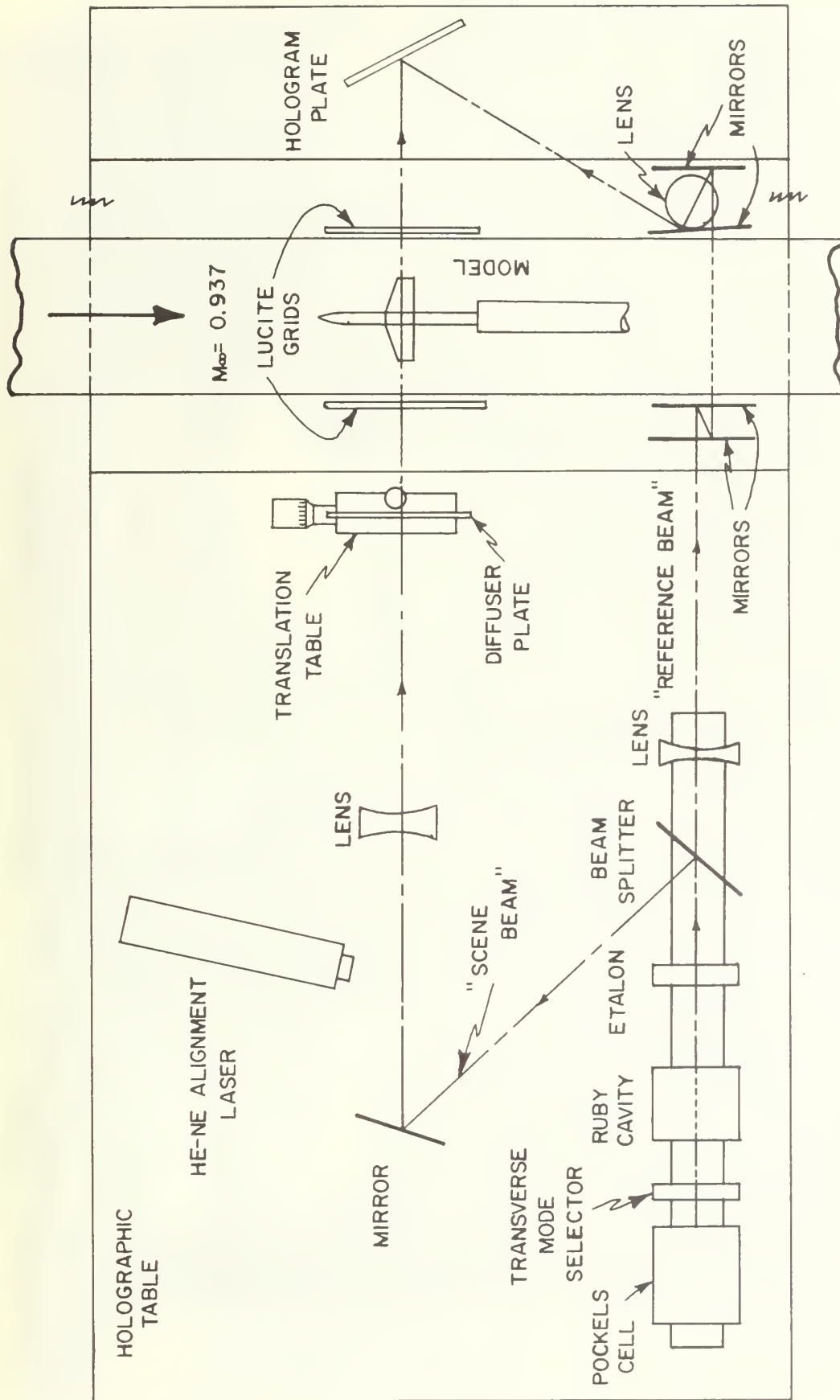


FIGURE 3. SCHEMATIC DRAWING OF THE HOLOGRAPHIC ARRANGEMENT

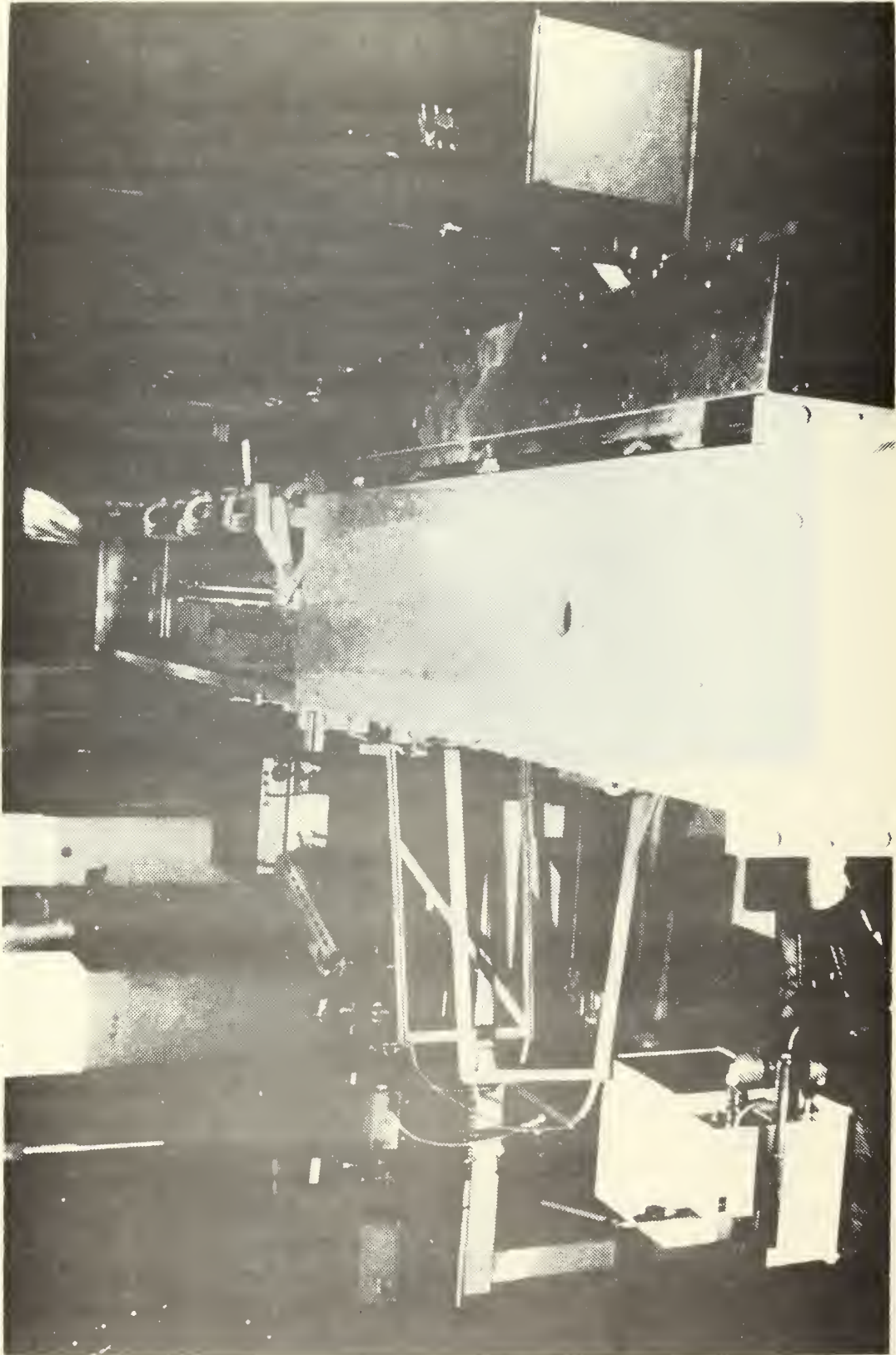


FIGURE 4. OVERHEAD VIEW OF TUNNEL AND ENTIRE HOLOGRAPHIC SYSTEM

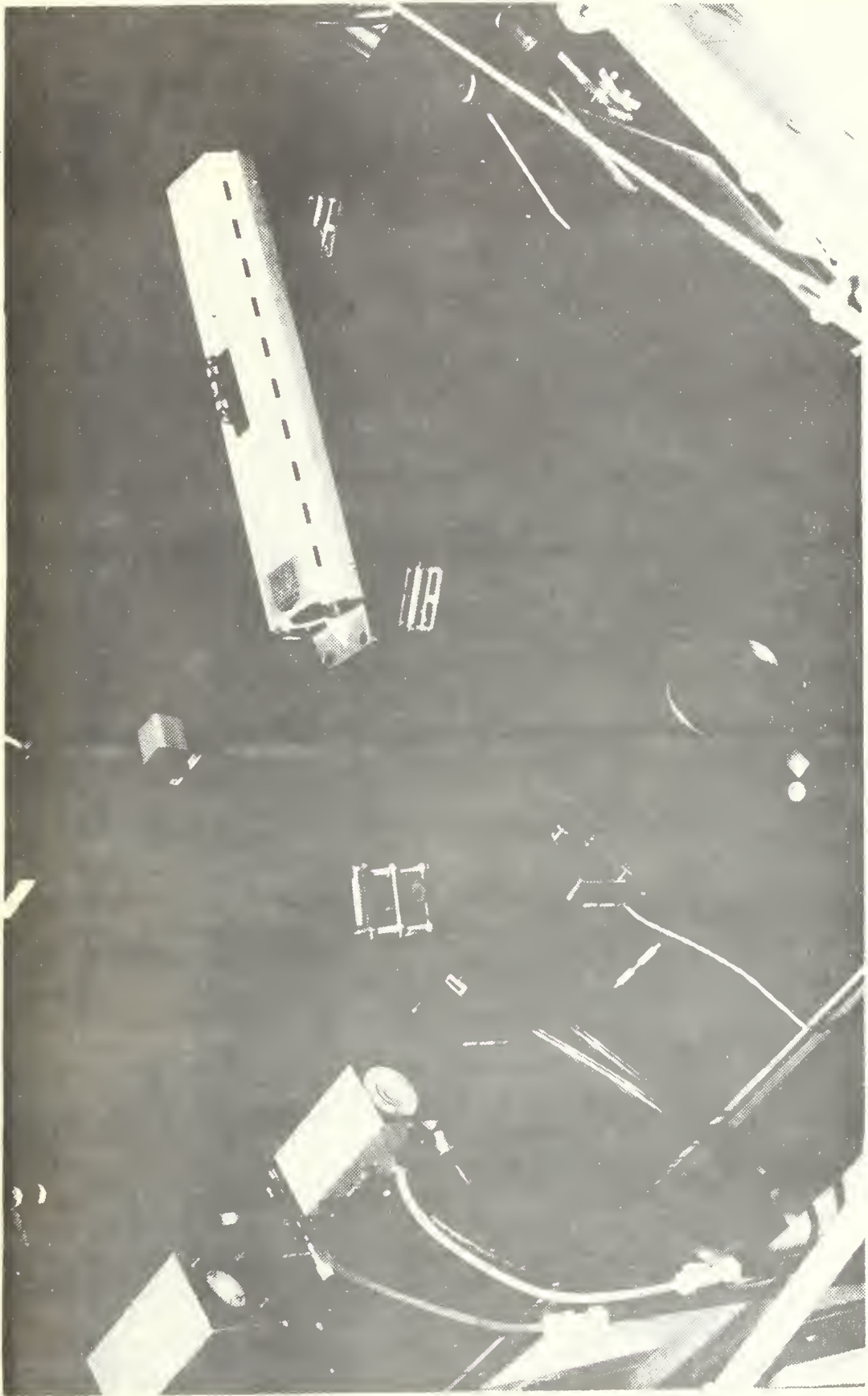


FIGURE 5. OBLIQUE VIEW OF HOLOGRAPHIC TABLE

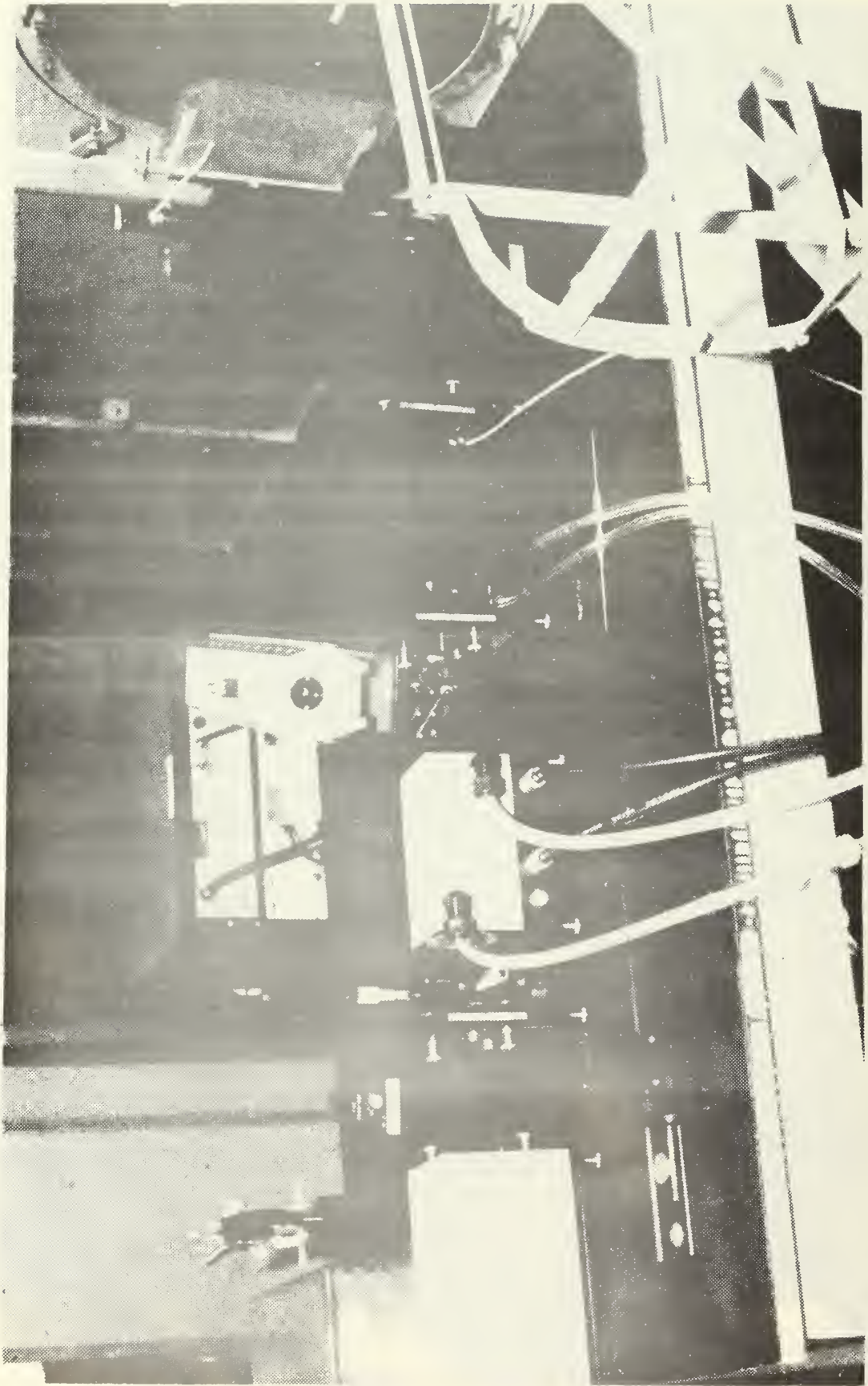


FIGURE 6. OBLIQUE VIEW OF HOLOGRAPHIC TABLE

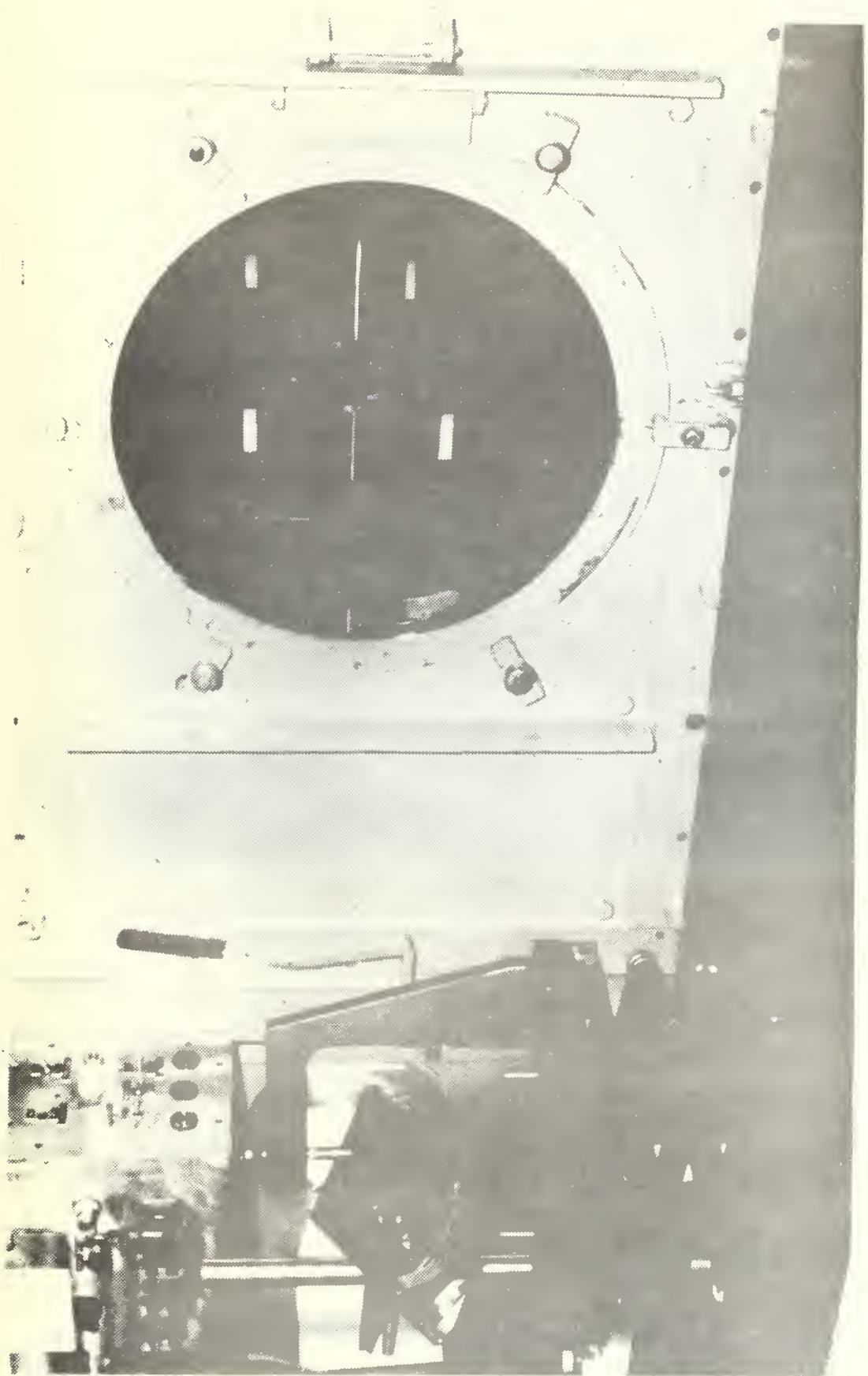


FIGURE 7. DETAIL OF MODEL MOUNTING AND REFERENCE GRIDS



FIGURE 8. AERODYNAMIC TEST MODEL; 0 DEG. ROLL ANGLE

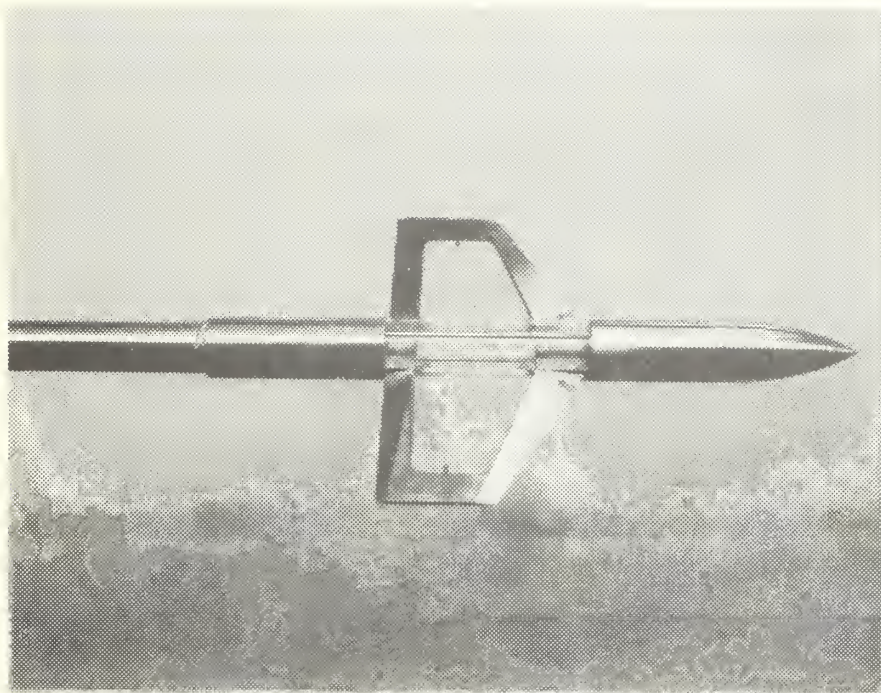


FIGURE 9. AERODYNAMIC TEST MODEL; 45 DEG. ROLL ANGLE

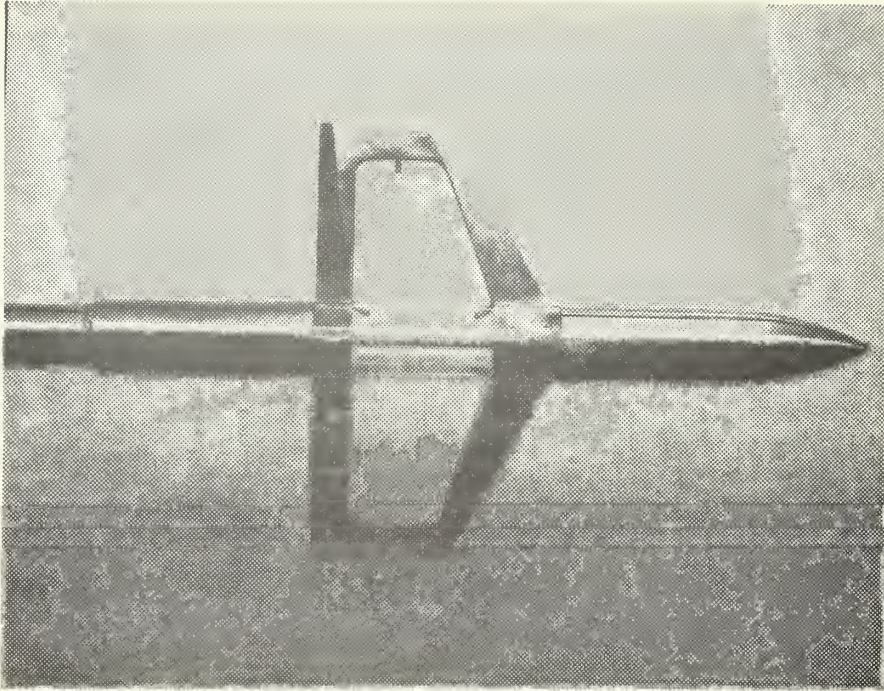
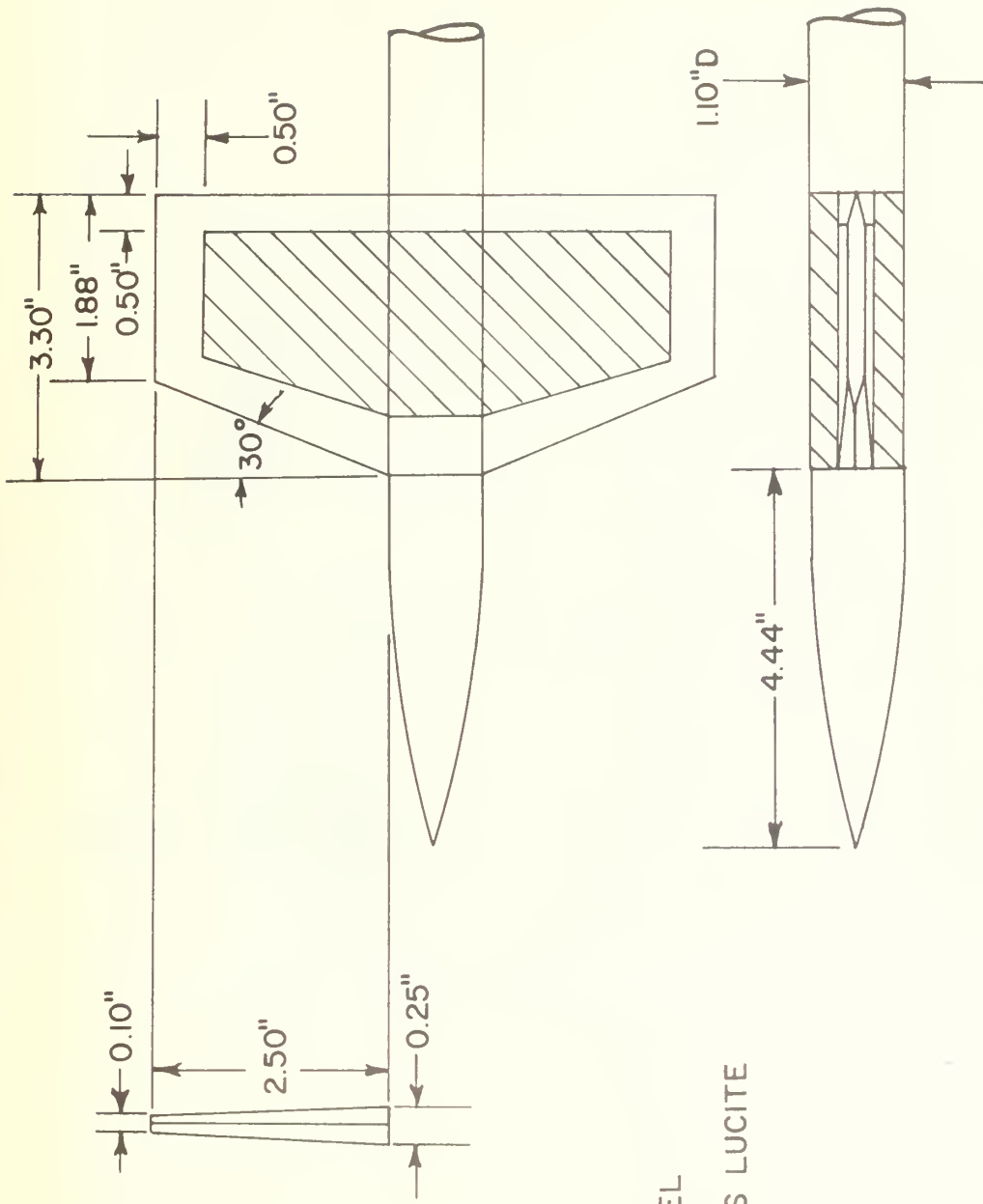


FIGURE 10. AERODYNAMIC TEST MODEL; 90 DEG. ROLL ANGLE



NO SCALE

STAINLESS STEEL

HATCHED AREAS LUCITE

FIGURE 11. DETAILS OF THE AERODYNAMIC TEST MODEL

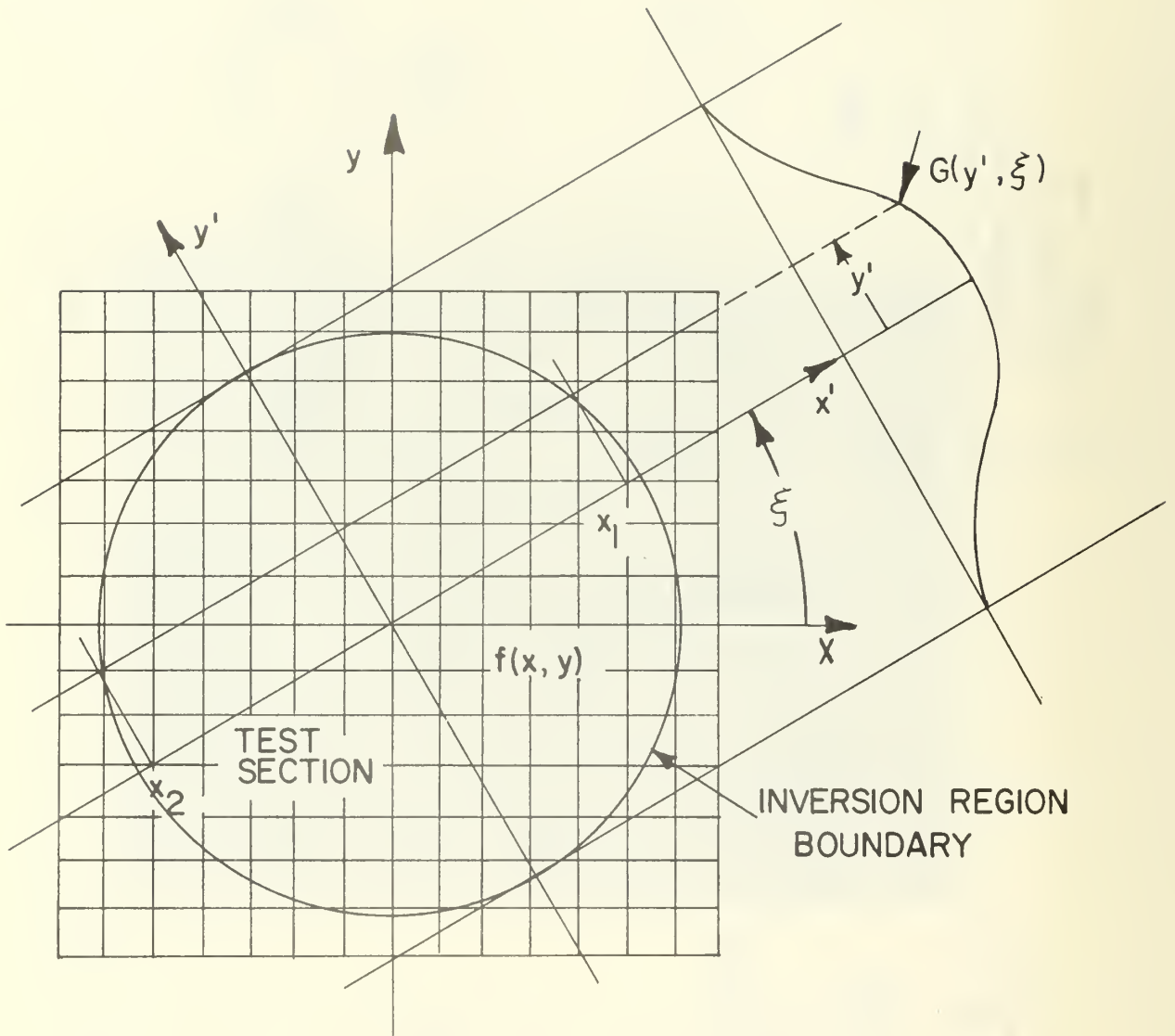


FIGURE 12. CO-ORDINATE SYSTEM USED FOR INVERSION OF FRINGE NUMBER TO DENSITY



FIGURE 13. SCHLIEREN PHOTOGRAPH; 0 DEG. ROLL ANGLE,
0.967 MACH NUMBER

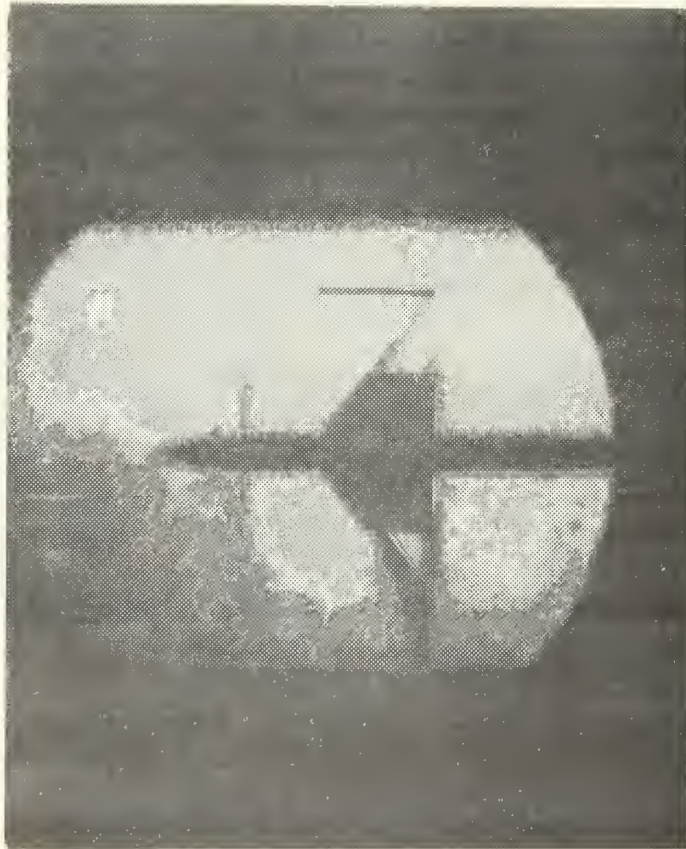


FIGURE 14. SCHLIEREN PHOTOGRAPH; 45 DEG. ROLL ANGLE,
0.967 MACH NUMBER



FIGURE 15. SCHLIEREN PHOTOGRAPH; 90 DEG. ROLL ANGLE,
0.967 MACH NUMBER

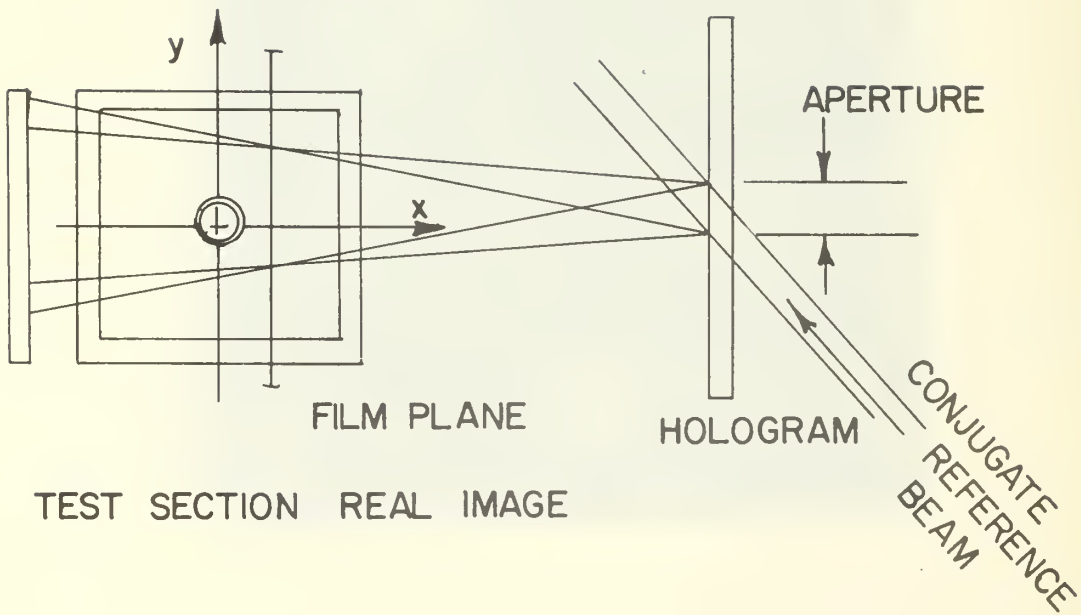


FIGURE 16. LENSLESS PHOTOGRAPHIC TECHNIQUE USING A CONJUGATE REFERENCE BEAM OF SMALL DIAMETER

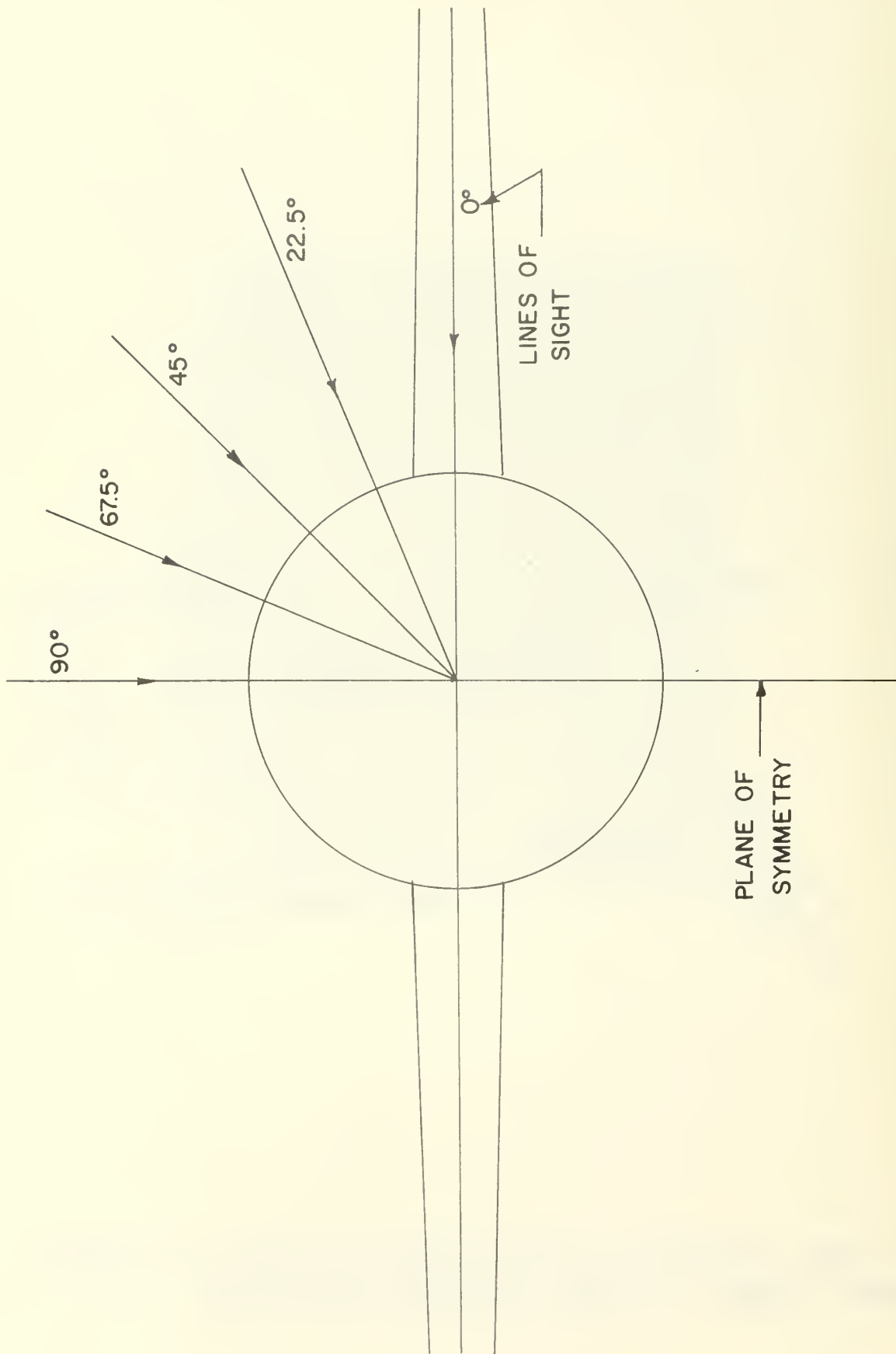


FIGURE 18. FRINGE DATA INPUT INFORMATION

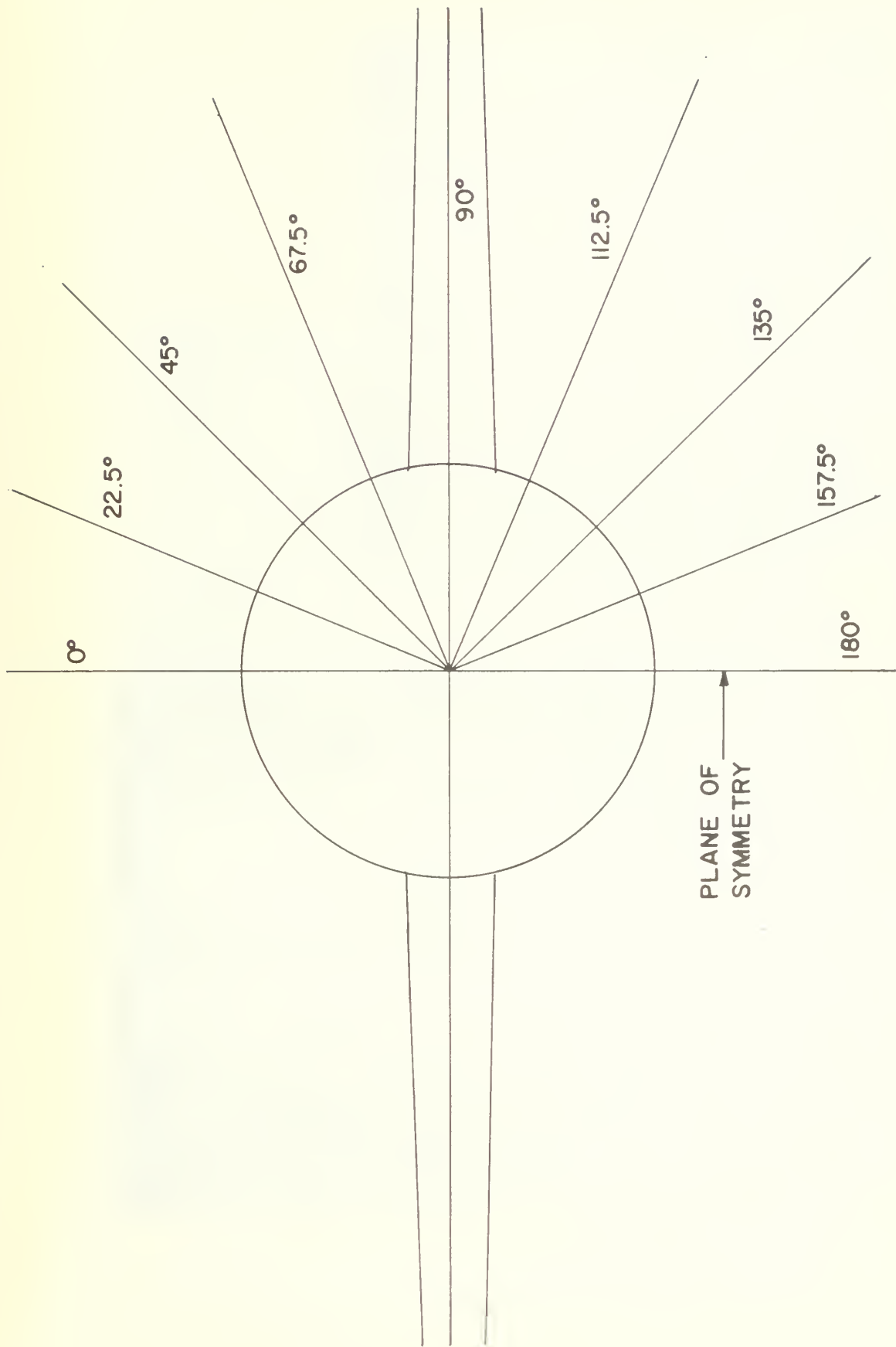
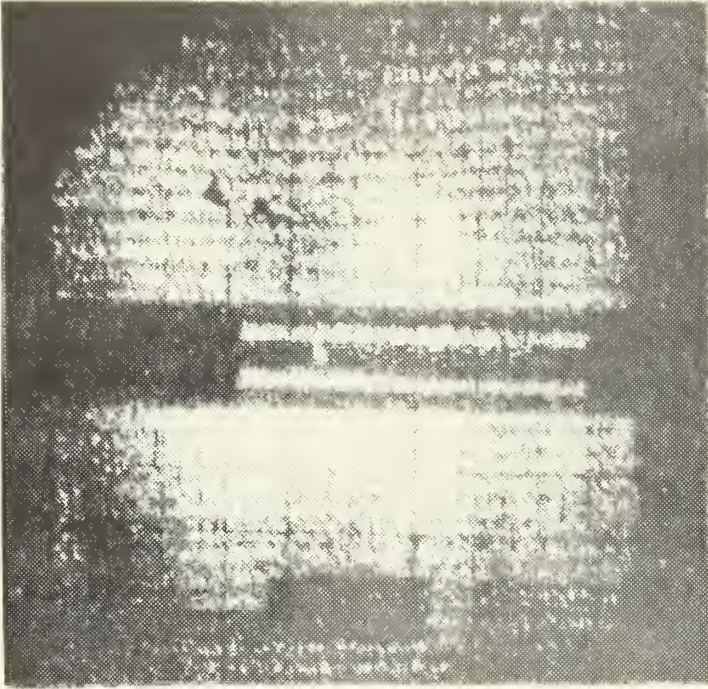
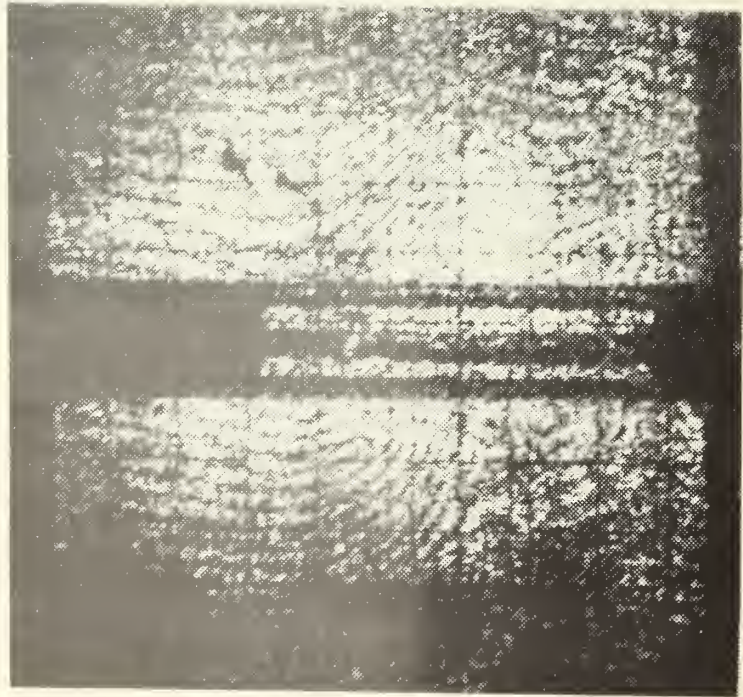


FIGURE 19. DENSITY DATA OUTPUT INFORMATION

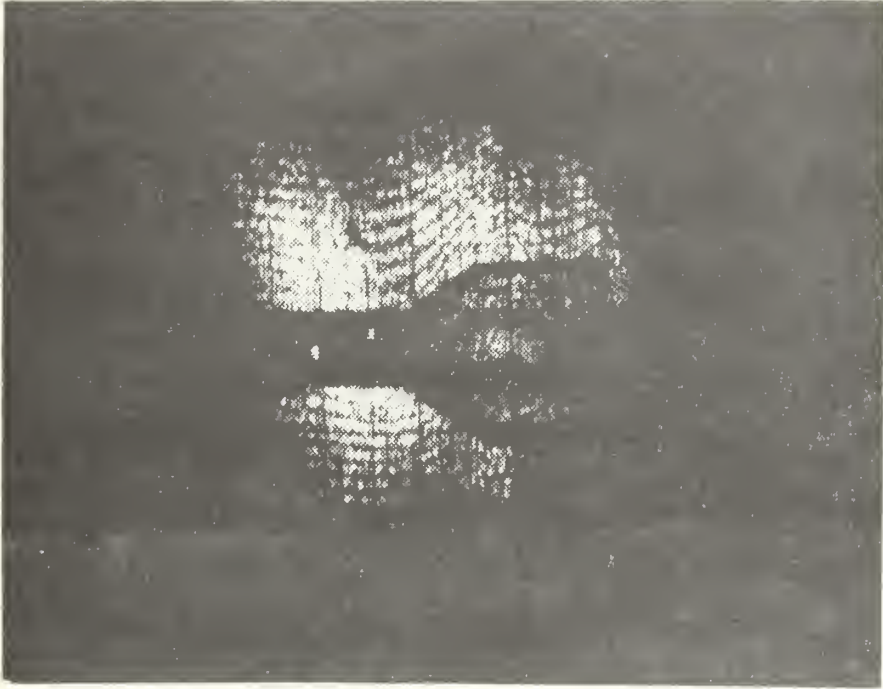


DOUBLE-STATIC
INTERFEROGRAM



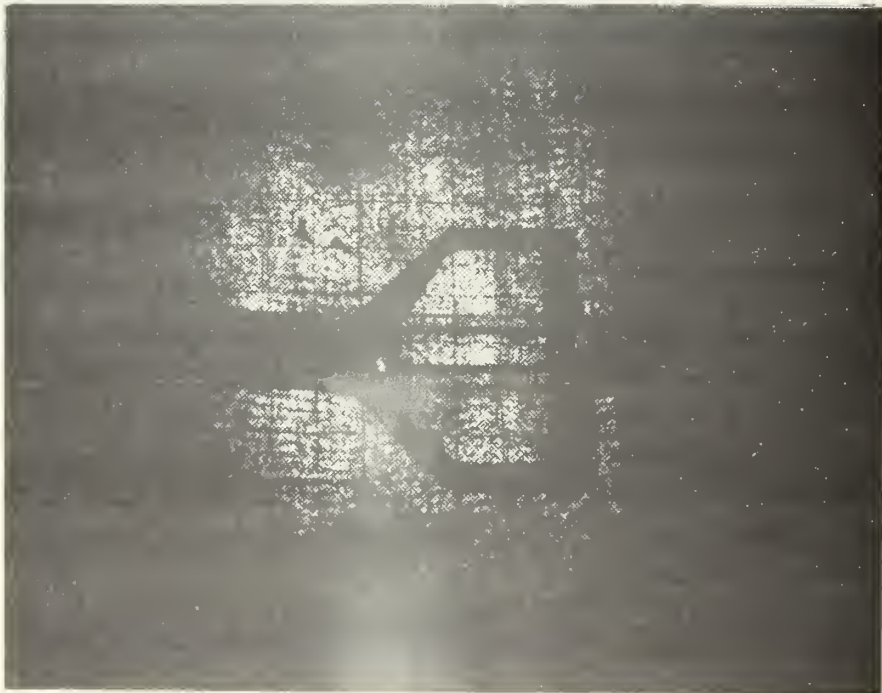
STATIC-DYNAMIC
INTERFEROGRAM

FIGURE 20. PHOTOGRAPHIC INTERFEROGRAMS
FOR 0 DEG. VIEWING ANGLE



21

FIGURE 21. STATIC-DYNAMIC INTERFEROGRAM
FOR $22\frac{1}{2}$ DEG. VIEWING ANGLE



5

FIGURE 22. STATIC-DYNAMIC INTERFEROGRAM
FOR 45 DEG. VIEWING ANGLE

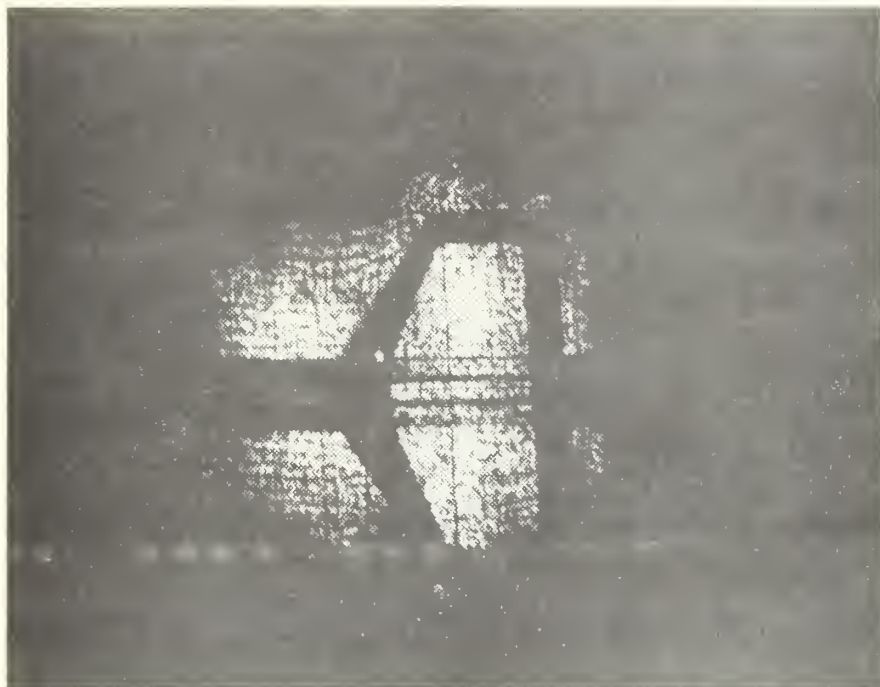
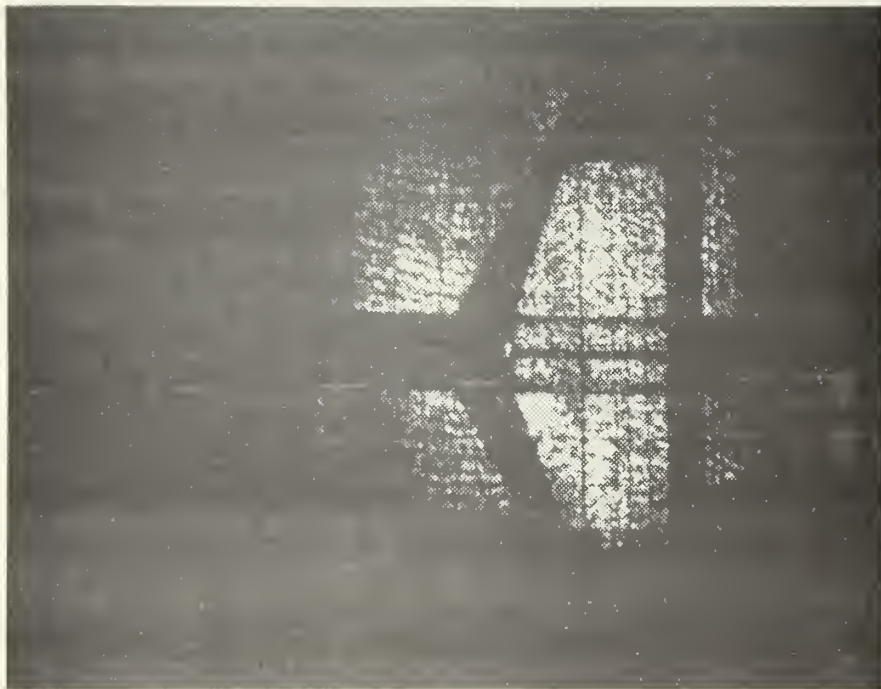


FIGURE 23. STATIC-DYNAMIC INTERFEROGRAM
FOR $67\frac{1}{2}$ DEG. VIEWING ANGLE



c

FIGURE 24. STATIC-DYNAMIC INTERFEROGRAM
FOR 90 DEG. VIEWING ANGLE

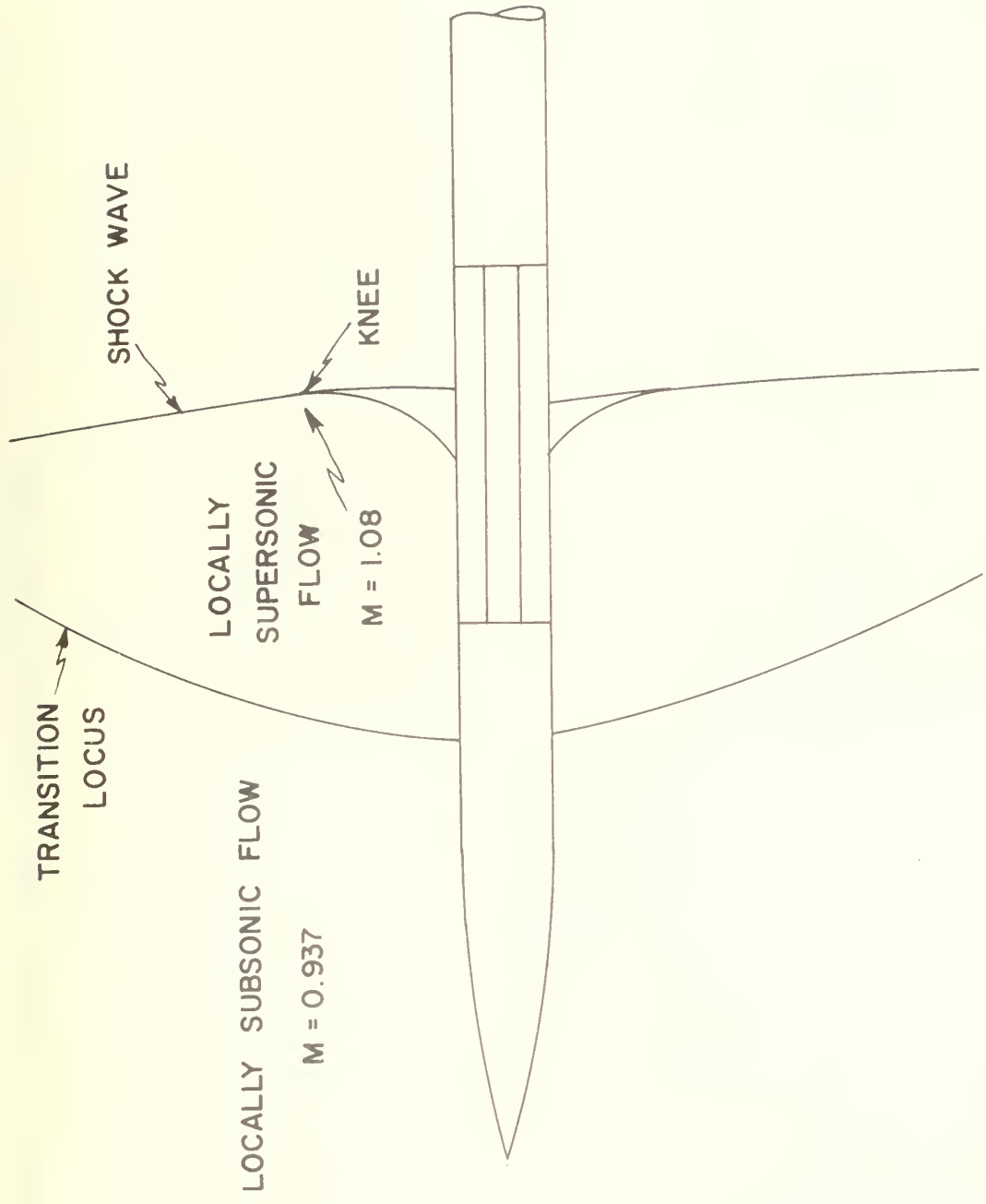


FIGURE 25.
 CHARACTERISTIC TRANSONIC FLOW REGIONS; FROM SEVERAL INTERFEROGRAMS

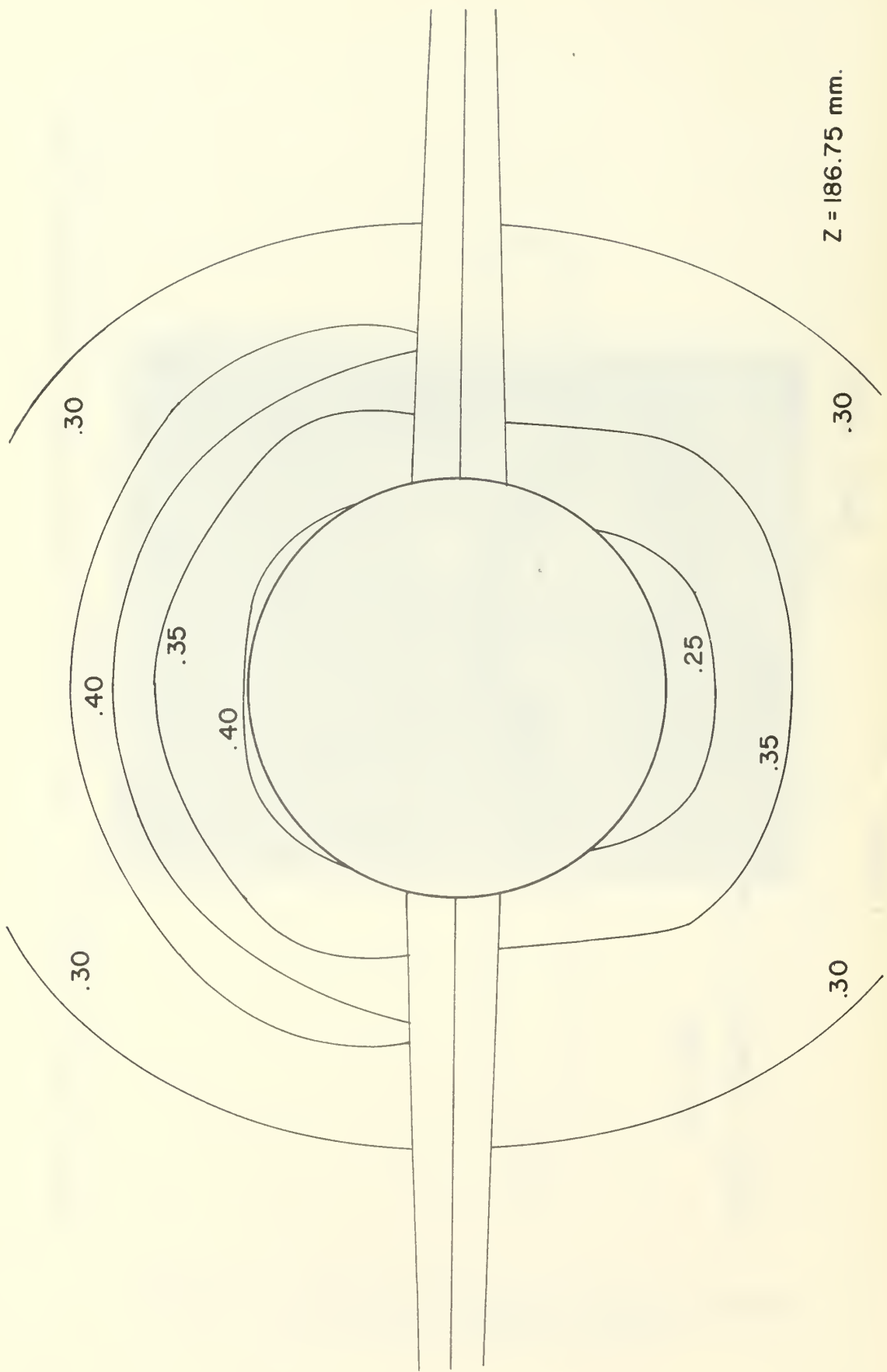


FIGURE 26. CONTOUR PLOT OF DENSITY FUNCTION, $(\rho / \rho_{\infty}) - 1$, FOR GIVEN CROSS-SECTIONAL PLANE

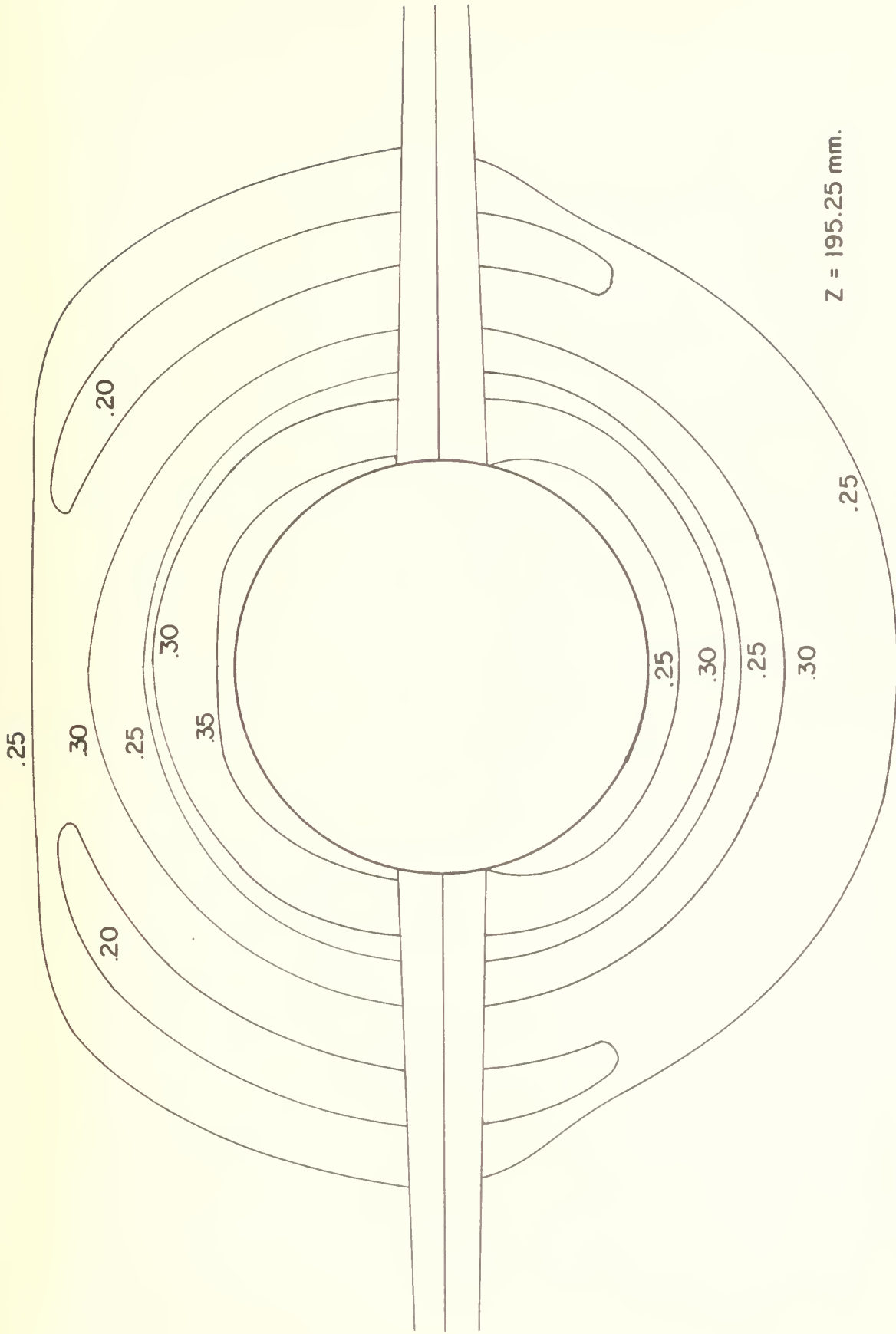


FIGURE 27.
 CONTOUR PLOT OF DENSITY FUNCTION, $(\rho / \rho_0) - 1$, FOR GIVEN CROSS-SECTIONAL PLANE

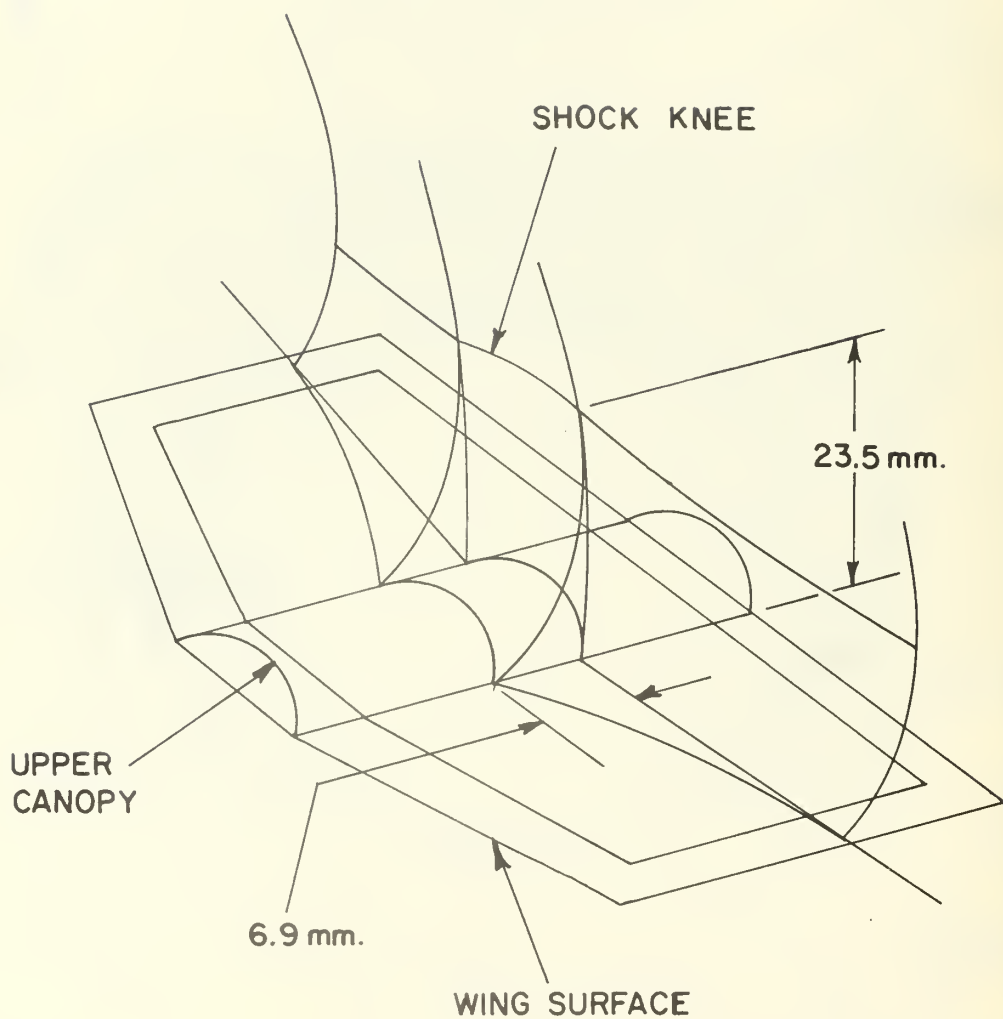


FIGURE 28. THREE DIMENSIONAL SCHEMATIC OF SHOCK WAVE STRUCTURE; CONSTRUCTED USING SEVERAL INTERFEROGRAM VIEWS

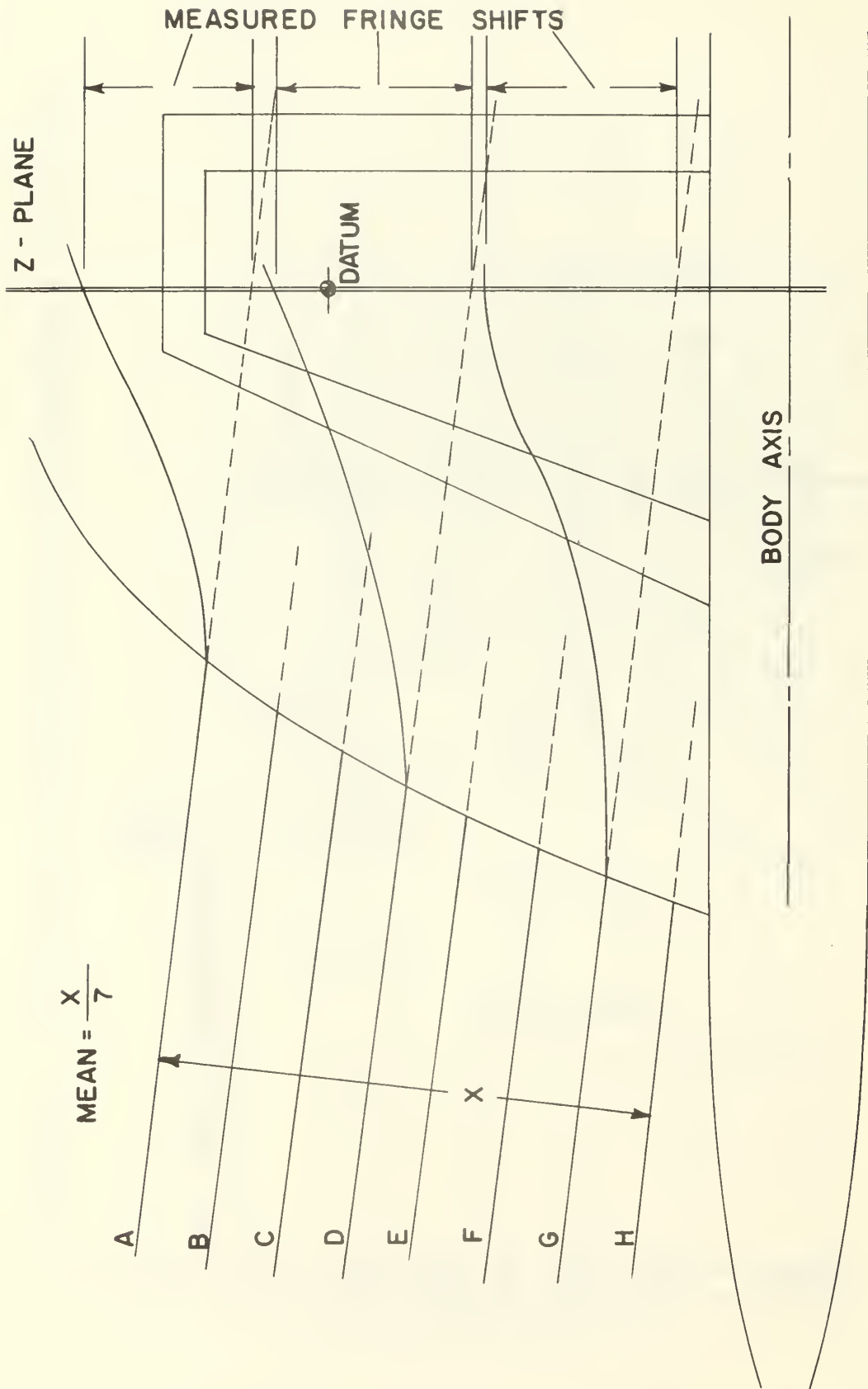


FIGURE 30. STATIC-DYNAMIC HOLOGRAM REDUCTION PROCESS; Z = 186.75 mm.

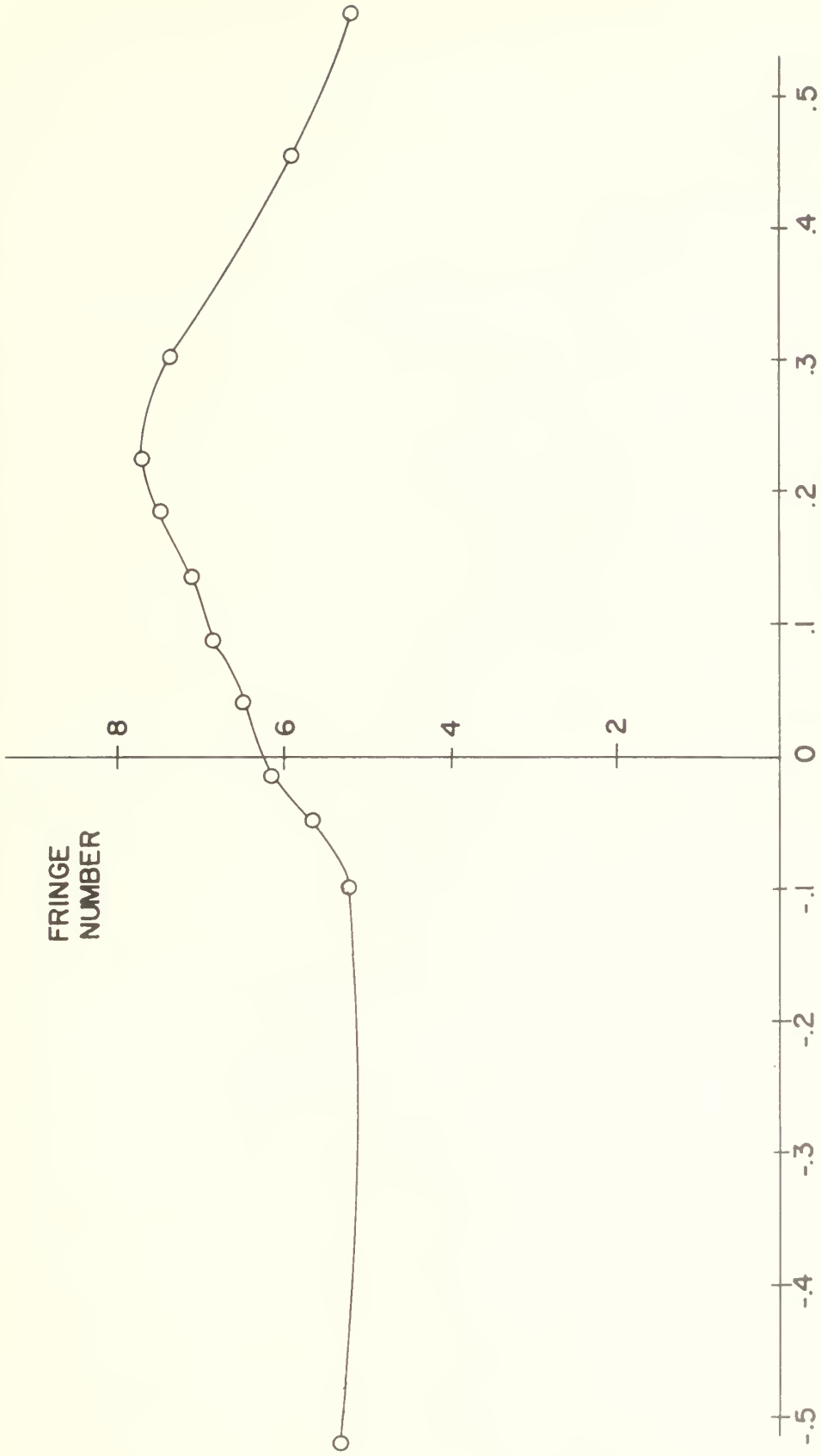


FIGURE 31. RADIAL VARIATION OF FRINGE NUMBER;
ZERO DEGREE VIEW, $Z = 186.75$ mm.

RUN NUMBER	HOLOGRAM NUMBER	DOUBLE EXPOSURE	ROLL ANGLE	P _A (psi)	P _T (psi)	T _T (deg. F)	MACH NUMBER
1	9	S/S	0.00				
2	10	S/D	0.00	14.781	14.181	64.6	.9371
3	23	S/S	11.25				
4	24	S/D	11.25	14.820	14.228	64.2	.9398
5	19	S/S	22.50				
6	20	S/D	22.50	14.784	14.187	64.6	.9361
7	15	S/S	33.75				
8	16	S/D	33.75	14.800	14.206	64.2	.9392
9	11	S/S	45.00				
10	12	S/D	45.00	14.785	14.185	64.6	.9391
11	25	S/S	56.25				
12	26	S/D	56.25	14.830	14.237	64.3	.9361
13	21	S/S	67.50				
14	22	S/D	67.50	14.787	14.195	64.3	.9365
15	17	S/S	78.75				
16	18	S/D	78.75	14.870	14.285	64.8	.9342
17	13	S/S	90.00				
18	14	S/D	90.00	14.787	14.195	64.6	.9402
19	35	S/S	101.25				
20	36	S/D	101.25	14.781	14.274	61.5	.9392
21	27	S/S	112.50				
22	28	S/D	112.50	14.875	14.281	62.5	.9371
23	37	S/S	123.75				
24	38	S/D	123.75	14.878	14.284	61.0	.9369
25	29	S/S	135.00				
26	30	S/D	135.00	14.875	14.278	62.0	.9372
27	39	S/S	146.25				
28	40	S/D	146.25	14.881	14.286	60.3	.9352
29	31	S/S	157.50				
30	32	S/D	157.50	14.875	14.276	61.8	.9350
31	41	S/S	168.75				
32	42	S/D	168.75	14.881	14.287	61.0	.9371
33	33	S/S	180.00				
34	34	S/D	180.00	14.875	14.282	62.0	.9357

TABLE I. EXPERIMENTAL DATA FOR WIND TUNNEL RUNS AT NSRDC

I. D.	FRINGE MEASURED		CORRECTED SHIFT	FRINGE NUMBER	DISTANCE FROM DATUM	DE MAG. DISTANCE	DISTANCE FROM AXIS	NONDIMEN. LOCATION
	SHIFT	SHIFT						
A	25.0	21.475	3.53	-27.0	-25.1	-63.8	--.798	
B	29.6	26.075	4.29	-23.2	-21.6	-59.8	--.748	
C	30.4	26.875	4.42	-18.5	-17.2	-55.4	--.693	
D	31.6	28.075	4.62	-13.0	-12.1	-50.3	--.623	
E	35.5	31.975	5.23	- 9.5	- 8.8	-47.0	--.588	
F	36.0	32.475	5.34	- 3.6	- 3.4	-41.6	--.520	
G	34.0	30.475	5.23	+32.8	+30.5	- 7.7	--.096	
H	36.4	32.875	5.64	+37.0	+34.4	- 3.8	--.048	
I	40.0	36.475	6.26	+40.0	+37.2	- 1.0	--.013	
J	41.5	37.975	6.51	+44.4	+41.3	+ 3.1	+ .039	
K	43.5	39.975	6.86	+48.5	+45.2	+ 7.0	+ .088	
L	45.3	41.775	7.17	+52.7	+49.1	+10.9	+ .136	
M	47.4	43.875	7.53	+57.0	+53.1	+14.9	+ .186	
N	48.6	45.075	7.73	+60.5	+56.3	+18.1	+ .226	
O	46.8	43.275	7.42	+67.0	+62.4	+24.2	+ .303	
P	38.5	34.975	5.99	+80.3	+74.8	+36.6	+ .458	
Q	34.0	30.475	5.23	+89.6	+83.4	+45.2	+ .565	

Mean free stream spacing = 5.96 mm.

Diffraction Correction = 3.525 mm.

Magnification factor = 1.074

Body axis location = +38.2 mm

All measurements in millimeters

- = above, + = below

TABLE II.

RECORDED DATA FOR ZERO DEGREE VIEW AT Z = 186.75 mm. FROM BODY NOSE

APPENDIX A

REDUCTION OF AN INTERFEROGRAM TO OBTAIN FRINGE SHIFT DATA

The reduction of data for a cross-sectional plane of interest involved a complete analysis of both doubly exposed holograms, and their corresponding interferograms, for each viewing angle.

For each view, or line of sight, the double-static exposure was first placed face down on a light table. The average fringe spacing was recorded on the back by measuring the perpendicular distance between two sufficiently separated fringe lines in the free stream and dividing by the number of spacings in between. The method is portrayed in Figure 29. Of primary importance was the measurement of the uniform shift of fringe lines due to the beam diffractive quality of the lucite sections of the model; this was taken to be the average distance between hypothetically unaltered fringe lines and the corresponding shifted fringes at their intersection with the z-plane.

The static-dynamic exposure was then placed face down on the light table and the fringe and model contours traced on the back, as shown in Figure 30. Again, the average free stream fringe line spacing was measured and checked against the value from the double-static exposure. A reference point, or datum, was selected at the intersection of a well-defined horizontal grid line and the z-plane of interest. Fringe shifts were computed in the following manner:

1. The distance from datum to a hypothetically undeviated fringe line at its intersection with the z-plane was measured in millimeters.
2. The distance from datum to the actual deviated, or shifted, fringe at its intersection with the z-plane was measured in millimeters. Measured shifts should be made perpendicular to the fringe direction. The present procedure is convenient and only introduces an error of about 1% in the overall level of the density field.
3. The raw fringe shift distance was then the distance in 1. above minus the distance in 2.
4. To correct for diffraction error, the uniform shift measured in the double-static exposure was then subtracted from the distance in 3.

Fringe numbers were calculated by dividing the shift for each fringe by the average free stream spacing for the exposure. Magnification factors were computed for each exposure by comparing photographically recorded model diameter with actual model diameter.

Since the datum location varied slightly from exposure to exposure, it was necessary to reference all measurements to a central point for each plane of analysis. This point was taken to be the intersection of the longitudinal axis of the model fuselage and the cross-sectional plane of interest. The intersections of shifted fringe lines with the z-plane were referenced to this fixed point and demagnified. The resulting distances were then nondimensionalized using the selected inversion circle radius. Table II contains typical data recorded for the zero degree view at the 186.75 mm. plane of interest.

A plot of fringe numbers versus nondimensionalized fringe location was produced for each viewing angle using data obtained from the interferograms. Fringe numbers at 201 equidistant points, as required for input into Mode 3 of the inversion computer program, were recorded from the resulting curves. The curve plotted using the data from Table II is shown in Figure 31.

APPENDIX B

APPLICATION OF COMPUTER PROGRAM "HOLOFER"

The computer program used in this study is designed to invert an array of fringe numbers across a field to obtain the associated density field using a special adaptation of the inversion technique first proposed by C. D. Maldonado [5, 6]. Three different modes of operation are available to the operator, as described below:

(a) Mode 1

This mode provides the basic self-testing capability of the computer program. It can either generate its own input density field using Subroutine FUNCT or read in a density field through Subroutine FREAD. The fringe number array corresponding to the input density data is first generated; this information is then used as the input for the inversion to obtain the original density distribution once again. This self-testing procedure was utilized in the present investigation to determine the best value of the scale factor, α , required to assure accurate density in the region of inversion.

(b) Mode 2

This mode generates the fringe array at regular intervals across the test field from irregularly spaced fringe values read in through Subroutine SHEET. Simulated fringe arrays may be generated

by one of the functions specified in Subroutine FUNCT if NCODE = 1 is specified.. Mode 2 has not been utilized in the present investigation.

(c) Mode 3

Mode 3 operation reads in a regularly spaced array of input density values directly utilizing Subroutine READ, which is first called by Subroutine GARRAY. The parameters in the first two cards preceding the input fringe data serve to identify the size, location and symmetry of the fringe field. The following parameters were used in calculating the asymmetric density field in the present experiment:

<u>PARAMETER</u>	<u>INPUT</u>
NOF	Run Number
IMAX	201
JMAX	20
ISYM	1
JSYM	1
IMS	201
JMS	5
Z	0.0, 1.0
XO	0.0
YO	0.0
PHISYM	0.0

Amplifying details and applications of the inversion computer program are found in References [3, 7, 9]. A listing of the program is included in this appendix for reference.

```

CAL00010
CAL00020
CAL00030
CAL00040
CAL00050
CAL00060
CAL00070
CAL00080
CAL00090
CAL00100
CAL00110
CAL00120
CAL00130
CAL00140
CAL00150
CAL00160
CAL00170
CAL00180
CAL00190
CAL00200
CAL00220

CAL00230
CAL00240
CAL00250
CAL00260
CAL00270
CAL00280
CAL00290
CAL00300
CAL00310
CAL00320
CAL00330
CAL00340
CAL00350
CAL00360
CAL00370
CAL00380
CAL00390
CAL00400
CAL00410
CAL00420
CAL00430
CAL00440
CAL00450
CAL00460
CAL00470

*****HOLLOVERT*****
HOLLOVERT INVERTS THE FIELD AT AN ARRAY OF POINTS IN A VARIABLE
COORDINATE SYSTEM. IT SURVEYS NPTS POINTS EACH FOR A SET OF NLINS
LINES ACROSS THE FIELD.

COMMON IMAX, JMAX, IIMX, JIMX, IJMX, ALPHA, SIZE, EPS, MODE, BOX, SD, IX, Z
COMMON /TAB/ INDEX, KEXTRA, MEXTRA, KLIMIT, MLIMIT, KOUT, MOUT
COMMON /TAB2/ IPT, KPT, LPT, BND, NPTS, NLINS, RHOINF, RLAMDA, BETA
COMMON /OUT/ XP, THEO, CALC, ERR, RHO, CA, FA
COMMON /EQPAR/ A, B, C, D, E, P, Q, S, T, U, V, W, RO, RA, NO, NA, NOF, NAF
COMMON /SYM/ ISYM, JSYM, MSYM, FCU, IMS, JMS, QSYM
COMMON /IO/ CMS, IN1, IN2, IN4
DATA BL, PL, ST, EX, OH, SC, DH, BR/1H, 1H+, 1H*, 1HX, 1HO, 1H-, 1H1/
DIMENSION RB(7), TL(62), RO(101), RA(101)

-----
DIMENSION G(5151), GA(5151), H(202, 5), SCF(73, 6), BDA(4000)
DIMENSION THEO(51, 11), CALC(51, 11), ERR(51), RHO(51)
DIMENSION CA(51), FA(51, 11), AR(42), XP(51), YP(51)
CMS=0.

-----
REWIND 3
IN1=5
IN2=5
IN4=5
IF (CMS.NE.1.) GO TO 20
IN1=1
IN2=2
IN4=4
IF (CMS.EQ.1.) REWIND 4
READ (IN4, 89) (AR(I), I=1, 42)
IMAX=AR(1)
JMAX=AR(2)*2
IF (JMAX.LE.0) JMAX=1
KLIMIT=AR(3)
MLIMIT=AR(4)
KEXTRA=AR(5)
MEXTRA=AR(6)
ALPHA=AR(14)
SIZE=AR(8)
EPS=AR(9)
MODE=AR(13)
DGN=AR(17)
RHOINF=AR(10)
RLAMDA=AR(11)*1.E-8
BETA=AR(12)

```



```

NF=INI
IF ((MODE.EQ.1.) .AND. (NOF.EQ.8) .AND. (DGN.GE.1.)) WRITE (6,69)
IF ((MODE.EQ.1.) .AND. (NOF.EQ.8)) CALL FREAD (NO,RO,NF,ZD)
Z=ZD
IF (DGN.GE.1.) WRITE (6,68)
CALL GARRAY (G,GA,NOF,DGN,MONE,XO,YO,PHISYM)
LM=1
IF ((LPT.EQ.0) .AND. (BND.EQ.0)) LM=0
IIMX=IMAX+1
JMX=JMAX+1
IJMX=IMAX*JMAX
NBD=1
IF (JSYM.EQ.0) NBD=2
KBD=KLIMIT*NBD
DO 15 IJ=1, IJMX
GA(IJ)=0
IF (NAF.EQ.0) GO TO 16
NF=IN2
IF ((NAF.EQ.8) .AND. (DGN.GE.1.)) WRITE (6,69)
IF (NAF.EQ.8) CALL FREAD (NA,RA,NF,ZD)
MST=MODE
MODE=1
IF (DGN.GE.1.) WRITE (6,68)
IF (NAF.NE.0) CALL GARRAY (GA,G,NAF,DGN,NTWO,XO,YO,PHISYM)
MODE=MST
DO 6 IJ=1, IJMX
G(IJ)=G(IJ)+GA(IJ)
RLINS=NLINS
IF (NAF.EQ.8) WRITE (6,88) NA,(RA(L),L=1,NA)
IF (NOF.EQ.8) WRITE (6,87) NO,(RO(I),I=1,NO)
IF (LM.EQ.0) GO TO 14
RB(I)=-1.
DO 1 I=2,7
RB(I)=RB(I-1)+.5
TPIE=2.*PIE
MPIE=-PIE
DYP=0.
DXP=0.
IF (NLINS.GT.1) DYP=YPRNG/(RLINS-1.)
IF (NPTS.GT.1) DXP=XPRNG/(RPTS-1.)
IF ((DGN.GE.1.) .AND. (NNN.EQ.2)) WRITE (6,64)
IF (NNN.EQ.2) CALL BDGEN (G,H,SCF,DGN,NBD,BDA,KBD)
DO 5 J=1,NLINS
IF (DGN.GE.1.) WRITE (6,67) J
RJM=J-1
PHI=PHIZ+DELPHI*RJM
YP(J)=YPZERO+DYP*RJM
PSI=(PHI+90.)*PIE/180.

```

15

6
16

1

CAL01180
CAL01190
CAL01200
CAL01210
CAL01220
CAL01230
CAL01240
CAL01250
CAL01260
CAL01270
CAL01280
CAL01290
CAL01300
CAL01310
CAL01320
CAL01330
CAL01340
CAL01350
CAL01360
CAL01370
CAL01380
CAL01390
CAL01400
CAL01410
CAL01420
CAL01430
CAL01440
CAL01450
CAL01460
CAL01470
CAL01480
CAL01490
CAL01500
CAL01510
CAL01520
CAL01530
CAL01540
CAL01550
CAL01560
CAL01570
CAL01580
CAL01590
CAL01600
CAL01610
CAL01620
CAL01630
CAL01640
CAL01650

CAL01660
 CAL01670
 CAL01680
 CAL01690
 CAL01700
 CAL01710
 CAL01720
 CAL01730
 CAL01740
 CAL01750
 CAL01760
 CAL01770
 CAL01780
 CAL01790
 CAL01800
 CAL01810
 CAL01820
 CAL01830
 CAL01840
 CAL01850
 CAL01860
 CAL01870
 CAL01880
 CAL01890
 CAL01900
 CAL01910
 CAL01920
 CAL01930
 CAL01940
 CAL01950
 CAL01960
 CAL01970
 CAL01980
 CAL01990
 CAL02000
 CAL02010
 CAL02020
 CAL02030
 CAL02040
 CAL02050
 CAL02060
 CAL02070
 CAL02080
 CAL02090
 CAL02100
 CAL02110
 CAL02120
 CAL02130

```

TAU=PSI-PHISYM
IF (LPT.EQ.0) GO TO 9
IF (LPT.LE.1) WRITE (6,78) (ST,I=1,124)
IF (LPT.GT.1) WRITE (6,74) (ST,I=1,95)
IF ((CMS.EQ.1).AND.(LPT.GT.1)) READ (5,79) ZZ
WRITE (6,86)
WRITE (6,85) Z,PHI,YP(J)
WRITE (6,76)
IF (MODE.EQ.1) WRITE (6,83) (RB(I),I=1,7)
IF (MODE.GT.1) WRITE (6,80) (RB(I),I=1,7)
WRITE (6,81) (DH,I=1,54),(PL,I=1,13)
IC=0
DO 3 I=1,NPTS
RIM=I-1
THEO(I,J)=0.
CA(I)=0.
FA(I,J)=0.
ERR(I)=0.
CALC(I,J)=0.
RHO(I)=0.
XP(I)=XPZERO+XP*RI
XPII=ABS(XP(I))
IF (XPII.LT.1.E-13) XP(I)=0.
RS=SQRT(XP(I)**2+YP(J)**2)/HS
IF (RS.GT.1.) GO TO 13
THT=ATANM(YP(J),XP(I))
IF (XPII.EQ.0.) THT=0.
SIG=TAU-PIE/2.+THT
IF (SIG.GT.PIE) SIG=SIG-TPIE
IF (SIG.LT.MPIE) SIG=SIG+TPIE
SIGI=SIG
XS=RS*COS(SIG)
IF (DGN.GE.1.) WRITE (6,44) SIG
FORMAT (' SIG=',E10.3)
YS=RS*SIN(SIG)
IF (DGN.GE.5) WRITE (6,57) PHI,DELPHI,PSI,TAU,THT,SIG,SIGI,XS,YS
R1=I
F=0.
IF (DGN.GE.2.) WRITE (6,66) I
CALL FUNCT (XS,YS,FA(I,J),NAF,DGN,NTWO)
IF (MODE.EQ.1) CALL FUNCT (XS,YS,F,NOF,DGN,MONE)
THEO(I,J)=F
IF (NNN.GE.2) REWIND 3
IF (NNN.GE.2) CALL FIELD (RS,SIGI,SOLN,NBD,BDA,DGN,KBD)
IF (NNN.EQ.1) CALL FIELD2 (RS,SIGI,SOLN,G,H,SCF,DGN)
CA(I)=SOLN/BOX/HS
CALC(I,J)=CA(I)-FA(I,J)

```

9

44

57

CAL02140
 CAL02150
 CAL02163
 CAL02170
 CAL02180
 CAL02193
 CAL02200
 CAL02210

CAL02260
 CAL02273
 CAL02280
 CAL02290
 CAL02333
 CAL02310
 CAL02320
 CAL02330
 CAL02340
 CAL02353
 CAL02360
 CAL02370
 CAL02383
 CAL02390
 CAL02400
 CAL02410
 CAL02420
 CAL02430
 CAL02440
 CAL02450
 CAL02460
 CAL02470
 CAL02480
 CAL02493
 CAL02500
 CAL02510
 CAL02520
 CAL02530
 CAL02543
 CAL02550
 CAL02560
 CAL02570
 CAL02580
 CAL02590
 CAL02600
 CAL02610

```

RHO(I)=RHOINF*(CALC(I,J)+1.)
ERR(I)=CA(I)
IF (MODE.EQ.1) ERR(I)=(CALC(I,J)-THEO(I,J))
IF (MODE.GT.1) THEO(I,J)=FA(I,J)
IF (LPT.EQ.0) GO TO 3
LC=0
TL(1)=BL
TTL=0
IF ((XP(I).GT.XPM).AND.(XP(I).LT.XPR)) TTL=1.
IF (IC.EQ.5) IC=0
IF (IC.EQ.0) TL(1)=PL
DO 2 L=2,62
  TL(L)=BL
  IF ((I.EQ.1).OR.(TTL.EQ.1).OR.(I.EQ.NPTS)) TL(L)=PL
  IF (LC.EQ.1) LC=0
  IF ((IC.EQ.0).AND.(LC.EQ.0)) TL(L)=PL
  LC=LC+1
  TL(2)=PL
  TL(22)=PL
  TL(62)=PL
  IC=IC+1
  RLW=(CA(I)+1.)*20.+2.5
  LW=RLW
  IF (LW.GT.62) LW=62
  IF (LW.LT.2) LW=2
  TL(LW)=SC
  RLY=(FA(I,J)+1.)*20.+2.5
  LY=RLY
  IF (LY.GT.62) LY=62
  IF (LY.LT.2) LY=2
  IF (NAF.NE.3) TL(LY)=ST
  RLX=(THEO(I,J)+1.)*20.+2.5
  LX=RLX
  IF (LX.GT.62) LX=62
  IF (LX.LT.2) LX=2
  IF (MODE.EQ.1) TL(LX)=OH
  RLZ=(CALC(I,J)+1.)*20.+2.5
  LZ=RLZ
  IF (LZ.GT.62) LZ=62
  IF (LZ.LT.2) LZ=2
  TL(LZ)=EX
WRITE (6,82)MOUT,KOUT,INDEX,THEO(I,J),ERR(I),CALC(I,J),RHO(I),
1XP(I),(TL(L),L=1,62)
IF ((NPTS.LE.20).AND.(I.NE.NPTS)) WRITE (6,79)
CONTINUE
IF (LPT.NE.0) WRITE (6,81) (DH,I=1,54),(PL,I=1,13)
TMAX=0.
TMIN=0.

```

13

2

3

```

CAL02620
CAL02630
CAL02640
CAL02650
CAL02660
CAL02670
CAL02680
CAL02690
CAL02700
CAL02710
CAL02720
CAL02730
CAL02740
CAL02750
CAL02760
CAL02770
CAL02780
CAL02790
CAL02800
CAL02810
CAL02820
CAL02830
CAL02840
CAL02850
CAL02860
CAL02870
CAL02880
CAL02890
CAL02900
CAL02910
CAL02920
CAL02930
CAL02940
CAL02950
CAL02960
CAL02970
CAL02980
CAL02990
CAL03000
CAL03010
CAL03020
CAL03030
CAL03040
CAL03050
CAL03060
CAL03070
CAL03080
CAL03090

IE=0
BE=0
EB=0
DO 4 I=1,NPTS
  TH=THEO(I,J)
  IF (TH.GT.TMAX) TMAX=TH
  IF (TH.LT.TMIN) TMIN=TH
  ER=ABS(CALC(I,J)-TH)
  IF (ER.LE.BE) GO TO 4
BE=ER
IE=I
CONTINUE
TMM=TMAX-TMIN
EB=RHOINF*(CALC(IE,J)-THEO(IE,J))*100./TMM
IF (TMM.NE.0) BE=(CALC(IE,J)-THEO(IE,J))*100./TMM
IF ((MUDE.EQ.1).AND.(LPT.NE.0)) WRITE (6,75) EB,XP(IE),BE
IF ((DELPHI.NE.3) YP(J)=PHI
CONTINUE
IF (BND.EQ.0) GO TO 14
IF (LPT.EQ.1) WRITE (6,78) (ST,I=1,124)
IF (LPT.GT.1) WRITE (6,74) (ST,I=1,95)
IF ((CMS.EQ.1).AND.(LPT.GT.1)) READ (5,79) ZZ
IF (DGN.EQ.1) WRITE (6,63)
CALL MAP (NPTS,NLINS,CALC,NOF,Z,BND)
IF (NAF.EQ.0) GO TO 10
NAO=10*NOF+NAF
IF ((DGN.EQ.1).AND.(NGP.EQ.-3)) WRITE (6,62)
IF (NGP.EQ.-3) CALL GPUNCH (Z,XO,YO,PHISYM,NAO,IMAX,JMAX,G)
DO 7 IJ=1,IJMX
  G(IJ)=G(IJ)-GA(IJ)
  IF ((IPT.LE.0) GO TO 11
  IF ((IPT.EQ.1).OR.(IPT.EQ.3)) WRITE (6,78) (ST,I=1,124)
  IF ((IPT.EQ.2).OR.(IPT.GE.4)) WRITE (6,74) (ST,I=1,95)
  IF ((CMS.EQ.1).AND.(IPT.EQ.2).OR.(IPT.GE.4)) READ (5,79) ZZ
  CALL GPRINT (G,MONE)
  IF (NGP.EQ.-1) CALL GPUNCH (Z,XO,YO,PHISYM,NOF,IMAX,JMAX,G)
  IF ((IPT.EQ.3) WRITE (6,78) (ST,I=1,124)
  IF ((IPT.GE.4) WRITE (6,74) (ST,I=1,95)
  IF ((CMS.EQ.1).AND.(IPT.GE.4)) READ (5,79) ZZ
  IF (IPT.GE.3) CALL GPRINT (GA,NTWO)
  IF ((KPT.LE.0) GO TO 12
  IF ((KPT.EQ.1).OR.(KPT.EQ.3)) WRITE (6,78) (ST,I=1,124)
  IF ((KPT.EQ.2).OR.(KPT.GE.4)) WRITE (6,74) (ST,I=1,95)
  IF ((CMS.EQ.1).AND.(KPT.EQ.2).OR.(KPT.GE.4)) READ (5,79) ZZ
  IF (DGN.GE.1) WRITE (6,61)
  CALL GPLOT (G,GA,JMS)
  WRITE (6,73) (EX,I=1,124)
  AGAIN=ST
12

```

```

89 IF (CMS.NE.1.) READ(5,60) AGAIN
88 IF (AGAIN.EQ.BL) GO TO 20
WRITE (6,77)
FORMAT (6F12.7)
THE INPUT DATA FOR ADD-ON FUNCTION NO.8 (' ,I3,
1, POINTS) WAS: /7(11F10.3//)
THE INPUT DATA FOR THE TEST FUNCTION NO.8, (' ,I3,
1, POINTS) WAS: /7(11F10.3//)
THE INVERTED CROSS SECTION FOR:
FORMAT (1H1//, ' CM.,F8.3, ' CM.,/10X, ' PHI=',F8.3, ' DEGREES'/10X,
14HY. =, F8.3, ' CM.,44X,0 = ORIGINAL FUNCTION'/
270X, '* = ADD-ON FUNCTION')
FORMAT ( ' ADJUST PAGE, HIT SPACE AND RETURN. ')
FORMAT ( ' LIMIT MAX ORIGINAL ABS. COMPUTED (MG/CC)'/
K TERM FUNCTION ERROR FUNCTION DENSITY ',6H X',F4.1,
1 26F10.1)
(2X,I2,1X,I3,1X,I4,1X,F9.4,2X,F7.3,1X,F9.4,1X,F7.3,
FORMAT (1X,62A1)
1 F7.3,1X
(3X,54A1,2X,A1,12(4X,A1))
FORMAT ( ' LIMIT MAX,3X,ADD-ON',6X, 'THE',4X, 'DENSITY (MG/CC)'/
K TERM,2X, 'FUNCTION',5X, 'SUM',3X, 'FUNCTION DENSITY ',
1 25H X',F4.1,6F10.1)
FORMAT (1X,F10.3)
FORMAT (1X,124A1)
79
78
77
76
1, INVERTED SUM,70X, 'X = COMPUTED FUNCTION')
FORMAT (4X, 'FUNCTION = (RHO/RHO-INFINITY)-1.0',33X, ': = THE'
1, 'INVERTED SUM',LARGEST ERROR: ',F8.6, ' GMS/CC;
1, 'AT ',3HX' =,F6.3
1, '4X,F10.2, ' PERCENT, 'HIT SPACE, RETURN ',48A1)
FORMAT (1X,47A1, ' SET PAGE,
FORMAT ( ' CALL FREAD')
FORMAT ( ' CALL GARRAY')
FORMAT ( ' LINE, I3, ' DO LOOP')
FORMAT ( ' POINT, I3, ' CALL FUNCT')
FORMAT ( ' CALL FIELD')
FORMAT ( ' CALL BDGEN')
FORMAT ( ' CALL MAP')
FORMAT ( ' CALL GPUNCH')
FORMAT ( ' CALL GPLOT')
FORMAT (80A1)
STOP
END
C000001
C

```

```

CAL03100
CAL03110
CAL03120
CAL03130
CAL03140
CAL03150
CAL03160
CAL03170
CAL03180
CAL03190
CAL03200
CAL03210
CAL03220
CAL03230
CAL03240
CAL03250
CAL03260
CAL03270
CAL03280
CAL03290
CAL03300
CAL03310
CAL03320
CAL03330
CAL03340
CAL03350
CAL03360
CAL03370
CAL03380
CAL03390
CAL03400
CAL03410
CAL03420
CAL03430
CAL03440
CAL03450
CAL03460
CAL03470
CAL03480
CAL03490
CAL03500
CAL03510
CAL03520
SUB00010
SUB00020

```

```

SUBROUTINE BDGEN (G,H,SCF,DGN,NBD,BDA,KBD)
C
C BDGEN EVALUATES THE B AND D COEFFICIENTS FOR ALL M AND K, AND WRITES
C THE ARRAY LINEARLY ON DISK.
C
COMMON IMAX,JMAX,IIMX,JJMX,IJMX,ALPHA,SIZE,EPS,MODE,BOX,SD,IX,Z
COMMON /TAB/ INDEX,KEXTRA,MEXTRA,KLIMIT,MLIMIT,KOUT,MOUT
COMMON /SYM/ ISYM,MSYM,FCU,IMS,JMS,QSYM
DIMENSION G(IJMX),H(IIMX,5),SCF(JJMX,6),BDA(KBD)
C INITIALIZE THE VALUES:
INDEX=0
KL2=NBD*KLIMIT
REWIND 3
JJMX6=JJMX*6
IIMX2=(IIMX+1)/2
PIE=3.141592653589793
RIMAX=IMAX
KLMP=KLIMIT+1
DX=2./RIMAX
RJMAX=JMAX
DXI=2.*PIE/FCU
C INITIALIZE THE MODIFIED HERMITE POLYNOMIAL ARRAY: VECTORS:
(1)=H1,(2)=H2,(3)=ALPHA*X(I),(4)=HM+2 STORED,(5)=HM+1 STORED
DO 1 I=1,IIMX2
RII=IIMX-I+1
IIM=IIMX-I+1
H(II,3)=ALPHA*(RII*DX-DX-1.)
H(II,3)=-H(II,3)
H(II,1)=2.*H(II,3)
H(II,2)=(H(II,3)*H(II,1)-1.)/3.
H(II,1)=-H(II,1)
H(II,2)=H(II,2)
H(II,5)=H(II,2)
H(II,4)=H(II,1)
H(II,4)=H(II,1)
SIGN=1.
C INITIALIZE THE SIN/COS ARRAY:
DO 2 J=1,JJMX
RJM=J-1
SCF(J,1)=0.
SCF(J,2)=1.
SCF(J,3)=SIN(RJM*DXI-PIE/2.)
SCF(J,4)=COS(RJM*DXI-PIE/2.)
SCF(J,5)=0.
SCF(J,6)=0.
MS=0
C COMMENCE THE M LOOP:
SUB000030
SUB000040
SUB000050
SUB000060
SUB000070
SUB000080
SUB000090
SUB000100
SUB000110
SUB000120
SUB000130
SUB000140
SUB000150
SUB000160
SUB000170
SUB000180
SUB000190
SUB000200
SUB000210
SUB000220
SUB000230
SUB000240
SUB000250
SUB000260
SUB000270
SUB000280
SUB000290
SUB000300
SUB000310
SUB000320
SUB000330
SUB000340
SUB000350
SUB000360
SUB000370
SUB000380
SUB000390
SUB000400
SUB000410
SUB000420
SUB000430
SUB000440
SUB000450
SUB000460
SUB000470
SUB000480
SUB000490
SUB000500

```

SUB000510
 SUB000520
 SUB000530
 SUB000540
 SUB000550
 SUB000560
 SUB000570
 SUB000580
 SUB000590
 SUB000600
 SUB000610
 SUB000620
 SUB000630
 SUB000640
 SUB000650
 SUB000660
 SUB000670
 SUB000680
 SUB000690
 SUB000700
 SUB000710
 SUB000720
 SUB000730
 SUB000740
 SUB000750
 SUB000760
 SUB000770
 SUB000780
 SUB000790
 SUB000800
 SUB000810
 SUB000820
 SUB000830
 SUB000840
 SUB000850
 SUB000860
 SUB000870
 SUB000880
 SUB000890
 SUB000900
 SUB000910
 SUB000920
 SUB000930
 SUB000940
 SUB000950
 SUB000960
 SUB000970

```

DO 7 MP=1,MLIMIT
M=MP-1
RM=M
SIGN=-SIGN
IF (DGN.LE.-4) WRITE (6,88) SCF(1,1),SCF(2,1),SCF(1,2),SCF(2,2)
TEST FOR SYMMETRY SKIPS:
IF (MS.EQ.MSYM) MS=0
TOTAL=0.
MS=MS+1
IF (MS.NE.1) GO TO 6
COMMENT THE K LOOP:
DO 5 KP=1,KLIMIT
K=KP-1
PK=KP
RK=K
INDEX=INDEX+1
CALL THE B & D COEFFICIENTS AND WRITE THEM ON DISK:
CALL BD (M,K,G,H,SCF,B,D,JJMX6)
IF (DGN.EQ.3.) WRITE(6,89) M,K,B,D
IF (DGN.LE.-2) WRITE (6,89) M,K,B,D
IF (DGN.LE.-4) WRITE (6,88) H(1,1),H(1,2),H(1,4),H(1,5)
KK=K*NBD+1
K2=KP*NBD
BDA(K2)=B
BDA(KK)=B
ORDER=M+2*KP+1
HA=SQRT((PK+RM))/ORDER
HB=2.*SQRT((PK+1.))*(RM+PK+1.)/((ORDER+1.))/(ORDER+2.)
DO 5 II=1,IIWX2
IIM=IIMX-II+1
H(II,1)=2.*(H(II,3)*H(II,2))-HA*H(II,1))
H(II,1)=SIGN*H(II,1)
H(II,2)=HB*(H(II,3)*H(II,1))-ORDER*H(II,2))
ADVANCE THE SIN/COS ARRAY FOR THE NEXT M:
DO 3 J=1,JJMX
IF (DGN.LE.-5) WRITE (6,87) (SCF(J,NT),NT=1,6)
IF (FORMAT(, SIN/COS MXI:8E10.3)
STEPM=SCF(J,1)
SCF(J,1)=SCF(J,1)+SCF(J,2)*SCF(J,3)
SCF(J,2)=SCF(J,2)-STEMP*SCF(J,3)
DO 4 J=1,JJMAX
SCF(J,5)=SCF(J+1,1)-SCF(J,1)
SCF(J,6)=SCF(J+1,2)-SCF(J,2)
WRITE (3) (BDA(I),I=1,KBD)
IF (DGN.LE.-3) WRITE (6,88) (BDA(I),I=1,10)
IF (JSYM.GT.JMAX) RETURN
RM=RM+1

```



```

C REGENERATE THE HERMITE ARRAY FOR NEW M, K=0:
DO 7 II=1,IIMX2
  IIM=IIMX-II+1
  H(II,2)=H(II,4)*SQRT(RM)/(RM+1.)
  H(II,1)=H(II,5)*(RM+2.)
  H(IIM,1)=-SIGV*H(II,1)
  H(II,2)=2.*SQRT(RM+1)*H(II,3)*H(II,1)-(RM+1.)*H(II,2))
  H(II,4)=H(II,2)/(RM+2.)/(RM+3.)
  H(II,5)=H(II,2)
  H(IIM,5)=H(II,2)
  FORMAT (I4,M=,I4, B=,E10.4, D=,E10.4)
89 FORMAT (2X,10E10.3)
88 RETURN
END
C000002
C

```

```

SUB00980
SUB00990
SUB01000
SUB01010
SUB01020
SUB01030
SUB01040
SUB01050
SUB01060
SUB01070
SUB01080
SUB01090
SUB01100
SUB01110
SUB01120
SUB01130

```

```

C SUBROUTINE FIELD (RS,SIG,SOLN,NBD,BDA,DGN,KBD)
C FIELD EVALUATES THE VALUE OF THE FIELD FUNCTION AT A PARTICULAR
C POINT DESIGNATED IN CYLINDRICAL COORDINATES, BY USING THE INVERSION
C EQUATION OF MALDONADO, ET.AL. FIELD USES THE ARRAY OF B & D
C COEFFICIENTS GENERATED IN SUBROUTINE BDGEN.

```

```

SUB01140
SUB01150
SUB01160
SUB01170
SUB01180
SUB01190
SUB01200
SUB01210
SUB01220
SUB01230
SUB01240
SUB01250
SUB01260
SUB01270
SUB01280
SUB01290
SUB01300
SUB01310
SUB01320
SUB01330
SUB01340
SUB01350
SUB01360
SUB01370
SUB01380
SUB01390
SUB01400
SUB01410
SUB01420
SUB01430

```

```

COMMON IMAX,JMAX,IIMX,JJMX,IJMX,ALPHA,SIZE,EPS,MODE,BOX,SD,IX,Z
COMMON /TAB/ INDEX,KEXTRA,MEXTRA,KLIMIT,MLIMIT,KOUT,MOUT
COMMON /SYM/ ISYM,JSYM,MSYM,FCU,IMS,JMS,QSYM
DIMENSION BDA(52),STK(52),STM(52)
C INITIALIZE THE VALUES:
INDEX=0
MTIMER=0
KOUT=0
MOUT=0
MMAX=0
KMAX=0
TOTAL=0.
JJMX6=JJMX*6
REWIND 3
AR=ALPHA*R
ARG=AR**2
EXPON=EXP(-ARG)
PIE=3.141592653589793
APP=ALPHA/PIE/PIE
M=0
RM=M
RIMAX=IMAX
DX=2./RIMAX

```


SUB01440
 SUB01450
 SUB01460
 SUB01470
 SUB01480
 SUB01490
 SUB01500
 SUB01510
 SUB01520
 SUB01530
 SUB01540
 SUB01550
 SUB01560
 SUB01570
 SUB01580
 SUB01590
 SUB01600
 SUB01610
 SUB01620
 SUB01630
 SUB01640
 SUB01650
 SUB01660
 SUB01670
 SUB01680
 SUB01690
 SUB01700
 SUB01710
 SUB01720
 SUB01730
 SUB01740
 SUB01750
 SUB01760
 SUB01770
 SUB01780
 SUB01790
 SUB01800
 SUB01810
 SUB01820
 SUB01830
 SUB01840
 SUB01850
 SUB01860
 SUB01870
 SUB01880
 SUB01890
 SUB01900
 SUB01910

```

R-JMAX=JMAX
SIGN=1.0
STK(1)=0.
STM(1)=0.
SMS=0.
CMS=1.
SMI=SIN(SIG)
CMI=COS(SIG)
MEP=MEXTRA+1
DO 16 MB=1,MEP
  STM(MB)=0.
  FM=1.
  MS=0.
  C COMMENT THE M LOOP:
  2 SIGN=-SIGN
  K=0
  RK=K
  RM=M
  ARM=1. NE.0) ARM=AR**M
  IF (M.NE.0)
  KTIMER=0
  KEP=KEXTRA+1
  DO 15 KB=1,KEP
  STK(KB)=0.
  SIGNK=-1.
  C COMPUTE THE K=0 & K=1 ORDERS OF LAGUERRE POLYNOMIAL FOR GIVEN M:
  PM=0.
  P=SQRT(1./FM)
  PP=(RM+1.-ARG)*SQRT(1./FM/(RM+1.))
  C TEST FOR SYMMETRY SKIPS:
  IF (MS.EQ.MSYM) MS=0
  MS=MS+1
  IF (MS.NE.1) GO TO 7 COEFFICIENTS FOR GIVEN M:
  C READ A LINE OF B & D
  READ (3) (BDA(I),I=1,KB)
  IF (DGN.LE.-6) WRITE (6,88) (BDA(I),I=1,10)
  C COMMENT THE K LOOP:
  3 INDEX=INDEX+1
  SIGNK=-SIGNK
  C COMPUTE THE M,K SUMMATION TERM:
  KK=K*NBD+1
  B=BDA(KK)
  D=0.
  IF (NBD.EQ.2) D=BDA(KK+1)
  BRACKET=B
  IF (RM.EQ.0.) GO TO 4
  BRACKET=B*CMS+D*SMS
  ADD=SIGNK*BRACKET*P*ARM
  4

```

```

TOTAL=TOTAL+ADD
IF (DGN.GT.-5) GO TO 5
STOT=TOTAL*EXPON*APP/BOX/SIZE
WRITE (6,89) M,K,STOT,ADD,BRACKET,P,ARM,B,CMS,D,SMS
ESTABLISH CHECK AS THE RELATIVE SIZE OF THE M,K TERM OF THE SERIES:
5 CHECK=ABS(ADD)
IF (TOTAL.GT.EPS) CHECK=ABS(ADD/TOTAL)
C ADVANCE THE K INDEX:
K=K+1
RK=K
DO 10 KA=1,KEXTRA
KB=KEXTRA-KA+1
STK(KB+1)=STK(KB)
STK(2)=TOTAL
ORDER=M+2*K+1
C GENERATE THE NEXT ORDER OF LAGUERRE POLYNOMIAL FOR NEW K:
PM=PP
P=PP
PP=PP*(ORDER-ARG)-PM*SQRT(RK*(RM+RK))
PP=PP/SQRT((RK+1.)*(RM+RK+1.))
C SET K TIMER TO PROVIDE EXTRA K TERMS AFTER CHECK < EPS:
KTIMER=KTIMER+1
IF (K.GE.KLIMIT) GO TO 6
IF (CHECK.GE.EPS) KTIMER=0
IF (KTIMER.LE.KEXTRA) GO TO 3
GO TO 7
6 KOUT=KOUT+1
IF (KEXTRA.EQ.0) GO TO 7
TOTAL=0
DO 11 KA=1,KEXTRA
TOTAL=TOTAL+STK(KA+1)
RKX=KEXTRA
TOTAL=TOTAL/RKX
C END OF K LOOP: ADVANCE M:
M=M+1
RM=M
STP=SMS
SMS=SMS*CMI+CMS*SMI
CMS=CMS*CMI-STP*SMI
IF (K.GT.KMAX) KMAX=K
FM=FM*RM
DO 12 MA=1,MEXTRA
MB=MEXTRA-MA+1
STM(MB+1)=STM(MB)
STM(2)=TOTAL
C SET M TIMER FOR EXTRA M TERMS:
IF (MS.EQ.1) MTIMER=MTIMER+1
IF (JSYM.GT.JMAX) GO TO 9

```

```

SUB01920
SUB01930
SUB01940
SUB01950
SUB01960
SUB01970
SUB01980
SUB01990
SUB02000
SUB02010
SUB02020
SUB02030
SUB02040
SUB02050
SUB02060
SUB02070
SUB02080
SUB02090
SUB02100
SUB02110
SUB02120
SUB02130
SUB02140
SUB02150
SUB02160
SUB02170
SUB02180
SUB02190
SUB02200
SUB02210
SUB02220
SUB02230
SUB02240
SUB02250
SUB02260
SUB02270
SUB02280
SUB02290
SUB02300
SUB02310
SUB02320
SUB02330
SUB02340
SUB02350
SUB02360
SUB02370
SUB02380
SUB02390

```



```

C THE INPUT PARAMETER.
C FIELD EVALUATES THE VALUE OF THE FIELD FUNCTION AT A PARTICULAR
C POINT DESIGNATED IN CYLINDRICAL COORDINATES, BY USING THE INVERSION
C EQUATION OF MALDONADO, ET AL. FIELD CALLS SUBROUTINES BD & GARRAY.
C
COMMON IMAX, JMAX, IIMX, JJMX, IJMX, ALPHA, SIZE, EPS, MUDE, BOX, SD, IX, Z
COMMON /TAB/ INDEX, KEXTRA, MEXTRA, KLIMIT, MLIMIT, KOUT, MOUT
COMMON /SYM/ ISYM, MSYM, FCU, IMS, JMS, QSYM
DIMENSION G(IJMX), H(IIMX,5), SCF(JJMX,6)
C INITIALIZE THE VALUES:
INDEX=0
IMTIMER=0
KOUT=0
MOUT=0
NMAX=0
KMAX=0
TOTAL=0
JJMX6=JJMX*6
IIMX2=(IIMX+1)/2
ARG=ALPHA*RS
ARG=ARG**2
EXPON=EXP(-ARG)
PIE=3.141592653589793
APP=ALPHA/PIE/PIE
M=0
RM=M
RIMAX=IMAX
DX=2./RIMAX
RJMAX=JMAX
DXI=2.*PIE/FCU
C INITIALIZE THE MODIFIED HERMITE POLYNOMIAL ARRAY; VECTORS:
(1)=H1, (2)=H2, (3)=ALPHA*X(I), (4)=HM+2 STORED, (5)=HM+1 STORED
DO 1 I=1, IIMX2
RII=II
IIM=IIMX-I+1
H(II,3)=ALPHA*(RII*DX-DX-1.)
H(II,3)=-H(II,3)
H(II,1)=2.*H(II,3)
H(II,2)=(H(II,3)*H(II,1)-1.)/3.
H(II,1)=-H(II,1)
H(II,2)=H(II,2)
H(II,5)=H(II,2)
H(II,5)=H(II,4,2)
H(II,4)=H(II,1)
H(II,4)=H(II,4)
SIGN=1.
FM=1.
C INITIALIZE THE SIN/COS ARRAY:

```

```

SUB03310
SUB03320
SUB03330
SUB03340
SUB03350
SUB03360
SUB03370
SUB03380
SUB03390
SUB03400
SUB03410
SUB03420
SUB03430
SUB03440
SUB03450
SUB03460
SUB03470
SUB03480
SUB03490
SUB03500
SUB03510
SUB03520
SUB03530
SUB03540
SUB03550
SUB03560
SUB03570
SUB03580
SUB03590
SUB03600
SUB03610
SUB03620
SUB03630
SUB03640
SUB03650
SUB03660
SUB03670
SUB03680
SUB03690
SUB03700
SUB03710
SUB03720
SUB03730
SUB03740
SUB03750
SUB03760
SUB03770
SUB03780

```

```

SUB03790
SUB03800
SUB03810
SUB03820
SUB03830
SUB03840
SUB03850
SUB03860
SUB03870
SUB03880
SUB03890
SUB03900
SUB03910
SUB03920
SUB03930
SUB03940
SUB03950
SUB03960
SUB03970
SUB03980
SUB03990
SUB04000
SUB04010
SUB04020
SUB04030
SUB04040
SUB04050
SUB04060
SUB04070
SUB04080
SUB04090
SUB04100
SUB04110
SUB04120
SUB04130
SUB04140
SUB04150
SUB04160
SUB04170
SUB04180
SUB04190
SUB04200
SUB04210
SUB04220
SUB04230
SUB04240
SUB04250
SUB04260

11 DO 11 J=1,JJMX
    RJM=J-1
    SCF(J,1)=0.
    SCF(J,2)=1.
    SCF(J,3)=SIN(RJM*DXI-PIE)
    SCF(J,4)=COS(RJM*DXI-PIE)
    SCF(J,5)=0.
    SCF(J,6)=0.
    MS=0
    COMMENTE THE M LOOP:
    SIGN=-SIGN
    K=0
    RK=K
    ARM=1.
    IF (M.NE.0) ARM=AR**M
    KTIMER=0
    SIGNK=-1.
    COMPUTE THE K=0 & K=1 ORDERS OF LAGUERRE POLYNOMIAL FOR GIVEN M:
    PM=0.
    P=SQRT(1./FM)
    PP=(RM+1.-ARG)*SQRT(1./FM/(RM+1.))
    C ADVANCE THE SIN/COS ARRAY FOR NEW M:
    DO 12 J=1,JJMX
        SCF(J,1)=SCF(J,1)*SCF(J,4)+SCF(J,2)*SCF(J,3)
        SCF(J,2)=SCF(J,2)*SCF(J,1)-SCF(J,3)
    DO 13 J=1,JMAX
        SCF(J,5)=SCF(J+1,1)-SCF(J,1)
        SCF(J,6)=SCF(J+1,2)-SCF(J,2)
    C TEST FOR SYMMETRY SKIPS:
    IF (MS.EQ.MSYM) MS=0
    TOTAL=0.
    MS=MS+1
    IF (MS.NE.1) GO TO 7
    RMS=RM*SIG
    CMS=COS(RMS)
    SMS=SIN(RMS)
    COMMENTE THE K LOOP:
    INDEX=INDEX+1
    SIGNK=-SIGNK
    CALL THE B & D COEFFICIENTS AND COMPUTE THE M,K SUMMATION TERM:
    CALL BD (M,K,G,H,SCF,B,D,JJMX6)
    IF (DGN.LE.-2.) WRITE (6,89) M,K,B,D
    BRACKET=B
    IF(RM.EQ.0.) GO TO 4
    BRACKET=B*CMS+D*SMS
    ADD=SIGNK*BRACKET*P*ARM
    TOTAL=TOTAL+ADD
    C ESTABLISH CHECK AS THE RELATIVE SIZE OF THE M,K TERM OF THE SERIES:

```



```

SUB04270
SUB04280
SUB04290
SUB04300
SUB04310
SUB04320
SUB04330
SUB04340
SUB04350
SUB04360
SUB04370
SUB04380
SUB04390
SUB04400
SUB04410
SUB04420
SUB04430
SUB04440
SUB04450
SUB04460
SUB04470
SUB04480
SUB04490
SUB04500
SUB04510
SUB04520
SUB04530
SUB04540
SUB04550
SUB04560
SUB04570
SUB04580
SUB04590
SUB04600
SUB04610
SUB04620
SUB04630
SUB04640
SUB04650
SUB04660
SUB04670
SUB04680
SUB04690
SUB04700
SUB04710
SUB04720
SUB04730
SUB04740

CHECK=ABS(ADD)
IF (TOTAL.GT.EPS) CHECK=ABS(ADD/TOTAL)
ADVANCE THE K INDEX:
K=K+1
RK=K
ORDER=M+2*K+1
GENERATE THE NEXT ORDER OF LAGUERRE POLYNOMIAL FOR NEW K:
P=PP
PP=PP*(ORDER-ARG)-PM*SQRT(RK*(RM+RK))
PP=PP/SQRT((RK+1.)*(RM+RK+1.))
GENERATE THE NEXT ORDER OF THE SET OF HERMITE POLYNOMIALS FOR NEW K:
HA=SQRT(RK*(RK+RM))/ORDER
HB=2.*SQRT((RK+1.)*(RM+RK+1.))/(ORDER+1.)/(ORDER+2.)
DO 5 II=1, IIMX2
IIM=IIMX-II+1
H(II,1)=2.*(H(II,3)*H(II,2)-HA*(H(II,1)))
H(II,1)=SIGN*(H(II,1))
H(II,2)=HB*(H(II,3)*H(II,1)-ORDER*(H(II,2)))
5 SET K TIMER TO PROVIDE EXTRA K TERMS AFTER CHECK < EPS:
KTIMER=KTIMER+1
IF (K.GE.KLIMIT) GO TO 6
IF (CHECK.GE.EPS) KTIMER=0
IF (KTIMER.LE.KEXTRA) GO TO 3
GO TO 7
C END OF K LOOP: ADVANCE M AND COMPUTE NEW TOTAL:
6 KOUT=KOUT+1
7 M=M+1
IF (K.GT.KMAX) KMAX=K
RM=M
FM=FM*RM
C REGENERATE THE HERMITE ARRAY FOR NEW M, K=0:
DO 8 II=1, IIMX2
IIM=IIMX-II+1
H(II,2)=H(II,4)*SQRT(RM)/(RM+1.)
H(II,1)=H(II,5)*(RM+2.)
H(II,1)=-SIGN*(H(II,1))
H(II,2)=-SQRT(RM+1.)*H(II,3)+H(II,1)*H(II,2)
H(II,4)=H(II,1)
H(II,5)=H(II,2)
8 SET M TIMER FOR EXTRA M TERMS:
IF (MSE.EQ.1) MTIMER=MTIMER+1
IF (JSYM.GT.JMAX) GO TO 9
IF (K.GT.KEXTRA) MTIMER=0
IF (M.GE.MLIMIT) GO TO 9
IF (MTIMER.LE.MEXTRA) GO TO 2
C END OF M LOOP: COMPUTE OUTPUT SOLN.

```

```

9      MOUT=M-1
      IF (KOUT.EQ.0) KOUT=KMAX-1
      SOLN=TOTAL*EXPON*APP/2.
      FORMAT ('M=',I4,' K=',I4,' B=',E10.4,' D=',E10.4)
      RETURN
      END
C000005
C
SUBROUTINE GARRAY (G,GA,NOF,DGN,NUMB,XO,YO,PHISYM)
C
C      GARRAY FILLS THE DATA ARRAY OVER AN ORTHOGONAL AREA WITH
C      THE REGULAR DATA OBTAINED BY THE METHOD CORRESPONDING TO THE
C      PARTICULAR MODE:
C
C      MODE 1 -- DATA OBTAINED BY SAMPLING A KNOWN FUNCTION SUPPLIED
C      IN SUBROUTINE FUNCT AND SAMPLED IN SUBROUTINE GOLF.
C
C      MODE 2 -- DATA OBTAINED BY GENERATING A REGULAR ARRAY FROM
C      IRREGULAR EXPERIMENTAL INPUT DATA READ IN. CALLS
C      SUBROUTINE SHEET. (EXPERIMENTAL DATA MAY
C      BE SIMULATED, SEE 'SHEET')
C
C      MODE 3 -- UTILIZES RAW DATA TAKEN AT THE PROPER INTERVAL,
C      OR PREVIOUSLY GENERATED, AND READ DIRECTLY INTO THE
C      GARRAY. CALLS SUBROUTINE READ.
C
COMMON IMAX,JMAX,IMX,JMX,IJMX,ALPHA,SIZE,EPS,MODE,BOX,SD,IX,Z
COMMON /SYM/ ISYM,JSYM,MSYM,FCU,IMS,JMS,QSYM
COMMON /IO/ CMS,IN1,IN2,IN4
DIMENSION G(IMAX,JMAX),GA(IMAX,JMAX)
PIE=3.141592653589793
HS=SIZE/2.
IF (MODE.GT.3) MODE=1
RIMX=IMAX
RJMX=JMAX
DELR=SIZE/RIMX
DELXI=2.*PIE/FCU
IF (MODE.GT.1) GO TO 2
DO 1 J=1,JMS
RJ=J
XI=(RJ-.5)*DELXI-PIE
J2=J+2*(JMS-J)
J3=J+JMAX/2
J4=J2+JMAX/2
SUB04750
SUB04760
SUB04770
SUB04780
SUB04790
SUB04800
SUB04810
SUB04820
SUB00010
SUB00020
SUB00030
SUB00040
SUB00050
SUB00060
SUB00070
SUB00080
SUB00090
SUB00100
SUB00110
SUB00120
SUB00130
SUB00140
SUB00150
SUB00160
SUB00170
SUB00180
SUB00190
SUB00200
SUB00210
SUB00220
SUB00230
SUB00240
SUB00250
SUB00260
SUB00270
SUB00280
SUB00290
SUB00300
SUB00310
SUB00320
SUB00330
SUB00340
SUB00350
SUB00360
SUB00370
SUB00380

```

```

SUB000390
SUB000400
SUB000410
SUB000420
SUB000430
SUB000440
SUB000450
SUB000460
SUB000470
SUB000480
SUB000490
SUB000500
SUB000510
SUB000520
SUB000530
SUB000540
SUB000550
SUB000560
SUB000570
SUB000580
SUB000590
SUB000600
SUB000610
SUB000620

DO 1 I=1,IMS
RI=I
II=IMAX+1-I
R=(RI-.5)*DELR-HS
CALL GOLF (R,XI,GIJ,NOF,DGN,NUMB)
G(I,J)=GIJ
IF (ISYM.EQ.2) G(II,J)=GIJ
IF (ISYM.EQ.2) GO TO 1
G(II,J3)=GIJ
IF (JSYM.EQ.0) GO TO 1
G(II,J2)=GIJ
G(II,J4)=GIJ
CONTINUE
GO TO 4
1 IF (MODE.GT.2) GO TO 3
2 CALL SHEET (G,GA,XO,YO,PHISYM,NOF)
GO TO 4
3 CALL READ (Z,XO,YO,PHISYM,NOF,IMAX,JMAX,G)
4 IF (DGN.GE.2) WRITE (6,39)
39 RETURN
FORMAT (' GARRAY RETURNS')
END
C000006
C

```

```

SUB000630
SUB000640
SUB000650
SUB000660
SUB000670
SUB000680
SUB000690
SUB000700
SUB000710
SUB000720
SUB000730
SUB000740
SUB000750
SUB000760
SUB000770
SUB000780
SUB000790
SUB000800
SUB000810
SUB000820
SUB000830
SUB000840

SUBROUTINE GOLF (R,XI,GIJ,NOF,DGN,NUMB)
C
C GOLF COMPUTES THE FUNCTION G(R,XI) FOR A PARTICULAR LINE OF SIGHT
C FROM A KNOWN FUNCTION CONTAINED IN SUBROUTINE FUNCT.
C
COMMON IMAX,JMAX,IIMX,JJMX,IJMX,ALPHA,SIZE,EPS,MODE,BOX,SD,IX,Z
ZERO=0.
LMAX=IMAX*3
RLMAX=LMAX
DELXP=SIZE/RLMAX
SXI=SIN(XI)
CXI=COS(XI)
DELYS=DELXP*CXI
DELYS=DELXP*SXI
XP=DELXP*.5-SIZE/2.
XS=XP*CXI-R*SXI
YS=XP*SXI+R*CXI
GIJ=0.
DO 1 L=1,LMAX
RL=L
CALL FUNCT(XS,YS,F,NOF,DGN,NUMB)
GIJ=GIJ+F

```

```

SUB00850
SUB00860
SUB00870
SUB00880
SUB00890
SUB00900
SUB00910
SUB00920
SUB00930
SUB00940
SUB00950
SUB00960
SUB00970
SUB00980

XS=XS+DELYS
YS=YS+DELYS
IF (GIJ.NE.0.) GIJ=GIJ*DELXP*BOX
IF ((SD.EQ.0.) OR (NUMB.EQ.1)) GO TO 2
IF (DGN.GE.3) WRITE (6,28) IX
CALL GAUSS (IX,SD,ZERO,RV)
GIJ=GIJ+RV
IF (DGN.GE.3) WRITE (6,29) R,XI,GIJ
RETURN
FORMAT (' R= ',F8.3,' ', XI=' ',F8.3,' ', GIJ=' ',F8.3)
FORMAT (' GAUSS; IX= ',I8)
END
C000007
C

```

```

SUBROUTINE FUNCT (XS,YS,F,NOF,DGN,NUMB)
C
SUB00990
SUB01000

```

```

CP67USERID 1095BOXJ
C
C FUNCT EVALUATES AS INPUT FUNCTION AT POSITION (X,Y) IN THE TEST
C SECTION COORDINATE SYSTEM. NOF IDENTIFIES THE EQUATION USED.
C
COMMON IMAX,JMAX,IIMX,JJMX,IJMX,ALPHA,SIZE,EPS,MODE,BOX,SD,IX,Z
CCMMON /EQPAR/ A,B,C,D,E,P,Q,S,T,U,V,W,RO,RA,NO,NA,NI,N2
DIMENSION RO(101),RA(101)
AA=A
BB=B
CC=C
DD=D
EE=E
PP=P
IF (NUMB.LE.1) GO TO 50
AA=S
BB=T
CC=U
DD=V
EE=W
PP=Q
PIE=3.141592653589793
HS=SIZE/2.
R=SQRT(XS**2+YS**2)/HS
F=0.
IF (R.GT.1.) GO TO 11
IF (NOF.LE.0) GO TO 11
C 1. AXISYMMETRIC GAUSSIAN:
SUB01020
SUB01030
SUB01040
SUB01050
SUB01060
SUB01070
SUB01080
SUB01090
SUB01100
SUB01110
SUB01120
SUB01130
SUB01140
SUB01150
SUB01160
SUB01170
SUB01180
SUB01190
SUB01200
SUB01210
SUB01220
SUB01230
SUB01240
SUB01250
SUB01260
SUB01270
SUB01280

```

```

1      IF (NOF.GT.1) GO TO 2
      F=AA*EXP(-1.*(R*HS/BB)**2)
      GO TO 11
C
2      2. ADJUSTABLE RECTANGULAR STEP FUNCTION:
      IF (NOF.GT.2) GO TO 3
      F=PP
      IF ((ABS(XS-DD).LE.BB).AND.(ABS(YS-EE).LE.CC)) F=AA
      GO TO 11
C
3      3. DISPLACABLE ELLIPTICAL GAUSSIAN:
      IF (NOF.GT.3) GO TO 4
      F=AA*EXP(-1.*(XS-DD)/BB)**2+((YS-EE)/CC)**2)
      GO TO 11
C
4      4. CONSTANT:
      IF (NOF.GT.4) GO TO 5
      F=AA
      GO TO 11
C
5      5. ADJUSTABLE AND DISPLACABLE ELLIPTIC RAMP FUNCTION:
      IF (NOF.GT.5) GO TO 6
      RBC=SQRT((XS-DD)/BB)**2+((YS-EE)/CC)**2)
      F=0.
      IF (RBC.LT.1.) F=AA*((1.-RBC)**PP)
      GO TO 11
C
6      6. DISPLACABLE ELLIPTIC STEP FUNCTION:
      IF (NOF.GT.6) GO TO 7
      RBC=SQRT((XS-DD)/BB)**2+((YS-EE)/CC)**2)
      F=0.
      IF (RBC.LT.1.) F=AA
      GO TO 11
C
7      7. CIRCULAR COSINE-SQUARED FUNCTION OF BB MAXIMA:
      IF (NOF.GT.7) GO TO 8
      F=AA*COS((2.*BB-1.)*PIE/R/2.))**2
      GO TO 11
C
8      8. NUMERICAL FUNCTION: REQUIRES AN INPUT ARRAY READ IN BY
      SUBROUTINE FREAD; N FOLLOWED BY N POINT VALUES. (101 MAX)
      A CONSTANT VALUE AA IS ADDED TO THE FUNCTION.
      IF (NOF.GT.8) GO TO 9
      IF (NUMB.LE.1) N=NO
      IF (NUMB.GT.1) N=NA
      NM=N-1
      NMM=N-2
      RN=N
SUB01290
SUB01300
SUB01310
SUB01320
SUB01330
SUB01340
SUB01350
SUB01360
SUB01370
SUB01380
SUB01390
SUB01400
SUB01410
SUB01420
SUB01430
SUB01440
SUB01450
SUB01460
SUB01470
SUB01480
SUB01490
SUB01500
SUB01510
SUB01520
SUB01530
SUB01540
SUB01550
SUB01560
SUB01570
SUB01580
SUB01590
SUB01600
SUB01610
SUB01620
SUB01630
SUB01640
SUB01650
SUB01660
SUB01670
SUB01680
SUB01690
SUB01700
SUB01710
SUB01720
SUB01730
SUB01740
SUB01750
SUB01760

```

```

SUB01770
SUB01780
SUB01790
SUB01800
SUB01810
SUB01820
SUB01830
SUB01840
SUB01850
SUB01860
SUB01870
SUB01880
SUB01890
SUB01900
SUB01910
SUB01920
SUB01930
SUB01940
SUB01950
SUB01960
SUB01970
SUB01980
SUB01990
SUB02000
SUB02010
SUB02020
SUB02030

SUB02040
SUB02050
SUB02060
SUB02070
SUB02080
SUB02090
SUB02100
SUB02110
SUB02120
SUB02130
SUB02140
SUB02150
SUB02160

RI=R*(RN-1.)+1.
IR=INT(RI)
RIR=FLOAT(IR)
DI=RIR-RIR
IF (NUMB.LE.1) F=RO(IR)
IF (NUMB.GT.1) F=RA(IR)
IF ((IR.NE.N).AND.(NUMB.LE.1)) F=F+DI*(RO(IR+1)-RO(IR))
IF ((IR.NE.N).AND.(NUMB.GT.1)) F=F+DI*(RA(IR+1)-RA(IR))
F=F*AA+BB
GO TO 11

C 9. SPECIAL FUNCTION: MAY BE WRITTEN FOR THE OCCASION AND
C INSERTED IN SUBROUTINE SPFUN
C 9 IF (NOF.GT.9) GO TO 10
C CALL SPFUN (XS,YS,F)
C GO TO 11

C EQUATIONS NO. 10 AND BEYOND ARE SET TO ZERO.
10 F=0.
C
C 11 IF (DGN.GE.4) WRITE (6,99) XS,YS,F
99 FORMAT (' F8.3',, YS=' F8.3',, F=' F8.3')
RETURN
END
C000008
C

SUBROUTINE SPFUN (XS,YS,F)
C SPFUN IS A SPECIAL ROUTINE FOR EQ'N NO. 9. ANY FUNCTION MAY BE
C ENTERED.
C CCMON /EQPAR/ A,B,C,D,E,P,Q,S,T,U,V,W,RO,RA,NG,NA,N1,N2
C DIMENSION RO(101),RA(101)
F=0.
IF ((ABS(XS).LE.B).AND.(ABS(YS).LE.C)) F=A
RETURN
END
C000009
C

```



```

SUBROUTINE SHEET (G,D,XO,YO,PHISYM,NOF)
SHEET READS IRREGULARLY SPACED VALUES OF THE LINE INTEGRAL, AS
OBTAINED FROM HOLOGRAPHIC INTERFEROGRAMS. THE INTEGRAL LINES MAY BE
DEFINED EITHER BY GRID INTERCEPT POSITIONS, OR BY ANGLE AND RADIUS
ABOUT THE CENTER OF THE LABORATORY COORDINATE SYSTEM CENTER. LINES
MUST BE ENTERED IN CONSECUTIVE ORDER FROM LOWEST (NEG.) TO HIGHEST
(POS.) RADIUS. DATA MAY BE SIMULATED BY SPECIFYING NCODE=1,
FOLLOWED BY APERTURE POSITIONS FOR A FUNCTION NUMBER IN 'SUBFUNCT'.
C          CCMON I MAX, JMAX, IIMX, JJMX, IJMX, ALPHA, SIZE, EPS, MODE, BOX, SD, IX, Z
C          COMMON /SYM/ ISYM, JSYM, MSYM, FCU, IMS, JMS, QSYM
C          COMMON /IO/ CMS, IN1, IN2, IN4
C          DIMENSION G(I MAX, JMAX), D(I MAX, JMAX), XI(303), RR(303)
C          DIMENSION XG(303), XD(303), YG(303), YD(303), XY(303)
C          NAR=303
C          PIE=3.141592653589793
C          MP IE=-PIE
C          TP IE=2.*PIE
C          MP IT=MP IE/2.
C          PI ET=PI E/2.
C          ZERO THE ARRAYS:
C          DO 1 J=1, JMAX
C          DO 1 I=1, I MAX
C          G(I, J)=0.
C          D(I, J)=0.
C          DO 2 I=1, NAR
C          XG(I)=0.
C          XD(I)=0.
C          YG(I)=0.
C          YD(I)=0.
C          XY(I)=0.
C          XI(I)=0.
C          RR(I)=0.
C          READ THE BASIC DATA:
C          IF (CMS.EQ.1.) REWIND 1
C          READ (IN1, 59) NOF, NCODE
C          READ (IN1, 58) Z, XO, YO, PHISYM, XMN, YMN, YMX, YMN
C          READ (IN1, 59) JM
C          RIMX=I MAX
C          DR=SIZE/RIMX
C          R=(-DR-SIZE)/2.
C          RZO=SQRT(XO**2+YO**2)
C          GAM=ATANM(YO, XO)
C          TP=3- ISYM
C          BT=JSYM
C          DAN=PIE*TP/BT
C          HS=SIZE/2.
SUB02170
SUB02180
SUB02190
SUB02200
SUB02210
SUB02220
SUB02230
SUB02240
SUB02250
SUB02260
SUB02270
SUB02280
SUB02290
SUB02300
SUB02310
SUB02320
SUB02330
SUB02340
SUB02350
SUB02360
SUB02370
SUB02380
SUB02390
SUB02400
SUB02410
SUB02420
SUB02430
SUB02440
SUB02450
SUB02460
SUB02470
SUB02480
SUB02490
SUB02500
SUB02510
SUB02520
SUB02530
SUB02540
SUB02550
SUB02560
SUB02570
SUB02580
SUB02590
SUB02600
SUB02610
SUB02620
SUB02630
SUB02640

```

SUB02650
 SUB02660
 SUB02670
 SUB02680
 SUB02690
 SUB02700
 SUB02710
 SUB02720
 SUB02730
 SUB02740
 SUB02750
 SUB02760
 SUB02770
 SUB02780
 SUB02790
 SUB02800
 SUB02810
 SUB02820
 SUB02830
 SUB02840
 SUB02850
 SUB02860
 SUB02870
 SUB02880
 SUB02890
 SUB02900
 SUB02910
 SUB02920
 SUB02930
 SUB02940
 SUB02950
 SUB02960
 SUB02970
 SUB02980
 SUB02990
 SUB03000
 SUB03010
 SUB03020
 SUB03030
 SUB03040
 SUB03050
 SUB03060
 SUB03070
 SUB03080
 SUB03090
 SUB03100
 SUB03110
 SUB03120

```

MXY=1
IF((XMX.NE.0.)OR.(XMN.NE.0.)OR.(YMX.NE.0.)OR.(YMN.NE.0.))MXY=0
IF (MXY.EQ.1) GO TO 3
XMX=XO+HS
YMX=YO+HS
XMN=XO-HS
YMN=YO-HS
C COMMENCE THE READ AND FILL LOOP:
3 DO 12 J=1, JM
  READ (INI,59) IM
  MN=0
  XH=0.
  YH=0.
C READ THE LINES, DETERMINE CODE, CALCULATE RADIUS & ANGLE FOR CODE 1:
DO 5 I=1, IM
  IF(NCODE.LE.0)READ(INI,58) XD(I), YD(I), XG(I), YG(I), D(I, J), RR(I),
  1 XI(I), XY(I)
  IF(NCODE.GE.1)CALL SIM(XD(I), YD(I), XG(I), YG(I), RR(I), XI(I),
  1 XY(I), XO, YO, PHISYM, XMX, XMN, YMX, YMN, NOF, I, IM)
  IF ((XY(I)).EQ.3.) GO TO 5
  IF ((XD(I)).NE.0.)OR.(YD(I).NE.0.)) XY(I)=1.
  IF ((XG(I)).NE.0.)OR.(YG(I).NE.0.)) XY(I)=1.
  IF ((RR(I)).NE.0.)OR.(XI(I).NE.0.))AND.(XY(I).EQ.0.) XY(I)=2.
  IF ((XY(I)).EQ.0.)AND.(D(I, J).NE.0.)) XY(I)=2.
  IF ((XY(I)).NE.1.) GO TO 4
  DEN=SQRT((XG(I)-XD(I)-YD(I))*2)
  IF (DEN.EQ.0.) XY(I)=4.
  IF (XY(I).EQ.4.) GO TO 4
  RR(I)=((XO-XD(I))*(YG(I)-YD(I))-(XG(I)-XD(I))*(YO-YD(I)))/DEN
  XI(I)=ATANM((YG(I)-YD(I)), (XG(I)-XD(I)))
  XIM=XI(I)
  IF (XY(I).EQ.2.) XIM=XI(I)
  XIN=XIM
  IF(XY(I).EQ.2.) RR(I)=RR(I)+RZO*SIN(GAM-XI(I))
  CONTINUE
C COMPUTE MAX AND MIN ANGLE INDEXES FOR APERATURE POSITION LOCATION:
DO 6 I=1, IM
  IF((XY(I)).NE.1.)OR.(XY(I).NE.2.) GO TO 6
  IF (XI(I)).GT.XIM) XIM=XI(I)
  IF (XI(I)).GT.XIM) IMT=I
  IF (XI(I)).LT.XIN) XIN=XI(I)
  IF (XI(I)).LE.XIN) INT=I
  CONTINUE
6 DETERMINE APERATURE LOCATION:
LPR=0
XID=XI(IMT)-XI(INT)
IF(ABS(XID).LT.00001) LPR=1
XIH=(XI(IMT)+XI(INT))/2.

```

SUB03130
 SUB03140
 SUB03150
 SUB03160
 SUB03170
 SUB03180
 SUB03190
 SUB03200
 SUB03210
 SUB03220
 SUB03230
 SUB03240
 SUB03250
 SUB03260
 SUB03270
 SUB03280
 SUB03290
 SUB03300
 SUB03310
 SUB03320
 SUB03330
 SUB03340
 SUB03350
 SUB03360
 SUB03370
 SUB03380
 SUB03390
 SUB03400
 SUB03410
 SUB03420
 SUB03430
 SUB03440
 SUB03450
 SUB03460
 SUB03470
 SUB03480
 SUB03490
 SUB03500
 SUB03510
 SUB03520
 SUB03530
 SUB03540
 SUB03550
 SUB03560
 SUB03570
 SUB03580
 SUB03590
 SUB03600

```

RRH=10000.
XH=RRH#COS(XIH)
YH=RRH#SIN(XIH)
IF (LPR.EQ.1) GO TO 7
YT X=-RR(IMT)*SIN(XI(IMT))-YO
YTN=-RR(INT)*SIN(XI(INT))-YO
XT X=RR(IMT)*COS(XI(IMT))-XO
XTN=RR(INT)*COS(XI(INT))-XO
UA=TAN(XI(IMT))
UC=TAN(XI(INT))
UB=YTX-UA*XTX
UD=YTN-UC*XTN
UH=XH#UA+UB
RRH=SQRT((XH-XO)**2+(YH-YO)**2)
XIH=ATANM((YH-YO),(XH-XO))
CONTINUE
7 C FILL THE ANGLE AND RADIUS FOR ANY CODE 3 OR 4 LINES:
DO 9 I=1,IM
IF(XY(I).NE.3.) GO TO 8
BAS=SQRT(RRH**2-RR(I)**2)
XI(I)=XIH-ATANM(RR(I),BAS)
GO TO 9
8 XI(I)=ATANM((YH-YD(I)),(XH-XD(I)))
RR(I)=RRH#SIN(XI(I)-XIH)
CONTINUE
9 C ANGLES AND RADII ARE NOW FILLED FOR ALL POINTS IN THIS LINE.
C VACATE THE SET OF VECTORS TO BE USED AS TEMPORARY STORAGE:
DO 10 I=1,IM
XD(I)=0.
YD(I)=0.
XG(I)=0.
YG(I)=RR(I)
XY(I)=D(I,J)
RR(I)=0.
DI(J)=0.
XI(I)=0.
10 C CONVERT THE LINE TO REGULAR RADII USING INTERPOLATION:
RR(1)=R+DR
CALL SPLINE(YG,XY,XY,IM,RR(1),D(1,J))
DO 11 I=2,IMAX
RI=I
RR(I)=R+DR*RI
CALL SPLINN(YG,XY,XY,IM,RR(I),D(I,J))
11 C GENERATE THE VECTOR OF ANGLES FOR THIS COLUMN AND STORE IN G ARRAY:
DO 12 I=1,IMAX
BAS=SQRT(RRH**2-RR(I)**2)
G(I,J)=XIH-ATANM(RR(I),BAS)

```

```

12 YG(I)=0.
C D(I,J)=XY(I)
C XY(I)=0.
C COLUMNS ARE NOW ALL REGULARLY FILLED.
C NEXT, INTERPOLATE EACH ROW REGULARLY OVER THE ANGLES.
C DO 23 I=1,IMAX
C EXPAND THE DATA TO 2 SETS TO ESTABLISH SMOOTH INTERPOLATION.
JM3=3*JM
II=IMAX+1-I
IF (JSYM.NE.0) GO TO 14
DO 13 J=1,JMS
J2=J+JMS
J3=J2+JMS
XD(J)=D(I,J)
XD(J2)=D(I,J)
XD(J3)=D(I,J)
XG(J)=G(I,J)-PIE-PHISYM
XG(J2)=G(I,J)-PIE-PHISYM
XG(J3)=G(I,J)-PHISYM
GO TO 16
DO 15 J=1,JMS
J1=JMS+1-J
J2=JMS+J
J3=JM3+1-J
XD(J1)=D(I,J)
XD(J2)=D(I,J)
XD(J3)=D(I,J)
XG(J1)=G(I,J)-2.*(G(I,J)-PHISYM)-PIE-PHISYM
XG(J2)=G(I,J)-PIE-PHISYM
XG(J3)=G(I,J)+2.*(DAN+PHISYM-G(I,J))-PIE-PHISYM
CONTINUE
JM2=2*JMS
JP=JMS/2
DO 17 J=1,JM2
XD(J)=XD(J+JP)
XG(J)=XG(J+JP)
JJS=JM2+1
DO 18 J=JJS,JM3
XD(J)=0.
XG(J)=0.
FIND THE SMALLEST ANGLE
XY(1)=1.
SA=XG(1)
DO 19 J=1,JM2
IF (XG(J).GE.SA) GO TO 19
SA=XG(J)
XY(1)=J
CONTINUE

```

```

SUB03610
SUB03620
SUB03630
SUB03640
SUB03650
SUB03660
SUB03670
SUB03680
SUB03690
SUB03700
SUB03710
SUB03720
SUB03730
SUB03740
SUB03750
SUB03760
SUB03770
SUB03780
SUB03790
SUB03800
SUB03810
SUB03820
SUB03830
SUB03840
SUB03850
SUB03860
SUB03870
SUB03880
SUB03890
SUB03900
SUB03910
SUB03920
SUB03930
SUB03940
SUB03950
SUB03960
SUB03970
SUB03980
SUB03990
SUB04000
SUB04010
SUB04020
SUB04030
SUB04040
SUB04050
SUB04060
SUB04070
SUB04080

```

```

C      FIND THA MAX ANGLE IN THE ROW:
XY(JM2)=JM2
SB=XG(JM2)
DO 20 J=1,JM2
IF (XG(J).LE.SB) GO TO 20
SB=XG(J)
XY(JM2)=J
CONTINUE
20  DETERMINE THE ORDER OF INCREASING ANGLE IN THE ROW
    SB=XG(JM2)
    JJ=2
    JSA=XY(JJ-1)
    SA=XG(JJ-1)
    JTS=0
    DO 22 J=1,JM2
    IF (XG(J).LE.SA) GO TO 22
    IF (XG(J).GT.SB) GO TO 22
    SB=XG(J)
    XY(JJ)=J
    JTS=1
    CONTINUE
22  IF (JTS.EQ.0) JM2=JJ
    JJ=JJ+1
    IF (JJ.LE.JM2) GO TO 21
    DO 23 J=1,JM2
    JX=XY(J)
    YD(J)=XD(JX)
23  INTERPOLATE:
    DXI=2.*PIE/FCU
    XI(J)=DXI/2.-PIE-PHISYM
    CALL SPLINE (XG,YD,JM2,XI(J),G(I,J))
    DO 24 J=2,JMS
    XI(J)=XI(J-1)+DXI
    CALL SPLINN (XG,YD,JM2,XI(J),G(I,J))
    DO 25 J=1,JMS
    XIJ=XI(J)
    XU=XXM
    IF ((XIJ.GE.0.).AND.(XIJ.LT.PIE)) XU=XMN
    YU=YMN
    IF ((XIJ.GE.MPIT).AND.(XIJ.LT.PIT)) YU=YMX
    XL=XMN
    IF ((XIJ.GE.0.).AND.(XIJ.LT.PIE)) XL=XXM
    YL=YMX
    IF ((XIJ.GE.MPIT).AND.(XIJ.LT.PIT)) YL=YMN
    SXIJ=SIN(XIJ)
    CXIJ=COS(XIJ)
    RMN=(XC-XL)*SXIJ-(YO-YL)*CXIJ
    RMX=(XO-XU)*SXIJ-(YO-YU)*CXIJ

```

```

SUB04090
SUB04100
SUB04110
SUB04120
SUB04130
SUB04140
SUB04150
SUB04160
SUB04170
SUB04180
SUB04190
SUB04200
SUB04210
SUB04220
SUB04230
SUB04240
SUB04250
SUB04260
SUB04270
SUB04280
SUB04290
SUB04300
SUB04310
SUB04320
SUB04330
SUB04340
SUB04350
SUB04360
SUB04370
SUB04380
SUB04390
SUB04400
SUB04410
SUB04420
SUB04430
SUB04440
SUB04450
SUB04460
SUB04470
SUB04480
SUB04490
SUB04500
SUB04510
SUB04520
SUB04530
SUB04540
SUB04550
SUB04560

```

```

SUB04570
SUB04580
SUB04590
SUB04600
SUB04610
SUB04620
SUB04630
SUB04640
SUB04650
SUB04660
SUB04670
SUB04680
SUB04690
SUB04700
SUB04710
SUB04720
SUB04730
SUB04740
SUB04750
SUB04760

SUB04780
SUB04790
SUB04800
SUB04810
SUB04820
SUB04830
SUB04840
SUB04850
SUB04860

SUB04870
SUB04880
SUB04890
SUB04900
SUB04910
SUB04920
SUB04930
SUB04940
SUB04950
SUB04960
SUB04970
SUB04980
SUB04990
SUB05000
SUB05010

DO 25 I=1,IMAX
IF (RR(I).LT.RMN) G(I,J)=0.
IF (RR(I).GT.RMX) G(I,J)=0.
CONTINUE
EXPAND SYMMETRY SECTOR INTO AN ORTHOGONAL INTERVAL.
IF (ISYM.EQ.2) GO TO 27
DO 26 J=1,JMS
J2=JMAX/2+1-J
J3=JMAX/2+J
J4=JMAX+1-J
DO 26 I=1,IMAX
II=IMAX+1-I
G(I,J2)=G(I,J)
G(II,J3)=G(I,J)
G(II,J4)=G(I,J)
RETURN
FOR EVEN SYMMETRY, AVERAGE THE GARRAY COLUMNS.
IMS=(2*IMAX+1)/2
DO 28 J=1,JMAX
DO 28 I=1,IMS
II=IMAX+1-I
GST=(G(I,J)+G(II,J))/2.
G(I,J)=GST
G(II,J)=GST
RETURN
FORMAT (5I5)
FORMAT (10F7.3)
END
C0J010
C

FUNCTION ATANM(Y,X)
C COMPUTES THE ARCTAN OF Y/X BETWEEN -PI AND +PI.
C
PIE=3.141592653589793
PI2=PIE/2.
ATANM=SIGN(PI2,Y)
IF(X.NE.0.) ATANM=ATAN(Y/X)
IF(X.GE.0.) RETURN
IF(Y.GE.0.) ATANM=PIE+ATANM
IF(Y.LT.0.) ATANM=-PIE+ATANM
RETURN
END
C000011
C

```



```

COMMON /IO/ CMS, IN1, IN2, IN4
DIMENSION G(IMAX, JMAX)
READ (IN1, 39) NOF, IMAX, JMAX, ISYM, JSYM, IMS, JMS
READ (IN1, 38) Z, XO, YO, PHISYM
READ (IN1, 38) ((G(I, J), I=1, IMS), J=1, JMS)
WRITE(6, 37) NOF, Z, XO, YO, PHISYM, IMAX, JMAX, JSYM
RJMX=JMAX
MSYM=JSYM
IF ((MSYM.EQ.0).OR.(MSYM.GT.JMAX)) MSYM=1
FCU=ISYM*JSYM*JMAX
IF (JSYM.GT.JMAX) FCU=JMAX
QSYM=FCU/RJMX
DO 4 J=1, JMS
IF (ISYM.EQ.1) GO TO 2
DO 1 I=1, IMS
II=IMAX+1-I
G(I, J)=G(I, J)
GO TO 4
J2=JMAX/2+1-J
J3=JMAX/2+J
J4=JMAX+1-J
DO 3 I=1, IMAX
II=IMAX+1-I
G(I, J2)=G(I, J)
G(I, J3)=G(I, J)
G(I, J4)=G(I, J)
CONTINUE
FORMAT (10I5)
FORMAT (10F7.3)
FORMAT (//, //, MDDE 3 READS GARRAY DIRECTLY: NOF='I4',
1, , XO='F7.3', YO='F7.3', PHISYM='F7.3',
2, , JMAX='I4', JSYM='I4//')
RETURN
END
C000016
C

SUBROUTINE MAP (IM, JM, A, N, Z, BAND)
C MAP CALLS SUBROUTINE MIMPII AND PLOTS A CONTOUR MAP OF THE ARRAY
C
DIMENSION A(IM, JM), T(24)
DATA BL/1H /
DO 1 I=1, 24
T(I)=BL
ICON=1
IF(BAND.LT.0.) ICON=0

```

SUB00950
SUB00960
SUB00970
SUB00980
SUB00990
SUB01000
SUB01010
SUB01020
SUB01030
SUB01040
SUB01050
SUB01060
SUB01070
SUB01080
SUB01090
SUB01100
SUB01110
SUB01120
SUB01130
SUB01140
SUB01150
SUB01160
SUB01170
SUB01180
SUB01190
SUB01200
SUB01210
SUB01220
SUB01230
SUB01240
SUB01250
SUB01260
SUB01270
SUB01280
SUB01290
SUB01300

SUB01310
SUB01320
SUB01330
SUB01340
SUB01350
SUB01360
SUB01370
SUB01380
SUB01390
SUB01400

Z='F7.3'
IMAX='I4',

NOF='I4',
PHISYM='F7.3',

YO='F7.3',
JSYM='I4//')

C000016
C

SUBROUTINE MAP (IM, JM, A, N, Z, BAND)
C MAP CALLS SUBROUTINE MIMPII AND PLOTS A CONTOUR MAP OF THE ARRAY
C

DIMENSION A(IM, JM), T(24)
DATA BL/1H /
DO 1 I=1, 24
T(I)=BL
ICON=1
IF(BAND.LT.0.) ICON=0

SUB01410
 SUB01420
 SUB01430
 SUB01440
 SUB01450
 SUB01460
 SUB01470
 SUB01480
 SUB01490
 SUB01500
 SUB01510
 SUB01520

```

IF(BAND.LT.0.) BAND=-BAND
AMIN=0.
IJT=0
AZ=1.
BZ=0.
WRITE(6,49) N,Z
CALL MTMPII(A,IM,JM,T,BAND,AZ,BZ,AMIN,IJT,ICON)
FORMAT (1H1//, THE FUNCTION SURFACE, TEST NO.,I3, Z=F5.3//)
RETURN
END
49          C000017
C

```

SUB01530
 SUB01540
 SUB01550
 SUB01560
 SUB01570
 SUB01580
 SUB01590
 SUB01600
 SUB01610
 SUB01620
 SUB01630
 SUB01640
 SUB01650
 SUB01660
 SUB01670
 SUB01680
 SUB01690
 SUB01700
 SUB01710
 SUB01720
 SUB01730
 SUB01740
 SUB01750
 SUB01760
 SUB01770
 SUB01780
 SUB01790
 SUB01800
 SUB01810
 SUB01820
 SUB01830
 SUB01840
 SUB01850
 SUB01860

```

SUBROUTINE GPLOT (G,GA,JMS)
C
C  GPLOT PRINTS A ROUGH PLOT OF THE LINE INTEGRAL FUNCTIONS IN GARRAY.
C
COMMON IMAX,JMAX,IIMX,JJMX,IJMX,ALPHA,SIZE,EPS,MODE,BOX,SD,IX,Z
COMMON /TAB/ INDEX(7),JSYM,ISYM
COMMON /TAB2/ IPT,KPT,LPT,MPT,REST(5)
DIMENSION G(IMAX,JMAX),GA(IMAX,JMAX),ROW(101)
DIMENSION A(201),B(101),C(201),D(101)
JM=101
DATA BL,PL,ST,DH,EX/1H,1H+,1H*,1H-,1HX/
JMS2=JMAX/2+1
IF(ISYM.EQ.2)JMS2=1
JMS3=JMS2+JMS-1
DO 8 J=JMS2,JMS3
WRITE(6,67) (ST,I=1,120)
DO 1 I=1,IMAX
A(I)=G(I,J)
C(I)=GA(I,J)
AS=.5
BS=.0
CALL INTERP (A,IMAX,AS,B,JM,BS)
CALL INTERP (C,IMAX,AS,D,JM,BS)
WRITE (6,69) J
BIG=0.
SMALL=0.
DO 2 I=1,IMAX
IF(A(I).GT.BIG) BIG=A(I)
IF(C(I).GT.BIG) BIG=C(I)
IF(A(I).LT.SMALL) SMALL=A(I)
IF(C(I).LT.SMALL) SMALL=C(I)
RANGE=BIG-SMALL
RINK=RANGE/80.
TOP=BIG+RINK

```



```

SUB01870
SUB01880
SUB01890
SUB01900
SUB01910
SUB01920
SUB01930
SUB01940
SUB01950
SUB01960
SUB01970
SUB01980
SUB01990
SUB02000
SUB02010
SUB02020
SUB02030
SUB02040
SUB02050
SUB02060
SUB02070
SUB02080
SUB02090
SUB02100
SUB02110
SUB02120
SUB02130
SUB02140
SUB02150
SUB02160
SUB02170
SUB02180
SUB02190
SUB02200
SUB02210

SUB02220
SUB02230
SUB02240
SUB02250
SUB02260
SUB02270
SUB02280
SUB02290
SUB02300
SUB02310
SUB02320

CEN=BIG
BOT=BIG-RINK
KC=0
DO 7 K=1,41
IC=0
DO 6 I=1,101
ROW(I)=BL
IF((I.EQ.1).OR.(I.EQ.51).OR.(I.EQ.101)) ROW(I)=PL
IF((K.EQ.1).OR.(K.EQ.41)) ROW(I)=PL
IF((TOP.GE.0.).AND.(BOT.LE.0.)) ROW(I)=DH
IF((IC.EQ.5) GO TO 3
GO TO 4
IC=0
IF(KC.EQ.10) ROW(I)=PL
IF(KPT.LE.2) GO TO 5
IF((D(I).LE.TOP).AND.(D(I).GE.BOT)) ROW(I)=ST
IF((B(I).LE.TOP).AND.(B(I).GE.BOT)) ROW(I)=EX
IC=IC+1
IF(KC.EQ.5) KC=0
IF(KC.NE.0) WRITE (6,65) (ROW(I),I=1,101)
IF(KC.EQ.0) WRITE (6,68) CEN,(ROW(I),I=1,101)
TOP = TOP-2.*RINK
CEN=CEN-2.*RINK
BOT=BOT-2.*RINK
KC=KC+1
WRITE (6,66) (ST,I=1,120)
FORMAT (//,13//)
FORMAT (1X,F8.3,1X,101A1)
FORMAT (1H1,//121A1//)
FORMAT (//121A1//)
FORMAT (10X,101A1)
RETURN
END
C000018
C

SUBROUTINE INTERP (A,IM,AS,B,JM,BS)
INTERP CONVERTS A REGULAR VECTOR A OF IM POINTS TO A REGULAR VECTOR
B OF JM POINTS. OS=.5 FOR A VECTOR WITH POINTS DEFINED IN THE
CENTER OF THE INTERVAL. AS AND BS ARE THE % OF AN INTERVAL FROM THE
EDGE OF THE FIELD TO THE FIRST POINT (.0 OR .5 FOR EDGE OR CENTER
DEFINED POINTS)
DIMENSION A(IM),B(JM)
RIM=IM
RJM=JM

```


SPL00340
 SPL00350
 SPL00360
 SPL00370
 SPL00380
 SPL00390
 SPL00400
 SPL00410
 SPL00420
 SPL00430

DETERMINE THE COEFFICIENTS TO BE USED IN PERFORMING THE
 INTERPOLATIONS. SEARCH FOR BRACKETING ABSCISSA VALUES IS
 ALWAYS MADE FROM THE REFERENCE LAST USED IN INTERPOLATING.

REFERENCE
 PENNINGTON, RALPH H., "INTRODUCTORY COMPUTER METHODS AND
 NUMERICAL ANALYSIS", THE MACMILLAN COMPANY, NEW YORK, 1965

SPL00440
 SPL00460
 SPL00470
 SPL00480
 SPL00490
 SPL00500
 SPL00510
 SPL00520
 SPL00530
 SPL00540
 SPL00550
 SPL00560
 SPL00570
 SPL00580
 SPL00590
 SPL00600
 SPL00610
 SPL00620
 SPL00630
 SPL00640
 SPL00650
 SPL00660
 SPL00670
 SPL00680
 SPL00690
 SPL00700
 SPL00710
 SPL00720

```

SUBROUTINE SPLINE(X,Y,M,XINT,YINT)
DIMENSION X(M),Y(M),C(4,300)
CALL SPLICO(X,Y,M,C)
K=1
ENTRY SPLINN(X,Y,M,XINT,YINT)
IF(XINT-X(1)) 70,1,2
3 70 K=1
1 GO TO 7
1 YINT=Y(1)
RETURN
2 IF(XINT-X(K+1)) 6,4,5
4 YINT=Y(K+1)
RETURN
5 K=K+1
71 IF(M-K) 71,71,3
71 K=M-1
6 GO TO 7
12 IF(XINT-X(K)) 13,12,11
12 YINT=Y(K)
RETURN
13 K=K-1
6 GO TO 6
7 PRINT 101,XINT
101 FORMAT(8H0XINT = E18.9,32H, OUT OF RANGE FOR INTERPOLATION)
11 YINT=(X(K+1)-XINT)*(C(1,K))*(X(K+1)-XINT)**2+C(3,K))
11 YINT=YINT+(XINT-X(K))*(C(2,K))*(XINT-X(K))**2+C(4,K)
RETURN
END
```

SPL00730
 SPL00750
 SPL00760
 SPL00770
 SPL00780
 SPL00790

```

SUBROUTINE SPLICO(X,Y,M,C)
DIMENSION X(M),Y(M),C(4,300),D(300),P(300),E(300),A(300,3),B(300),
1Z(300)
MM=M-1
DO 2 K=1,MM
D(K)=X(K+1)-X(K)
```


C OAKES CODE 5105 15 JAN 69

MET00610
MET00620

```

SUBROUTINE MTMPII(Y,N,M,T,BND,AZ,BZ,AMIN,IJT,ICON)
REAL*4 IH,KG,I TJZ
DIMENSION A(140),B(140),C(140),D(140),IH(20),Y(N,M),TP(10),TPX(10)
Z ,TPM(10),XMT(10),BTM(10),BTX(10),BT(10),KG(10),T(24)
DIMENSION E(140),F(140),G(140),H(140)

```

MET00630
MET00640
MET00650
MET00660
MET00670
MET00680
MET00690
MET00700
MET00710
MET00720
MET00730
MET00740
MET00750
MET00760
MET00770
MET00780
MET00790
MET00800
MET00810
MET00820
MET00830
MET00840
MET00850
MET00860
MET00870
MET00880
MET00890
MET00900
MET00910
MET00920
MET00930
MET00940
MET00950
MET00960
MET00970
MET00980
MET00990
MET01000
MET01010
MET01020
MET01030
MET01040
MET01050
MET01060

```

DATA DUE/4H /,EPL/4H+ /,EMI/4H- /,IH/1H0,1H ,1H1,1H ,1H2,
11H ,1H3,1H ,1H4,1H ,1H5,1H ,1H6,1H ,1H7,1H ,1H8,1H /,KG/
21H0,1H1,1H2,1H3,1H4,1H5,1H6,1H7,1H8,1H9/,BLK/4H

```

MET00700
MET00710
MET00720
MET00730
MET00740
MET00750
MET00760
MET00770
MET00780
MET00790
MET00800
MET00810
MET00820
MET00830
MET00840
MET00850
MET00860
MET00870
MET00880
MET00890
MET00900
MET00910
MET00920
MET00930
MET00940
MET00950
MET00960
MET00970
MET00980
MET00990
MET01000
MET01010
MET01020
MET01030
MET01040
MET01050
MET01060

```

10 YMIN=Y(1,1)
20 YMAX=Y(1,1)
DO 20 I=1,M
DO 10 J=1,N
YMIN=AMINI(YMIN,Y(J,I))
YMAX=AMAXI(YMAX,Y(J,I))
CONTINUE

```

MET00700
MET00710
MET00720
MET00730
MET00740
MET00750
MET00760
MET00770
MET00780
MET00790
MET00800
MET00810
MET00820
MET00830
MET00840
MET00850
MET00860
MET00870
MET00880
MET00890
MET00900
MET00910
MET00920
MET00930
MET00940
MET00950
MET00960
MET00970
MET00980
MET00990
MET01000
MET01010
MET01020
MET01030
MET01040
MET01050
MET01060

```

10 CONTINUE
20 DELY=YMAX-YMIN
IF(BND) 25,25,30
BND=DELY/15.0
30 IF (AMIN-YMIN) 31,31,32
31 IF (IJT) 33,32,33
32 PD=YMIN/BND
PF=ABS(PD-INT(PD))
IF (YMIN) 2,1,1
AMIN=YMIN-PF*BND
GO TO 33
2 AMIN=YMIN-(1.0-PF)*BND
33 AHLD=AZ
IF(AZ) 55,35,55
35 SM=AMAXI(ABS(YMIN),ABS(YMAX))
40 NS=NS+1
NS=10.0*SM
IF(SM-1.0) 40,50,45
45 NS=NS-1
SM=SM/10.0
IF(SM-1.0) 50,50,45
50 AHLD=BND/2.0
55 PRINT 70
PRINT 6,T

```

MET00700
MET00710
MET00720
MET00730
MET00740
MET00750
MET00760
MET00770
MET00780
MET00790
MET00800
MET00810
MET00820
MET00830
MET00840
MET00850
MET00860
MET00870
MET00880
MET00890
MET00900
MET00910
MET00920
MET00930
MET00940
MET00950
MET00960
MET00970
MET00980
MET00990
MET01000
MET01010
MET01020
MET01030
MET01040
MET01050
MET01060


```

6  FORMAT(5X,24A4,/)
PRINT 57,AHLD,BZ
57  FORMAT(IH0,65H THE FOLLOWING TRANSFORMATION WAS PERFORMED ON THE IN
      1PUT MATRIX /5X,1H(E12.5,8H*Y(I,J)+,E12.5,1H) //2X,73HAND THREE
      2 DIGITS TO THE RIGHT OF THE DECIMAL POINT ARE PRINTED IN THE MAP )
C
PRINT 54,YMAX,YMIN
54  FORMAT(/4X,5HYMAX=,E15.7,5X,5HYMIN=,E15.7)
5   IF (ICON)5,58,5
11  PRINT 11,BND
      1LS
      2)
      3)
      4)
      5)
      6)
      7)
      8)
      9)
      10)
      11)
      12)
      13)
      14)
      15)
      16)
      17)
      18)
      19)
      20)
      21)
      22)
      23)
      24)
      25)
      26)
      27)
      28)
      29)
      30)
      31)
      32)
      33)
      34)
      35)
      36)
      37)
      38)
      39)
      40)
      41)
      42)
      43)
      44)
      45)
      46)
      47)
      48)
      49)
      50)
      51)
      52)
      53)
      54)
      55)
      56)
      57)
      58)
      59)
      60)
      61)
      62)
      63)
      64)
      65)
      66)
      67)
      68)
      69)
      70)
      71)
      72)
      73)
      74)
      75)
      76)
      77)
      78)
      79)
      80)
      81)
      82)
      83)
      84)
      85)
      86)
      87)
      88)
      89)
      90)
      91)
      92)
      93)
      94)
      95)
      96)
      97)
      98)
      99)
      100)
      101)
      102)
      103)
      104)
      105)
      106)
      107)
      108)
      109)
      110)
      111)
      112)
      113)
      114)
      115)
      116)
      117)
      118)
      119)
      120)
      121)
      122)
      123)
      124)
      125)
      126)
      127)
      128)
      129)
      130)
      131)
      132)
      133)
      134)
      135)
      136)
      137)
      138)
      139)
      140)
      141)
      142)
      143)
      144)
      145)
      146)
      147)
      148)
      149)
      150)
      151)
      152)
      153)
      154)
      155)
      156)
      157)
      158)
      159)
      160)
      161)
      162)
      163)
      164)
      165)
      166)
      167)
      168)
      169)
      170)
      171)
      172)
      173)
      174)
      175)
      176)
      177)
      178)
      179)
      180)
      181)
      182)
      183)
      184)
      185)
      186)
      187)
      188)
      189)
      190)
      191)
      192)
      193)
      194)
      195)
      196)
      197)
      198)
      199)
      200)
      201)
      202)
      203)
      204)
      205)
      206)
      207)
      208)
      209)
      210)
      211)
      212)
      213)
      214)
      215)
      216)
      217)
      218)
      219)
      220)
      221)
      222)
      223)
      224)
      225)
      226)
      227)
      228)
      229)
      230)
      231)
      232)
      233)
      234)
      235)
      236)
      237)
      238)
      239)
      240)
      241)
      242)
      243)
      244)
      245)
      246)
      247)
      248)
      249)
      250)
      251)
      252)
      253)
      254)
      255)
      256)
      257)
      258)
      259)
      260)
      261)
      262)
      263)
      264)
      265)
      266)
      267)
      268)
      269)
      270)
      271)
      272)
      273)
      274)
      275)
      276)
      277)
      278)
      279)
      280)
      281)
      282)
      283)
      284)
      285)
      286)
      287)
      288)
      289)
      290)
      291)
      292)
      293)
      294)
      295)
      296)
      297)
      298)
      299)
      300)
      301)
      302)
      303)
      304)
      305)
      306)
      307)
      308)
      309)
      310)
      311)
      312)
      313)
      314)
      315)
      316)
      317)
      318)
      319)
      320)
      321)
      322)
      323)
      324)
      325)
      326)
      327)
      328)
      329)
      330)
      331)
      332)
      333)
      334)
      335)
      336)
      337)
      338)
      339)
      340)
      341)
      342)
      343)
      344)
      345)
      346)
      347)
      348)
      349)
      350)
      351)
      352)
      353)
      354)
      355)
      356)
      357)
      358)
      359)
      360)
      361)
      362)
      363)
      364)
      365)
      366)
      367)
      368)
      369)
      370)
      371)
      372)
      373)
      374)
      375)
      376)
      377)
      378)
      379)
      380)
      381)
      382)
      383)
      384)
      385)
      386)
      387)
      388)
      389)
      390)
      391)
      392)
      393)
      394)
      395)
      396)
      397)
      398)
      399)
      400)
      401)
      402)
      403)
      404)
      405)
      406)
      407)
      408)
      409)
      410)
      411)
      412)
      413)
      414)
      415)
      416)
      417)
      418)
      419)
      420)
      421)
      422)
      423)
      424)
      425)
      426)
      427)
      428)
      429)
      430)
      431)
      432)
      433)
      434)
      435)
      436)
      437)
      438)
      439)
      440)
      441)
      442)
      443)
      444)
      445)
      446)
      447)
      448)
      449)
      450)
      451)
      452)
      453)
      454)
      455)
      456)
      457)
      458)
      459)
      460)
      461)
      462)
      463)
      464)
      465)
      466)
      467)
      468)
      469)
      470)
      471)
      472)
      473)
      474)
      475)
      476)
      477)
      478)
      479)
      480)
      481)
      482)
      483)
      484)
      485)
      486)
      487)
      488)
      489)
      490)
      491)
      492)
      493)
      494)
      495)
      496)
      497)
      498)
      499)
      500)
      501)
      502)
      503)
      504)
      505)
      506)
      507)
      508)
      509)
      510)
      511)
      512)
      513)
      514)
      515)
      516)
      517)
      518)
      519)
      520)
      521)
      522)
      523)
      524)
      525)
      526)
      527)
      528)
      529)
      530)
      531)
      532)
      533)
      534)
      535)
      536)
      537)
      538)
      539)
      540)
      541)
      542)
      543)
      544)
      545)
      546)
      547)
      548)
      549)
      550)
      551)
      552)
      553)
      554)
      555)
      556)
      557)
      558)
      559)
      560)
      561)
      562)
      563)
      564)
      565)
      566)
      567)
      568)
      569)
      570)
      571)
      572)
      573)
      574)
      575)
      576)
      577)
      578)
      579)
      580)
      581)
      582)
      583)
      584)
      585)
      586)
      587)
      588)
      589)
      590)
      591)
      592)
      593)
      594)
      595)
      596)
      597)
      598)
      599)
      600)
      601)
      602)
      603)
      604)
      605)
      606)
      607)
      608)
      609)
      610)
      611)
      612)
      613)
      614)
      615)
      616)
      617)
      618)
      619)
      620)
      621)
      622)
      623)
      624)
      625)
      626)
      627)
      628)
      629)
      630)
      631)
      632)
      633)
      634)
      635)
      636)
      637)
      638)
      639)
      640)
      641)
      642)
      643)
      644)
      645)
      646)
      647)
      648)
      649)
      650)
      651)
      652)
      653)
      654)
      655)
      656)
      657)
      658)
      659)
      660)
      661)
      662)
      663)
      664)
      665)
      666)
      667)
      668)
      669)
      670)
      671)
      672)
      673)
      674)
      675)
      676)
      677)
      678)
      679)
      680)
      681)
      682)
      683)
      684)
      685)
      686)
      687)
      688)
      689)
      690)
      691)
      692)
      693)
      694)
      695)
      696)
      697)
      698)
      699)
      700)
      701)
      702)
      703)
      704)
      705)
      706)
      707)
      708)
      709)
      710)
      711)
      712)
      713)
      714)
      715)
      716)
      717)
      718)
      719)
      720)
      721)
      722)
      723)
      724)
      725)
      726)
      727)
      728)
      729)
      730)
      731)
      732)
      733)
      734)
      735)
      736)
      737)
      738)
      739)
      740)
      741)
      742)
      743)
      744)
      745)
      746)
      747)
      748)
      749)
      750)
      751)
      752)
      753)
      754)
      755)
      756)
      757)
      758)
      759)
      760)
      761)
      762)
      763)
      764)
      765)
      766)
      767)
      768)
      769)
      770)
      771)
      772)
      773)
      774)
      775)
      776)
      777)
      778)
      779)
      780)
      781)
      782)
      783)
      784)
      785)
      786)
      787)
      788)
      789)
      790)
      791)
      792)
      793)
      794)
      795)
      796)
      797)
      798)
      799)
      800)
      801)
      802)
      803)
      804)
      805)
      806)
      807)
      808)
      809)
      810)
      811)
      812)
      813)
      814)
      815)
      816)
      817)
      818)
      819)
      820)
      821)
      822)
      823)
      824)
      825)
      826)
      827)
      828)
      829)
      830)
      831)
      832)
      833)
      834)
      835)
      836)
      837)
      838)
      839)
      840)
      841)
      842)
      843)
      844)
      845)
      846)
      847)
      848)
      849)
      850)
      851)
      852)
      853)
      854)
      855)
      856)
      857)
      858)
      859)
      860)
      861)
      862)
      863)
      864)
      865)
      866)
      867)
      868)
      869)
      870)
      871)
      872)
      873)
      874)
      875)
      876)
      877)
      878)
      879)
      880)
      881)
      882)
      883)
      884)
      885)
      886)
      887)
      888)
      889)
      890)
      891)
      892)
      893)
      894)
      895)
      896)
      897)
      898)
      899)
      900)
      901)
      902)
      903)
      904)
      905)
      906)
      907)
      908)
      909)
      910)
      911)
      912)
      913)
      914)
      915)
      916)
      917)
      918)
      919)
      920)
      921)
      922)
      923)
      924)
      925)
      926)
      927)
      928)
      929)
      930)
      931)
      932)
      933)
      934)
      935)
      936)
      937)
      938)
      939)
      940)
      941)
      942)
      943)
      944)
      945)
      946)
      947)
      948)
      949)
      950)
      951)
      952)
      953)
      954)
      955)
      956)
      957)
      958)
      959)
      960)
      961)
      962)
      963)
      964)
      965)
      966)
      967)
      968)
      969)
      970)
      971)
      972)
      973)
      974)
      975)
      976)
      977)
      978)
      979)
      980)
      981)
      982)
      983)
      984)
      985)
      986)
      987)
      988)
      989)
      990)
      991)
      992)
      993)
      994)
      995)
      996)
      997)
      998)
      999)
      1000)
      1001)
      1002)
      1003)
      1004)
      1005)
      1006)
      1007)
      1008)
      1009)
      1010)
      1011)
      1012)
      1013)
      1014)
      1015)
      1016)
      1017)
      1018)
      1019)
      1020)
      1021)
      1022)
      1023)
      1024)
      1025)
      1026)
      1027)
      1028)
      1029)
      1030)
      1031)
      1032)
      1033)
      1034)
      1035)
      1036)
      1037)
      1038)
      1039)
      1040)
      1041)
      1042)
      1043)
      1044)
      1045)
      1046)
      1047)
      1048)
      1049)
      1050)
      1051)
      1052)
      1053)
      1054)
      1055)
      1056)
      1057)
      1058)
      1059)
      1060)
      1061)
      1062)
      1063)
      1064)
      1065)
      1066)
      1067)
      1068)
      1069)
      1070)
      1071)
      1072)
      1073)
      1074)
      1075)
      1076)
      1077)
      1078)
      1079)
      1080)
      1081)
      1082)
      1083)
      1084)
      1085)
      1086)
      1087)
      1088)
      1089)
      1090)
      1091)
      1092)
      1093)
      1094)
      1095)
      1096)
      1097)
      1098)
      1099)
      1100)
      1101)
      1102)
      1103)
      1104)
      1105)
      1106)
      1107)
      1108)
      1109)
      1110)
      1111)
      1112)
      1113)
      1114)
      1115)
      1116)
      1117)
      1118)
      1119)
      1120)
      1121)
      1122)
      1123)
      1124)
      1125)
      1126)
      1127)
      1128)
      1129)
      1130)
      1131)
      1132)
      1133)
      1134)
      1135)
      1136)
      1137)
      1138)
      1139)
      1140)
      1141)
      1142)
      1143)
      1144)
      1145)
      1146)
      1147)
      1148)
      1149)
      1150)
      1151)
      1152)
      1153)
      1154)
      1155)
      1156)
      1157)
      1158)
      1159)
      1160)
      1161)
      1162)
      1163)
      1164)
      1165)
      1166)
      1167)
      1168)
      1169)
      1170)
      1171)
      1172)
      1173)
      1174)
      1175)
      1176)
      1177)
      1178)
      1179)
      1180)
      1181)
      1182)
      1183)
      1184)
      1185)
      1186)
      1187)
      1188)
      1189)
      1190)
      1191)
      1192)
      1193)
      1194)
      1195)
      1196)
      1197)
      1198)
      1199)
      1200)
      1201)
      1202)
      1203)
      1204)
      1205)
      1206)
      1207)
      1208)
      1209)
      1210)
      1211)
      1212)
      1213)
      1214)
      1215)
      1216)
      1217)
      1218)
      1219)
      1220)
      1221)
      1222)
      1223)
      1224)
      1225)
      1226)
      1227)
      1228)
      1229)
      1230)
      1231)
      1232)
      1233)
      1234)
      1235)
      1236)
      1237)
      1238)
      1239)
      1240)
      1241)
      1242)
      1243)
      1244)
      1245)
      1246)
      1247)
      1248)
      1249)
      1250)
      1251)
      1252)
      1253)
      1254)
      1255)
      1256)
      1257)
      1258)
      1259)
      1260)
      1261)
      1262)
      1263)
      1264)
      1265)
      1266)
      1267)
      1268)
      1269)
      1270)
      1271)
      1272)
      1273)
      1274)
      1275)
      1276)
      1277)
      1278)
      1279)
      1280)
      1281)
      1282)
      1283)
      1284)
      1285)
      1286)
      1287)
      1288)
      1289)
      1290)
      1291)
      1292)
      1293)
      1294)
      1295)
      1296)
      1297)
      1298)
      1299)
      1300)
      1301)
      1302)
      1303)
      1304)
      1305)
      1306)
      1307)
      1308)
      1309)
      1310)
      1311)
      1312)
      1313)
      1314)
      1315)
      1316)
      1317)
      1318)
      1319)
      1320)
      1321)
      1322)
      1323)
      1324)
      1325)
      1326)
      1327)
      1328)
      1329)
      1330)
      1331)
      1332)
      1333)
      1334)
      1335)
      1336)
      1337)
      1338)
      1339)
      1340)
      1341)
      1342)
      1343)
      1344)
      1345)
      1346)
      1347)
      1348)
      1349)
      1350)
      1351)
      1352)
      1353)
      1354)
      1355)
      1356)
      1357)
      1358)
      1359)
      1360)
      1361)
      1362)
      1363)
      1364)
      1365)
      1366)
      1367)
      1368)
      1369)
      1370)
      1371)
      1372)
      1373)
      1374)
      1375)
      1376)
      1377)
      1378)
      1379)
      1380)
      1381)
      1382)
      1383)
      1384)
      1385)
      1386)
      1387)
      1388)
      1389)
      1390)
      1391)
      1392)
      1393)
      1394)
      1395)
      1396)
      1397)
      1398)
      1399)
      1400)
      1401)
      1402)
      1403)
      1404)
      1405)
      1406)
      1407)
      1408)
      1409)
      1410)
      1411)
      1412)
      1413)
      1414)
      1415)
      1416)
      1417)
      1418)
      1419)
      1420)
      1421)
      1422)
      1423)
      1424)
      1425)
      1426)
      1427)
      1428)
      1429)
      1430)
      1431)
      1432)
      1433)
      1434)
      1435)
      1436)
      1437)
      1438)
      1439)
      1440)
      1441)
      1442)
      1443)
      1444)
      1445)
      1446)
      1447)
      1448)
      1449)
      1450)
      1451)
      1452)
      1453)
      1454)
      1455)
      1456)
      1457)
      1458)
      1459)
      1460)
      1461)
      1462)
      1463)
      1464)
      1465)
      1466)
      1467)
      1468)
      1469)
      1470)
      1471)
      1472)
      1473)
      1474)
      1475)
      1476)
      1477)
      1478)
      1479)
      1480)
      1481)
      1482)
      1483)
      1484)
      1485)
      1486)
      1487)
      1488)
      1489)
      1490)
      1491)
      1492)
      1493)
      1494)
      1495)
      1496)
      1497)
      1498)
      1499)
      1500)
      1501)
      1502)
      1503)
      1504)
      1505)
      1506)
      1507)
      1508)
      1509)
      1510)
      1511)
      1512)
      1513)
      1514)
      1515)
      1516)
      1517)
      1518)
      1519)
      1520)
      1521)
      1522)
      1523)
      1524)
      1525)
      1526)
      1527)
      1528)
      1529)
      1530)
      1531)
      1532)
      1533)
      1534)
      1535)
      1536)
      1537)
      1538)
      1539)
      1540)
      1541)
      1542)
      1543)
      1544)
      1545)
      1546)
      1547)
      1548)
      1549)
      1550)
      1551)
      1552)
      1553)
      1554)
      1555)
      1556)
      1557)
      1558)
      1559)
      1560)
      1561)
      1562)
      1563)
      1564)
      1565)
      1566)
      1567)
      1568)
      1569)
      1570)
      1571)
      1572)
      1573)
      1574)
      1575)
      1576)
      1577)
      1578)
      1579)
      1580)
      1581)
      1582)
      1583)
      1584)
      1585)
      1586)
      1587)
      1588)
      1589)
      1590)
      1591)
      1592)
      1593)
      1594)
      1595)
      1596)
      1597)
      1598)
      1599)
      1600)
      1601)
      1602)
      1603)
      1604)
      1605)
      1606)
      1607)
      1608)
      1609)
      1610)
      1611)
      1612)
      1613)
      1614)
      1615)
      1616)
      1617)
      1618)
      1619)
      1620)
      1621)
      1622)
      1623)
      1624)
      1625)
      1626)
      1627)
      1628)
      1629)
      1630)
      1631)
      1632)
      1633)
      1634)
      1635)
      1636)
      1637)
      1638)
      1639)
      1640)
      1641)
      1642)
      1643)
      1644)
      1645)
      1646)
      1647)
      1648)
      1649)
      1650)
      1651)
      1652)
      1653)
      1654)
      1655)
      1656)
      1657)
      1658)
      1659)
      1660)
```



```

KI=L
IF(KI-100) 130,120,120
LL=KI/100
A(J)=KG(LL+1)
KI=KI-100*LL
GO TO 135
130 A(J)=KG(I)
135 J=J+1
IF(KI-10) 150,140,140
140 LL=KI/10
A(J)=KG(LL+1)
KI=KI-10*LL
GO TO 155
150 A(J)=KG(I)
155 J=J+1
A(J)=KG(KI+1)
160 CONTINUE
C SETUP FIRST ROW OF ARRAY
GO TO 260
170 NLINE=NLINE+1
LLINE=NLINE+1
IF(NLINE-N) 180,180,380
180 DO 190 I=1,135
A(I)=BLK
B(I)=BLK
C(I)=BLK
D(I)=BLK
E(I)=BLK
F(I)=BLK
G(I)=BLK
H(I)=BLK
190 CONTINUE
IF (ICON)195,260,195
195 NCY=NCCP-1
J=4
IF(NCY)200,200,210
J=5
200 NCY=NCY+1
210 IF(NCY-NCP) 220,220,260
220 IF(NCY-M) 230,260,260
230 NLINE = NLINE - 1
YD1 = Y(NLINE,NCY) - Y(NLINE+1,NCY)
YD2=Y(NLINE,NCY+1)-Y(NLINE+1,NCY+1)
TP(1) = Y(NLINE,NCY)-0.125*YD1
TPX(1)=Y(NLINE,NCY)-0.250*YD1
TPM(1)=Y(NLINE,NCY)-0.375*YD1
XMT(1)=Y(NLINE,NCY)-0.500*YD1
BTM(1)=Y(NLINE,NCY)-0.625*YD1

```

```

MET01550
MET01560
MET01570
MET01580
MET01590
MET01600
MET01610
MET01620
MET01630
MET01640
MET01650
MET01660
MET01680
MET01690
MET01700
MET01710
MET01720
MET01730
MET01740
MET01750
MET01760
MET01770
MET01780
MET01790
MET01800
MET01810
MET01820
MET01830
MET01840
MET01850
MET01860
MET01870
MET01880
MET01890
MET01900
MET01910
MET01920
MET01930
MET01940
MET01950
MET01960
MET01970
MET01980
MET01990
MET02000
MET02010
MET02020

```

MET02030
 MET02040
 MET02050
 MET02060
 MET02070
 MET02080
 MET02090
 MET02100
 MET02110
 MET02120
 MET02130
 MET02140
 MET02150
 MET02160
 MET02170
 MET02180
 MET02190
 MET02200
 MET02210
 MET02220
 MET02230
 MET02240
 MET02250
 MET02260
 MET02270
 MET02280
 MET02290
 MET02300
 MET02310
 MET02320
 MET02330
 MET02340
 MET02350
 MET02360
 MET02370
 MET02380
 MET02390
 MET02400
 MET02410
 MET02420
 MET02430
 MET02440
 MET02450
 MET02460
 MET02470
 MET02480
 MET02490
 MET02500

```

BTX(1)=Y(NLINE,NCY)-0.750*YD1
BT(1)=Y(NLINE,NCY)-0.875*YD1
TPX(10)=Y(NLINE,NCY+1)-0.125*YD2
TPM(10)=Y(NLINE,NCY+1)-0.250*YD2
XMT(10)=Y(NLINE,NCY+1)-0.375*YD2
BTM(10)=Y(NLINE,NCY+1)-0.500*YD2
BTX(10)=Y(NLINE,NCY+1)-0.625*YD2
BT(10)=Y(NLINE,NCY+1)-0.750*YD2
NLINE = NLINE + 1
D1=3.1 * (TPX(10)-TP(1))
D2=0.1 * (TPX(10)-TPM(1))
D3=0.1 * (TPM(10)-XMT(1))
D4=0.1 * (XMT(10)-BTM(1))
D5=0.1 * (BTM(10)-BTX(1))
D6=0.1 * (BTX(10)-BT(1))
D7=0.1 * (BT(10)-BT(1))
DO 240 I = 2,9
TP(I)=TP(I-1)+D1
TPX(I)=TPX(I-1)+D2
TPM(I)=TPM(I-1)+D3
XMT(I)=XMT(I-1)+D4
BTM(I)=BTM(I-1)+D5
BTX(I)=BTX(I-1)+D6
BT(I)=BT(I-1)+D7
240 CONTINUE
DO 250 I=1,10
J=J+1
I1=MOD(IFIX((TPX(I)-AMIN)/BND),20)+1
I2=MOD(IFIX((TPM(I)-AMIN)/BND),20)+1
I3=MOD(IFIX((XMT(I)-AMIN)/BND),20)+1
I4=MOD(IFIX((BTM(I)-AMIN)/BND),20)+1
I5=MOD(IFIX((BTX(I)-AMIN)/BND),20)+1
I6=MOD(IFIX((BT(I)-AMIN)/BND),20)+1
A(J)=IH(I1)
B(J)=IH(I2)
C(J)=IH(I3)
D(J)=IH(I4)
E(J)=IH(I5)
F(J)=IH(I6)
G(J)=IH(I7)
CONTINUE
GO TO 210
260 NCY=NCCP-1
J=-2
IF(NCY) 265,265,270
J=-1
265

```

```

270 GO TO 330
    NCY=NCY+1
    IF(NCY-NCP) 280,280,310
280 J=J+7
    THLD=AHLD*Y(NLINE,NCY)+BZ
    IF(THLD) 285,290,290
285 H(J)=EMI
    GO TO 295
290 H(J)=EPL
295 NUM=INT((ABS(THLD-INT(THLD)))*1000.0+0.5)
    NDS=100
    DO 300 KK=1,3
        J=J+1
        KI=NUM/NDS
        H(J)=KG(KI+1)
        NUM=NUM-KI*NDS
        NDS=NDS/10
300 CONTINUE
    GO TO 270
310 IF(NCP-M) 360,320,320
320 IF(J-127)330,330,360
330 J=J+3
    KI=NLINE
    IF(KI-100) 340,335,335
    LL=KI/100
    H(J)=KG(LL+1)
    KI=KI-100*LL
    GO TO 343
340 H(J)=KG(1)
343 J=J+1
    IF(KI-10) 350,345,345
345 LL=KI/10
    H(J)=KG(LL+1)
    KI=KI-10*LL
    GO TO 355
350 H(J)=KG(1)
355 H(J)=KG(KI+1)
        J=J-5
    IF(NCY-1) 270,270,360
    IF(NLINE-1)362,362,368
360 PRINT 370,(A(I),I=1,132),(B(IP1),IP1=1,132),(H(IP2),IP2=1,132)
362 GO TO 170
368 PRINT 370,(A(I),I=1,132),(B(IP1),IP1=1,132),(C(IP2),IP2=1,132),
    1(D(IP3),IP3=1,132),(E(IP4),IP4=1,132),(F(IP5),IP5=1,132),
    2(G(IP6),IP6=1,132),(H(IP7),IP7=1,132)
370 FORMAT(132A1)
    GO TO 170

```

```

MET02510
MET02520
MET02530
MET02540
MET02550
MET02560
MET02570
MET02580
MET02590
MET02600
MET02610
MET02620
MET02630
MET02640
MET02650
MET02660
MET02670
MET02680
MET02690
MET02700
MET02710
MET02720
MET02730
MET02740
MET02750
MET02760
MET02770
MET02780
MET02790
MET02800
MET02810
MET02820
MET02830
MET02840
MET02850
MET02860
MET02870
MET02880
MET02890
MET02900
MET02910
MET02920
MET02930
MET02940
MET02950
MET02960
MET02970
MET02980
MET02990

```

```

380 DO 390 I=1,135
    A(I)=BLK
    B(I)=BLK
    C(I)=BLK
    D(I)=BLK
390 CONTINUE
    J=-2
    IF(NCCP-1) 395,395,400
395 J=-1
400 DO 430 L=NCCP,NCP
    J=J+8
    KI=L
    IF(KI-100) 410,405,405
405 LL=KI/100
    C(J)=KG(LL+1)
    KI=KI-100*LL
    GO TO 412
410 C(J)=KG(1)
412 J=J+1
    IF(KI-10) 420,415,415
415 LL=KI/10
    C(J)=KG(LL+1)
    KI=KI-10*LL
    GO TO 422
420 C(J)=KG(1)
422 J=J+1
    C(J)=KG(KI+1)
430 CONTINUE
    PRINT 370, (B(IP1),IP1=1,132),(C(IP2),IP2=1,132)
    IF(NCP-M)60,500,500
500 RETURN
    END

```

```

MET02990
MET03000
MET03010
MET03020
MET03030
MET03040
MET03050
MET03060
MET03070
MET03080
MET03090
MET03100
MET03110
MET03120
MET03130
MET03140
MET03150
MET03160
MET03170
MET03180

```

```

MET03200
MET03210
MET03220
MET03230
MET03240
MET03250
MET03260
MET03270
MET03280
MET03290
MET03300

```

```

C000021
C .....
C SUBROUTINE GAUSS
C .....
C PURPOSE
C COMPUTES A NORMALLY DISTRIBUTED RANDOM NUMBER WITH A GIVEN
C MEAN AND STANDARD DEVIATION
C .....
C USAGE
C CALL GAUSS(IX,S,AM,V)
C .....
C DESCRIPTION OF PARAMETERS
C .....
GAUS 10
GAUS 20
GAUS 30
GAUS 40
GAUS 50
GAUS 60
GAUS 70
GAUS 80
GAUS 90
GAUS 100
GAUS 110
GAUS 120
GAUS 130

```


CC

AND PRODUCES A NEW INTEGER AND REAL RANDOM NUMBER.

USAGE
CALL RANDU(IX,IY,YFL)

DESCRIPTION OF PARAMETERS
IX -- FOR THE FIRST ENTRY THIS MUST CONTAIN ANY ODD INTEGER
NUMBER WITH NINE OR LESS DIGITS. AFTER THE FIRST ENTRY,
IX SHOULD BE THE PREVIOUS VALUE OF IY COMPUTED BY THIS
SUBROUTINE.
IY -- A RESULTANT INTEGER RANDOM NUMBER REQUIRED FOR THE NEXT
ENTRY TO THIS SUBROUTINE. THE RANGE OF THIS NUMBER IS
BETWEEN ZERO AND 2**31
YFL-- THE RESULTANT UNIFORMLY DISTRIBUTED, FLOATING POINT,
RANDOM NUMBER IN THE RANGE 0 TO 1.0

REMARKS

THIS SUBROUTINE IS SPECIFIC TO SYSTEM/360 AND WILL PRODUCE
2**29 TERMS BEFORE REPEATING. THE REFERENCE BELOW DISCUSSES
SEEDS (65539 HERE), RUN PROBLEMS, AND PROBLEMS CONCERNING
RANDOM DIGITS USING THIS GENERATION SCHEME. MACLAREN AND
MARSAGLIA, JACM 12, P. 83-89, DISCUSS CONGRUENTIAL
GENERATION METHODS AND TESTS. THE USE OF TWO GENERATORS OF
THE RANDU TYPE, ONE FILLING A TABLE AND ONE PICKING FROM THE
TABLE, IS OF BENEFIT IN SOME CASES. 65549 HAS BEEN
SUGGESTED AS A SEED WHICH HAS BETTER STATISTICAL PROPERTIES
FOR HIGH ORDER BITS OF THE GENERATED DEVIAE.
SEEDS SHOULD BE CHOSEN IN ACCORDANCE WITH THE DISCUSSION THAT
GIVEN IN THE REFERENCE BELOW. ALSO, IT SHOULD BE NOTED THAT
IF FLOATING POINT RANDOM NUMBERS ARE DESIRED, AS ARE
AVAILABLE FROM RANDU, THE RANDOM CHARACTERISTICS OF THE
FLOATING POINT DEVIATES ARE MODIFIED AND IN FACT THESE
DEVIATES HAVE HIGH PROBABILITY OF HAVING A TRAILING LOW
ORDER ZERO BIT IN THEIR FRACTIONAL PART.

SUBROUTINES AND FUNCTION SUBPROGRAMS REQUIRED
NONE

METHOD
POWER RESIDUE METHOD DISCUSSED IN IBM MANUAL C20-8011,
RANDOM NUMBER GENERATION AND TESTING

RAND 100
RAND 110
RAND 120
RAND 130
RAND 140
RAND 150
RAND 160
RAND 170
RAND 180
RAND 190
RAND 200
RAND 210
RAND 220
RAND 230
RAND 240
RAND 250
RAND 260
RAND 270
RAND 280
RAND 290
RAND 300
RAND 310
RAND 320
RAND 330
RAND 340
RAND 350
RAND 360
RAND 370
RAND 380
RAND 390
RAND 400
RAND 410
RAND 420
RAND 430
RAND 440
RAND 450
RAND 460
RAND 470
RAND 480
RAND 490
RAND 500
RAND 510
RAND 520
RAND 530


```
SUBROUTINE RANDU(IX,IY,YFL)
  IY=IX*65539
  IF(IY)5,6,6
  5 IY=IY+2147483647+1
  6 YFL=IY
  YFL=YFL*.4656613E-9
  RETURN
END
```

```
RAND 540
RAND 550
RAND 560
RAND 570
RAND 580
RAND 590
RAND 600
```

LIST OF REFERENCES

1. Heflinger, L. O., Wuerker, R. F., and Brooks, R. E., "Holographic Interferometry," Journal of Applied Physics, Vol. 37, No. 2, pp. 642-649, February 1966.
2. Brooks R. E., Heflinger, L. O., and Wuerker, R. F., "9A9 - Pulsed Laser Holograms," IEEE Journal of Quantum Electronics, Vol. EQ-2, No. 8, pp. 275-299, August 1966.
3. Matulka, R. D., The Application of Holographic Interferometry to The Determination of Asymmetric Three-Dimensional Density Fields in Free Jet Flow, PhD Thesis, Naval Postgraduate School, June 1970.
4. Matulka, R. D., and Collins, D. J., "Determination of Three-Dimensional Density Fields From Holographic Interferograms," Journal of Applied Physics, Vol. 42, No. 3, pp. 1109-1119, March 1971.
5. Maldonado, C. D., Caron, A. P., and Olsen, H. N., "New Method for Obtaining Emission Coefficients from Emitted Spectral Intensities. Part I - Circularly Symmetric Light Sources," Journal of The Optical Society of America, Vol. 55, No. 10, pp. 1247-1254, October 1965.
6. Maldonado, C. D., and Olsen, H. N., "New Method for Obtaining Emission Coefficients from Emitted Spectral Intensities. Part II - Asymmetric Sources," Journal of The Optical Society of America, Vol. 56, No. 10, pp. 1305-1312, October 1966.
7. Jagota, R. C., The Application of Holographic Interferometry to The Determination of The Flow Field Around a Right Circular Cone At Angle of Attack, Aeronautical Engineer's Thesis, Naval Postgraduate School, December 1970.
8. Jagota, R. C., and Collins, D. J., "Finite Fringe Holographic Interferometry Applied to A Right Circular Cone At Angle of Attack," ASME Paper No. 72-APM-PP, to appear in the Journal of Applied Mechanics.
9. Heyer, R. W., Holographic Interferometry of The Flow Field Between A Fin and Flat Plate, Master's Thesis, Naval Postgraduate School, March 1972.

10. Liepmann, H. W., and Roshko, A., Elements of Gas Dynamics, p. 165, John Wiley and Sons, Inc., 1957.
11. Collier, R. J., and others, Optical Holography, sect. 10.8.4, Academic Press, 1971.
12. Sweeney, D. W., and Vest, C. M., "Reconstruction of Three-Dimensional Refractive Index Fields by Holographic Interferometry," Applied Optics, Vol. 11, No. 1, pp. 205-207, January 1972.
13. Van Houten, P. E., Analysis of Discontinuous Three-Dimensional Density Fields Using Holographic Interferometry, Aeronautical Engineer's Thesis, Naval Postgraduate School, December 1972.
14. Junginger, H. G., and van Haeringen, W., "Calculation of Three-Dimensional Refractive Index Fields Using Phase Integrals," to appear in Optics Communications.

INITIAL DISTRIBUTION LIST

	No. Copies
1. Defense Documentation Center Cameron Station Alexandria, Virginia 22314	12
2. Library, Code 0212 Naval Postgraduate School Monterey, California 93940	2
3. Professor D. J. Collins, Code 57Co Department of Aeronautics Naval Postgraduate School Monterey, California 93940	1
4. LT Robert A. Kosakoski, USN The Arches, Apt #77 1235 Wildwood Avenue Sunnyvale, California 94086	1
5. Chairman, Department of Aeronautics Naval Postgraduate School Monterey, California 93940	1
6. Dean of Research Naval Postgraduate School Monterey, California 93940	1

DOCUMENT CONTROL DATA - R & D

(Security classification of title, body of abstract and indexing annotation must be entered when the overall report is classified)

1. ORIGINATING ACTIVITY (Corporate author) Naval Postgraduate School Monterey, California 93940		2a. REPORT SECURITY CLASSIFICATION Unclassified	
		2b. GROUP	
3. REPORT TITLE Application of Holographic Interferometry to Density Field Determination in Transonic Corner Flow			
4. DESCRIPTIVE NOTES (Type of report and, inclusive dates) Master's Thesis; December 1972			
5. AUTHOR(S) (First name, middle initial, last name) Robert A. Kosakoski			
6. REPORT DATE December 1972	7a. TOTAL NO. OF PAGES 120	7b. NO. OF REFS 14	
8a. CONTRACT OR GRANT NO.	9a. ORIGINATOR'S REPORT NUMBER(S)		
b. PROJECT NO.			
c.	9b. OTHER REPORT NO(S) (Any other numbers that may be assigned this report)		
d.			
10. DISTRIBUTION STATEMENT			
11. SUPPLEMENTARY NOTES		12. SPONSORING MILITARY ACTIVITY Naval Postgraduate School Monterey, California 93940	
13. ABSTRACT The successful application of holographic interferometry to the study of density fields around opaque bodies in wind tunnel experiments has been reported in the literature. The present report extends this technique to the study of the three-dimensional asymmetric flow fields encountered near the wing-fuselage junction of an aerodynamic model in the transonic flow regime. Finite fringe interferometry has been used to obtain fringe information about a partially transparent wind-body structure. A FORTRAN computer program was utilized to invert the fringe information and produce a plot of the density field around the model. The resulting asymmetric density field and shock wave structure are shown to be an accurate representation of the phenomena encountered in aerodynamic corner flow.			

14

KEY WORDS

LINK A

LINK B

LINK C

ROLE

WT

ROLE

WT

ROLE

WT

Holography

Interferometry

Transonic Flow

Corner Flow

Transparent Phase Object

Aerodynamic Model

Wing-Fuselage Junction

DISTRIBUTION

1.	Defense Documentation Center Cameron Station Alexandria, Virginia 22314	20
2.	Library (Code 0212) Naval Postgraduate School Monterey, California 93940	2
3.	Commander Naval Air Systems Command Department of the Navy Washington, D. C. 20360	
	Attn: AIR 310	2
	AIR 604	2
4.	Chairman Department of Aeronautics Code 57 Naval Postgraduate School Monterey, California 93940	1
5.	Professor D. J. Collins Department of Aeronautics Code 57C0 Naval Postgraduate School Monterey, California 93940	2
6.	Dean of Research Naval Postgraduate School Monterey, California 93940	2
7.	Dr. H. J. Mueller Naval Air Systems Command AIR 310 Department of the Navy Washington, D. C. 20360	2

DOCUMENT CONTROL DATA - R & D

(Security classification of title, body of abstract and indexing annotation must be entered when the overall report is classified)

<p>1 ORIGINATING ACTIVITY (Corporate author)</p> <p>Naval Postgraduate School Monterey, California 93940</p>	<p>2a. REPORT SECURITY CLASSIFICATION</p> <p>Unclassified</p> <p>2b. GROUP</p>
--	--

3 REPORT TITLE

Application of Holographic Interferometry to Density Field Determination in Transonic Corner Flow

4 DESCRIPTIVE NOTES (Type of report and inclusive dates)

Technical Report NPS-57C072121A

5 AUTHOR(S) (First name, middle initial, last name)

D. J. Collins and R. A. Kosakoski

<p>6 REPORT DATE</p> <p>December 1972</p>	<p>7a. TOTAL NO. OF PAGES</p> <p>127</p>	<p>7b. NO. OF REFS</p> <p>0</p>
---	--	---------------------------------

<p>8a. CONTRACT OR GRANT NO.</p> <p>b. PROJECT NO. Dr. H. Mueller ONR Req. 00014-2-000033, 15 Sep 71</p> <p>c. NASC W. R. 2-6059, 12 Jul 71</p> <p>d.</p>	<p>9a. ORIGINATOR'S REPORT NUMBER(S)</p> <p>9b. OTHER REPORT NO(S) (Any other numbers that may be assigned this report)</p>
---	---

10 DISTRIBUTION STATEMENT

Approved for public release; distribution unlimited.

<p>11. SUPPLEMENTARY NOTES</p>	<p>12. SPONSORING MILITARY ACTIVITY</p> <p>Office of Naval Research and Naval Air Systems Command</p>
--------------------------------	---

13. ABSTRACT

The successful application of holographic interferometry to the study of density fields around opaque bodies in wind tunnel experiments has been reported in the literature. The present report extends this technique to the study of the asymmetric flow fields encountered near the wing-fuselage junction of an aerodynamic model in the transonic flow regime. Finite fringe interferometry has been used to investigate the three dimensional density field about a partially transparent wing-body structure. The resulting asymmetric density field and shock wave structure are shown to be an accurate representation of the phenomena encountered in aerodynamic corner flow.

14 KEY WORDS	LINK A		LINK B		LINK C	
	ROLE	WT	ROLE	WT	ROLE	WT
Holography Interferometry Transonic Flow Corner Flow Transparent Phase Object Aerodynamic Model Wing-Fuselage Junction						

DUDLEY KNOX LIBRARY



3 2768 00391409 4